Univerza
v Ljubljani
Fakulteta
za gradbeništvo
in geodezijo

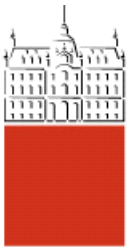

Benjamin Cerar

KALIBRACIJA ENAČB MEJNEGA STANJA ZA ARMIRANOBETONSKE KONSTRUKCIJE NA OSNOVI ZANESLJIVOSTI KONSTRUKCIJ

MAGISTRSKO DELO

MAGISTRSKI ŠTUDIJSKI PROGRAM DRUGE STOPNJE GRADBENIŠTVO

Ljubljana, 2020

Hrbtna stran: **CERAR BENJAMIN** 2020

Univerza
v Ljubljani

Fakulteta za
gradbeništvo in
geodezijo

Kandidat/-ka:

Benjamin Cerar

KALIBRACIJA ENAČB MEJNEGA STANJA ZA ARMIRANOBETONSKE KONSTRUKCIJE NA OSNOVI ZANESLJIVOSTI KONSTRUKCIJ

Magistrsko delo št.:

RELIABILITY-BASED CALIBRATION OF REINFORCED CONCRETE DESIGN FORMULAS

Master thesis No.:

Mentor/-ica:
prof. dr. Goran Turk

Predsednik komisije:

Somentorja:
dr. Árpád Rózsás, doc. dr. Yuguang Yang

Član komisije:

Ljubljana, _____

ERRATA

Page	Line	Instead of	Should be

BIBLIOGRAPHIC-DOCUMENTALISTIC INFORMATION AND ABSTRACT

UDC: **624.012.45(043.3)**
Author: **Benjamin Cerar**
Supervisor: **Prof. Goran Turk, Ph.D.**
Co-supervisors: **Assist. Prof. Yuguang Yang, Ph.D., Árpád Rózsás, Ph.D.**
Title: **Reliability-based calibration of reinforced concrete design formulas**
Document type: **Master Thesis**
Notes: **54 p., 43 fig., 15 tab., 30 eq.**
Keywords: **reliability analysis, structural design codes, uncertainty**

Abstract

Structural design codes are one of the most important components in the process of designing structures. In this thesis we deal with probabilistic calibration of existing design codes, specifically the Eurocodes. In the process of developing this thesis, we pose the following research question: What are the partial safety factors for concrete (γ_C) for the selected Eurocode 2 (EN 1992-1:2018 Draft 4) design expressions obtained by performing a reliability-based code calibration? To answer the question we use an implementation of a probabilistic (reliability-based) code calibration procedure, developed at TU Delft and TNO, which allows parameters of the resistance and the load effects to be considered as random variables. In this thesis, we consider the resistance model uncertainty as one of the random variables and estimate its parameters with the method of maximum likelihood using an experimental database. Reliability analysis is performed for a large number of design scenarios. The parameters of probabilistic models for the random variables are based either on literature or expert judgment. The partial factors are free parameters of a weighted objective function, which measures the absolute deviation of the calculated reliability levels from the target reliability for all design scenarios. Here we use a symmetric objective function, the target reliability $\beta_{\text{target}} = 4.7$, which corresponds to a 1-year reference period and consequence class 2 as defined in EN 1990, and a weight function that is based on our judgment of prevalent design scenarios. The calculated sensitivity factors α^2 indicate that only the model uncertainty is a significant parameter among the resistance variables with values between 0.5 and 0.7. For other random variables on the resistance side we mostly obtain α^2 values lower than 0.2. The reliability levels mostly follow the same behavior: the values range between 3.5 and 5.0 and are the lowest when the variable load represents most of the applied load (high load ratio values). The traffic load combination shows different behavior in terms of reliability levels, with few design scenarios achieving the target reliability. To answer the research question: the calibrated material partial factors are $\gamma_C = 1.54$ and $\gamma_C = 1.46$ for the two considered subsets of the one-way shear resistance formula, $\gamma_C = 1.61$ and $\gamma_C = 1.46$ for the subsets of the punching shear resistance formula. It appears that the partial factors are close to the present value $\gamma_C = 1.50$, however, more research should be done to investigate the reliability level when designing according to the traffic load combination. Additionally, we recommend exploring the calibration for different levels of target reliability, as well as performing a sensitivity analysis in order to determine whether it makes sense to include the random variables that show low α^2 values in the calibration.

BIBLIOGRAFSKO-DOKUMENTACIJSKA STRAN IN IZVLEČEK

UDK: **624.012.45(043.3)**
Avtor: **Benjamin Cerar**
Mentor: **prof. dr. Goran Turk**
Somentorja: **doc. dr. Yuguang Yang, dr. Árpád Rózsás**
Naslov: **Kalibracija enačb mejnega stanja za armirano betonske konstrukcije na osnovi zanesljivosti konstrukcij**
Tip dokumenta: **Magistrska naloga**
Obseg in oprema: **54 str., 43 sl., 15 pregl., 30 en.**
Ključne besede: **analiza zanesljivosti, enačbe mejnih stanj, negotovost**

Izvleček

Standardi za projektiranje gradbenih konstrukcij predstavljajo enega izmed najpomembnejših vidikov v procesu gradnje. V magistrski nalogi obravnavamo probabilistično kalibracijo enačb mejnih stanj v omenjenih standardih, natančneje v Evrokodih. Tekom te magistrske naloge postavimo raziskovalno vprašanje: kolikšna je vrednost delnega varnostnega faktorja za beton (γ_C) za izbrane enačbe mejnega stanja v EN 1992-1:2018 D4 ob kalibraciji na podlagi analize zanesljivosti? Na vprašanje odgovorimo z uporabo procedure za probabilistično kalibracijo mejnih stanj, ki so jo razvili raziskovalci iz organizacije TNO in Tehniške univerze v Delftu. V nalogi obravnavamo modelno negotovost kot slučajno spremenljivko. Parametre njene porazdelitve izračunamo z metodo največjega verjetja na podlagi eksperimentalnih podatkov. Analiza zanesljivosti je opravljena za veliko število generiranih projektnih scenarijev. V sklopu probabilistične kalibracije obravnavamo delne varnostne faktorje kot spremenljivke utežene ciljne funkcije, ki meri povprečno odstopanje izračunanih indeksov zanesljivosti od ciljne zanesljivosti. V tej nalogi uporabimo simetrično ciljno funkcijo, ter ciljno zanesljivost $\beta_{\text{target}} = 4.7$, ki po definiciji v EN 1990:2002 ustreza enoletnem referenčnem obdobju. Uporabimo tudi utežno funkcijo, ki je določena na podlagi lastne presoje o merodajnosti generiranih projektnih scenarijev. Faktorji občutljivosti α^2 nakazujejo na to, da je le modelska negotovost (vrednosti med 0.5 in 0.7) relevantna slučajna spremenljivka za odpornostni model, saj so preostale vrednosti manjše kot 0.2. Izračunani indeksi zanesljivosti so večinoma podobni za vse uporabljene obtežne kombinacije: vrednosti nihajo med 3.5 in 5.0 in so najmanjše, ko je spremenljiva obtežba prevladujoča. Izjema je obtežna kombinacija za promet, kjer večina projektnih scenarijev ne doseže ciljne zanesljivosti. Izračunani delni varnostni faktorji za beton so: $\gamma_C = 1.54$ in $\gamma_C = 1.46$ za pogoja projektne strižne odpornosti armiranobetonskih elementov brez strižne armature, ter $\gamma_C = 1.61$ in $\gamma_C = 1.46$ za pogoja projektne odpornosti proti preboju armiranobetonskih elementov brez strižne armature. Izračunani delni varnostni faktorji so podobni trenutni vrednosti $\gamma_C = 1.50$. Kljub temu bi bila potrebna nadaljna analiza stopnje zanesljivosti obeh projektnih enačb, še zlasti, ko je uporabljena obtežna kombinacija za promet. Priporočena je tudi kalibracija z drugimi vrednostmi indeksa ciljne zanesljivosti, kot tudi občutljivostna analiza, s katero bi bilo mogoče določiti vpliv slučajnih spremenljivk z nizkimi α^2 vrednosti na izračunani delni varnostni faktor.

ACKNOWLEDGEMENT

The primary, secondary, and tertiary degrees of my education were completed tuition-free thanks to the educational system of the Republic of Slovenia. A part of my graduate studies was completed at the RWTH Aachen with the support of the Erasmus+ programme, which is financed by the European Commission. I appreciate the (indirect) support of both. I would like to thank the Study board of the Department of Civil Engineering at the Faculty of Civil and Geodetic Engineering at the University of Ljubljana for enabling me to complete this thesis in English. I also acknowledge the Knowledge Investment Project (KIP) Concrete Structures at TNO, which facilitated this thesis.

My sincerest thanks to the supervisors of this thesis: Árpád Rózsás, Arthur Slobbe, Yuguang Yang, and Goran Turk. Without your patient guidance, support and understanding, this thesis would not have been completed. I would especially like to highlight Arthur who is unfortunately not officially credited for this thesis. You were the first one to give me a chance and enabled me to work at TNO – thank you!

During the course of my studies at the University of Ljubljana I have met a lot of interesting people. None were as influential on me as Amel, Doron and Nejc. Distance can separate us, but memories always bring us back together.

Thank you to Marjon, Cees and Koen for the support, council and for providing me with a roof over my head. You have made my first experiences in the Netherlands memorable. To Renske, for your companionship, for selfless support in the most difficult times and for putting up with me.

Finally, I would like to acknowledge my family, whose support I always had regardless the decisions I made. To my parents, Branko and Tatjana, who instilled in me the ideals of hard work, honesty and caring: you worked as much as me for my education. I am thankful.

TABLE OF CONTENTS

BIBLIOGRAPHIC-DOCUMENTALISTIC INFORMATION AND ABSTRACT **II**

BIBLIOGRAFSKO-DOKUMENTACIJSKA STRAN IN IZVLEČEK **III**

ACKNOWLEDGMENT **IV**

1 INTRODUCTION **1**

1.1 Motivation 1

1.2 Problem statement 1

1.3 Approach 2

1.4 Scope and limitations 2

1.5 Outline of the thesis 2

2 LITERATURE REVIEW **4**

2.1 Code calibration approaches 4

2.2 The Eurocodes 4

2.3 Concluding remarks 5

3 RELIABILITY-BASED CODE CALIBRATION IMPLEMENTATION **6**

3.1 Overview 6

3.2 Calibration procedure 6

3.3 Software engineering 10

4 DEMONSTRATION OF THE PROPOSED CALIBRATION APPROACH ON THE REVISED EUROCODE 2 DESIGN EQUATIONS **12**

4.1 One-way shear resistance of reinforced concrete members without shear reinforcement 12

4.1.1 Model uncertainty inference 12

4.1.2 Definition of design scenarios 14

4.1.3 Probabilistic description of resistance and load models for the calibration of one-way shear resistance expression 15

4.1.4 Results 22
4.2 Punching shear resistance of reinforced concrete members without shear reinforcement 32
4.2.1 Model uncertainty inference 33
4.2.2 Definition of design scenarios 35
4.2.3 Probabilistic description of resistance and load models for the calibration of punching shear resistance expression 36
4.2.4 Results 38

5 DISCUSSION 46

6 CONCLUSIONS AND RECOMMENDATIONS 47
6.1 Conclusions 47
6.2 Recommendations 47

POVZETEK 49

REFERENCES 54

LIST OF FIGURES

3.1 Flowchart of the probabilistic calibration procedure that was used in this thesis. 11

4.1 Relationship between experimental and model one-way shear resistance values for subset $a_{cs} \geq 4d$; the solid black line represents perfect model prediction; circles denote individual data points from the experimental database. 14

4.2 Relationship between experimental and model one-way shear resistance values for subset $a_{cs} \geq 4d$; the solid black line represents perfect model prediction; circles denote individual data points from the experimental database. 15

4.3 Sensitivity factors α^2 corresponding to subset $a_{cs} \geq 4d$ of the one-way shear resistance equation with the snow-wind load combination and with different effective depth d: a) 150 mm, (b) 520 mm, (c) 890 mm. 23

4.4 Sensitivity factors α^2 corresponding to subset $a_{cs} \geq 4d$ of the one-way shear resistance equation with the snow-wind load combination and with different effective depth d: (a) 1260 mm, (b) 1630 mm, (c) 2000 mm. 24

4.5 Reliability indices β as a function of load ratio χ_1 with $d = 150$ mm for the subset $a_{cs} \geq 4d$ corresponding to the one-way shear resistance formula. Columns present different load combinations, while rows different value of longitudinal reinforcement ratios. Colors represent different values of χ_2 load ratios, while the marker size shows the magnitude of the weight of prevalence. The black horizontal line indicates the target reliability (4.7). 25

4.6 Reliability indices β as a function of load ratio χ_1 with $d = 2000$ mm for the subset $a_{cs} \geq 4d$ corresponding to the one-way shear resistance formula. Columns present different load combinations, while rows different value of longitudinal reinforcement ratios. Colors represent different values of χ_2 load ratios, while the marker size shows the magnitude of the weight of prevalence. The black horizontal line indicates the target reliability (4.7). 26

4.7 Sensitivity factors α^2 corresponding to subset $a_{cs} < 4d$ of the one-way shear resistance equation with the snow-wind load combination and with different effective depth d: (a) 150 mm, (b) 520 mm, (c) 890 mm. 27

4.8 Sensitivity factors α^2 corresponding to subset $a_{cs} < 4d$ of the one-way shear resistance equation with the snow-wind load combination and with different effective depth d: (a) 1260 mm, (b) 1630 mm, (c) 2000 mm. 28

4.9 Reliability indices β as a function of load ratio χ_1 with $d = 150$ mm for the subset $a_{cs} < 4d$ corresponding to the one-way shear resistance formula. Columns present different load combinations, while rows different value of longitudinal reinforcement ratios. Colors represent different values of χ_2 load ratios, while the marker size shows the magnitude of the weight of prevalence. The black horizontal line indicates the target reliability (4.7). 29

4.10 Reliability indices β as a function of load ratio χ_1 with $d = 2000$ mm for the subset $a_{cs} < 4d$ corresponding to the one-way shear resistance formula. Columns present different load combinations, while rows different value of longitudinal reinforcement ratios. Colors represent different values of χ_2 load ratios, while the marker size shows the magnitude of the weight of prevalence. The black horizontal line indicates the target reliability (4.7). 30

4.11 Relationship between experimental and model punching shear resistance values for subset $a_p \leq 8d_v$; the solid black line represents perfect model prediction; circles denote individual data points from the experimental database. 34

4.12 Relationship between experimental and model punching shear resistance values for subset $a_p > 8d_v$; the solid black line represents perfect model prediction; circles denote individual data points from the experimental database. 35

4.13 Sensitivity factors α^2 corresponding to subset $a_p \leq 8d_v$ of the punching shear resistance equation with the snow-wind load combination and with different effective depth d: (a) 150 mm, (b) 300 mm, (c) 400 mm, (d) 500 mm. 39

4.14 Reliability indices β as a function of load ratio χ_1 with $d = 150$ mm for the subset $a_p \leq 8d_v$ corresponding to the punching shear resistance formula. Columns present different load combinations, while rows different value of longitudinal reinforcement ratios. Colors represent different values of χ_2 load ratios, while the marker size shows the magnitude of the weight of prevalence. The black horizontal line indicates the target reliability (4.7). 40

4.15 Reliability indices β as a function of load ratio χ_1 with $d = 500$ mm for the subset $a_p \leq 8d_v$ corresponding to the punching shear resistance formula. Columns present different load combinations, while rows different value of longitudinal reinforcement ratios. Colors represent different values of χ_2 load ratios, while the marker size shows the magnitude of the weight of prevalence. The black horizontal line indicates the target reliability (4.7). 41

4.16 Sensitivity factors α^2 corresponding to subset $a_p > 8d_v$ of the punching shear resistance equation with the snow-wind load combination and with different effective depth d: (a) 150 mm, (b) 300 mm, (c) 400 mm, (d) 500 mm. 42

4.17 Reliability indices β as a function of load ratio χ_1 with $d = 150$ mm for the subset $a_p > 8\,d_v$ corresponding to the punching shear resistance formula. Columns present different load combinations, while rows different value of longitudinal reinforcement ratios. Colors represent different values of χ_2 load ratios, while the marker size shows the magnitude of the weight of prevalence. The black horizontal line indicates the target reliability (4.7). 43

4.18 Reliability indices β as a function of load ratio χ_1 with $d = 500$ mm for the subset $a_p > 8\,d_v$ corresponding to the punching shear resistance formula. Columns present different load combinations, while rows different value of longitudinal reinforcement ratios. Colors represent different values of χ_2 load ratios, while the marker size shows the magnitude of the weight of prevalence. The black horizontal line indicates the target reliability (4.7). 44

B.1 Sensitivity factors α^2 corresponding to subset $a_{cs} \geq 4\,d$ of the one-way shear resistance equation with the snow-imposed load combination and with different effective depth d: (a) 150 mm, (b) 520 mm, (c) 890 mm 1

B.2 Sensitivity factors α^2 corresponding to subset $a_{cs} \geq 4\,d$ of the one-way shear resistance equation with the snow-imposed load combination and with different effective depth d: (a) 1260 mm, (b) 1630 mm, (c) 2000 mm. 2

B.3 Sensitivity factors α^2 corresponding to subset $a_{cs} \geq 4\,d$ of the one-way shear resistance equation with the wind-imposed load combination and with different effective depth d: (a) 150 mm, (b) 520 mm, (c) 890 mm. 3

B.4 Sensitivity factors α^2 corresponding to subset $a_{cs} \geq 4\,d$ of the one-way shear resistance equation with the wind-imposed load combination and with different effective depth d: (a) 1260 mm, (b) 1630 mm, (c) 2000 mm. 4

B.5 Reliability indices β as a function of load ratio χ_1 with $d = 520$ mm for the subset $a_{cs} \geq 4\,d$ corresponding to the one-way shear resistance formula. Columns present different load combinations, while rows different value of longitudinal reinforcement ratios. Colors represent different values of χ_2 load ratios, while the marker size shows the magnitude of the weight of prevalence. The black horizontal line indicates the target reliability (4.7). 5

B.6 Reliability indices β as a function of load ratio χ_1 with $d = 890$ mm for the subset $a_{cs} \geq 4\,d$ corresponding to the one-way shear resistance formula. Columns present different load combinations, while rows different value of longitudinal reinforcement ratios. Colors represent different values of χ_2 load ratios, while the marker size shows the magnitude of the weight of prevalence. The black horizontal line indicates the target reliability (4.7). 6

B.7 Reliability indices β as a function of load ratio χ_1 with $d = 1260$ mm for the subset $a_{cs} \geq 4d$ corresponding to the one-way shear resistance formula. Columns present different load combinations, while rows different value of longitudinal reinforcement ratios. Colors represent different values of χ_2 load ratios, while the marker size shows the magnitude of the weight of prevalence. The black horizontal line indicates the target reliability (4.7). 7

B.8 Reliability indices β as a function of load ratio χ_1 with $d = 1630$ mm for the subset $a_{cs} \geq 4d$ corresponding to the one-way shear resistance formula. Columns present different load combinations, while rows different value of longitudinal reinforcement ratios. Colors represent different values of χ_2 load ratios, while the marker size shows the magnitude of the weight of prevalence. The black horizontal line indicates the target reliability (4.7). 8

B.9 Sensitivity factors α^2 corresponding to subset $a_{cs} < 4d$ of the one-way shear resistance equation with the snow-imposed load combination and with different effective depth d: (a) 150 mm, (b) 520 mm, (c) 890 mm. 9

B.10 Sensitivity factors α^2 corresponding to subset $a_{cs} < 4d$ of the one-way shear resistance equation with the snow-imposed load combination and with different effective depth d: (a) 1260 mm, (b) 1630 mm, (c) 2000 mm. 10

B.11 Sensitivity factors α^2 corresponding to subset $a_{cs} < 4d$ of the one-way shear resistance equation with the wind-imposed load combination and with different effective depth d: (a) 150 mm, (b) 520 mm, (c) 890 mm. 11

B.12 Sensitivity factors α^2 corresponding to subset $a_{cs} < 4d$ of the one-way shear resistance equation with the wind-imposed load combination and with different effective depth d: (a) 1260 mm, (b) 1630 mm, (c) 2000 mm. 12

B.13 Reliability indices β as a function of load ratio χ_1 with $d = 520$ mm for the subset $a_{cs} < 4d$ corresponding to the one-way shear resistance formula. Columns present different load combinations, while rows different value of longitudinal reinforcement ratios. Colors represent different values of χ_2 load ratios, while the marker size shows the magnitude of the weight of prevalence. The black horizontal line indicates the target reliability (4.7). 13

B.14 Reliability indices β as a function of load ratio χ_1 with $d = 890$ mm for the subset $a_{cs} < 4d$ corresponding to the one-way shear resistance formula. Columns present different load combinations, while rows different value of longitudinal reinforcement ratios. Colors represent different values of χ_2 load ratios, while the marker size shows the magnitude of the weight of prevalence. The black horizontal line indicates the target reliability (4.7). 14

B.15 Reliability indices β as a function of load ratio χ_1 with $d = 1260$ mm for the subset $a_{cs} < 4d$ corresponding to the one-way shear resistance formula. Columns present different load combinations, while rows different value of longitudinal reinforcement ratios. Colors represent different values of χ_2 load ratios, while the marker size shows the magnitude of the weight of prevalence. The black horizontal line indicates the target reliability (4.7). 15

B.16 Reliability indices β as a function of load ratio χ_1 with $d = 1630$ mm for the subset $a_{cs} < 4d$ corresponding to the one-way shear resistance formula. Columns present different load combinations, while rows different value of longitudinal reinforcement ratios. Colors represent different values of χ_2 load ratios, while the marker size shows the magnitude of the weight of prevalence. The black horizontal line indicates the target reliability (4.7). 16

B.17 Sensitivity factors α^2 corresponding to subset $a_p \leq 8d_v$ of the punching shear resistance equation with the snow-imposed load combination and with different effective depth d: (a) 150 mm, (b) 300 mm, (c) 400 mm, (d) 500 mm. 17

B.18 Sensitivity factors α^2 corresponding to subset $a_p \leq 8d_v$ of the punching shear resistance equation with the wind-imposed load combination and with different effective depth d: (a) 150 mm, (b) 300 mm, (c) 400 mm, (d) 500 mm. 18

B.19 Reliability indices β as a function of load ratio χ_1 with $d = 300$ mm for the subset $a_p \leq 8d_v$ corresponding to the punching shear resistance formula. Columns present different load combinations, while rows different value of longitudinal reinforcement ratios. Colors represent different values of χ_2 load ratios, while the marker size shows the magnitude of the weight of prevalence. The black horizontal line indicates the target reliability (4.7). 19

B.20 Reliability indices β as a function of load ratio χ_1 with $d = 400$ mm for the subset $a_p \leq 8d_v$ corresponding to the punching shear resistance formula. Columns present different load combinations, while rows different value of longitudinal reinforcement ratios. Colors represent different values of χ_2 load ratios, while the marker size shows the magnitude of the weight of prevalence. The black horizontal line indicates the target reliability (4.7). 20

B.21 Sensitivity factors α^2 corresponding to subset $a_p > 8d_v$ of the punching shear resistance equation with the snow-imposed load combination and with different effective depth d: (a) 150 mm, (b) 300 mm, (c) 400 mm, (d) 500 mm. 21

B.22 Sensitivity factors α^2 corresponding to subset $a_p > 8d_v$ of the punching shear resistance equation with the wind-imposed load combination and with different effective depth d: (a) 150 mm, (b) 300 mm, (c) 400 mm, (d) 500 mm. 22

B.23 Reliability indices β as a function of load ratio χ_1 with $d = 300$ mm for the subset $a_p > 8\,d_v$ corresponding to the punching shear resistance formula. Columns present different load combinations, while rows different value of longitudinal reinforcement ratios. Colors represent different values of χ_2 load ratios, while the marker size shows the magnitude of the weight of prevalence. The black horizontal line indicates the target reliability (4.7). 23

B.24 Reliability indices β as a function of load ratio χ_1 with $d = 400$ mm for the subset $a_p > 8\,d_v$ corresponding to the punching shear resistance formula. Columns present different load combinations, while rows different value of longitudinal reinforcement ratios. Colors represent different values of χ_2 load ratios, while the marker size shows the magnitude of the weight of prevalence. The black horizontal line indicates the target reliability (4.7). 24

LIST OF TABLES

3.1 Values of weights of prevalence used in the presented calibrations. 9

3.2 Number of design scenarios that were used in the calibration of the considerd design formulas. 10

4.1 Estimated model uncertainty parameters of the design one-way shear resistance expression in comparison to the present value used for representing resistance model uncertainty. 13

4.2 Design scenario parameters and their discrete values that were used in the calibration of the one-way shear design expression. 16

4.3 Probabilistic description of random variables in the one-way shear resistance model. . 17

4.4 Parameters of random variables used in the permanent load model for the one-way shear expression. 17

4.5 Probabilistic description of random variables in the imposed load model for the one-way shear formula. 18

4.6 Probabilistic description of random variables in the traffic load model for the one-way shear formula. 19

4.7 Probabilistic descriptions of random variables in the snow load model for the one-way shear resistance formula. 20

4.8 Parameters of random variables used in the wind load model for the one-way shear resistance equation calibration. 21

4.9 Calculated partial safety factors for concrete for the design one-way shear resistance expression. 22

4.10 Estimated model uncertainty parameters of the design punching shear resistance expression in comparison to the present value used for representing resistance model uncertainty. 34

4.11 Design scenario parameters and their discrete values that were used in the calibration of the punching shear design expression. 36

4.12 Probabilistic description of random variables in the punching shear resistance model. . 37

4.13 Calculated partial safety factors for concrete for the design punching shear resistance expression. 38

SEZNAM SLIK

3.1 Diagram poteka procedure probabilistične kalibracije, uporabljene v tej magistrski nalogi. 11

4.1 Razmerje med eksperimentalnimi in modelnimi vrednostmi strižne odpornosti za pogoj $a_{cs} \geq 4d$; neprekinjena črta prikazuje idealno modelno napoved; krožne oznake prikazujo posamezne vrednosti iz nabora eksperimentov. 14

4.2 Razmerje med eksperimentalnimi in modelnimi vrednostmi strižne odpornosti za pogoj $a_{cs} < 4d$; neprekinjena črta prikazuje idealno modelno napoved; krožne oznake prikazujo posamezne vrednosti iz nabora eksperimentov. 15

4.3 Faktorji občutljivosti α^2, ki ustrezajo pogoju $a_{cs} \geq 4d$ enačbe strižne odpornosti za obtežno kombinacijo sneg-veter in projektne vrednosti višine prereza d: a) 150 mm, (b) 520 mm, (c) 890 mm. 23

4.4 Faktorji občutljivosti α^2, ki ustrezajo pogoju $a_{cs} \geq 4d$ enačbe strižne odpornosti za obtežno kombinacijo sneg-veter in projektne vrednosti višine prereza d: (a) 1260 mm, (b) 1630 mm, (c) 2000 mm. 24

4.5 Indeksi zanesljivosti β kot funkcija obtežnega faktorja χ_1 pri $d = 150$ mm za pogoj $a_{cs} \geq 4d$ enačbe strižne odpornosti; stolpci prikazujejo obtežne kombinacije, vrstice prikazujejo različne vrednosti koeficienta natezne armature; barve prikazujejo vrednosti obtežnega faktorja χ_2, velikost oznake na grafu prikazuje vrednost uteži; horizontalna polna črta prikazuje ciljni indeks zanesljivosti (4.7). 25

4.6 Indeksi zanesljivosti β kot funkcija obtežnega faktorja χ_1 pri $d = 2000$ mm za pogoj $a_{cs} \geq 4d$ enačbe strižne odpornosti; stolpci prikazujejo obtežne kombinacije, vrstice prikazujejo različne vrednosti koeficienta natezne armature; barve prikazujejo vrednosti obtežnega faktorja χ_2, velikost oznake na grafu prikazuje vrednost uteži; horizontalna polna črta prikazuje ciljni indeks zanesljivosti (4.7). 26

4.7 Faktorji občutljivosti α^2, ki ustrezajo pogoju $a_{cs} < 4d$ enačbe strižne odpornosti za obtežno kombinacijo sneg-veter in projektne vrednosti višine prereza d: (a) 150 mm, (b) 520 mm, (c) 890 mm. 27

4.8 Faktorji občutljivosti α^2, ki ustrezajo pogoju $a_{cs} < 4d$ enačbe strižne odpornosti za obtežno kombinacijo sneg-veter in projektne vrednosti višine prereza d: (a) 1260 mm, (b) 1630 mm, (c) 2000 mm. 28

4.9 Indeksi zanesljivosti β kot funkcija obtežnega faktorja χ_1 pri $d = 150$ mm za pogoj $a_{cs} \geq 4d$ enačbe strižne odpornosti; stolpci prikazujejo obtežne kombinacije, vrstice prikazujejo različne vrednosti koeficienta natezne armature; barve prikazujejo vrednosti obtežnega faktorja χ_2, velikost oznake na grafu prikazuje vrednost uteži; horizontalna polna črta prikazuje ciljni indeks zanesljivosti (4.7). 29

4.10 Indeksi zanesljivosti β kot funkcija obtežnega faktorja χ_1 pri $d = 2000$ mm za pogoj $a_{cs} \geq 4d$ enačbe strižne odpornosti; stolpci prikazujejo obtežne kombinacije, vrstice prikazujejo različne vrednosti koeficienta natezne armature; barve prikazujejo vrednosti obtežnega faktorja χ_2, velikost oznake na grafu prikazuje vrednost uteži; horizontalna polna črta prikazuje ciljni indeks zanesljivosti (4.7). 30

4.11 Razmerje med eksperimentalnimi in modelnimi vrednostmi odpornosti proti preboju za pogoj $a_p \leq 8d_v$; neprekinjena črta prikazuje idealno modelno napoved; krožne oznake prikazujo posamezne vrednosti iz nabora eksperimentov. 34

4.12 Razmerje med eksperimentalnimi in modelnimi vrednostmi odpornosti proti preboju za pogoj $a_p > 8d_v$; neprekinjena črta prikazuje idealno modelno napoved; krožne oznake prikazujo posamezne vrednosti iz nabora eksperimentov. 35

4.13 Faktorji občutljivosti α^2, ki ustrezajo pogoju $a_p \leq 8d_v$ enačbe odpornosti proti preboju za obtežno kombinacijo sneg-veter in projektne vrednosti višine prereza d: (a) 150 mm, (b) 300 mm, (c) 400 mm, (d) 500 mm. 39

4.14 Indeksi zanesljivosti β kot funkcija obtežnega faktorja χ_1 pri $d = 150$ mm za pogoj $a_p \leq 8d_v$ enačbe odpornosti proti preboju; stolpci prikazujejo obtežne kombinacije, vrstice prikazujejo različne vrednosti koeficienta natezne armature; barve prikazujejo vrednosti obtežnega faktorja χ_2, velikost oznake na grafu prikazuje vrednost uteži; horizontalna polna črta prikazuje ciljni indeks zanesljivosti (4.7). 40

4.15 Indeksi zanesljivosti β kot funkcija obtežnega faktorja χ_1 pri $d = 500$ mm za pogoj $a_p \leq 8d_v$ enačbe odpornosti proti preboju; stolpci prikazujejo obtežne kombinacije, vrstice prikazujejo različne vrednosti koeficienta natezne armature; barve prikazujejo vrednosti obtežnega faktorja χ_2, velikost oznake na grafu prikazuje vrednost uteži; horizontalna polna črta prikazuje ciljni indeks zanesljivosti (4.7). 41

4.16 Faktorji občutljivosti α^2, ki ustrezajo pogoju $a_p > 8d_v$ enačbe odpornosti proti preboju za obtežno kombinacijo sneg-veter in projektne vrednosti višine prereza d: (a) 150 mm, (b) 300 mm, (c) 400 mm, (d) 500 mm. 42

4.17 Indeksi zanesljivosti β kot funkcija obtežnega faktorja χ_1 pri $d = 150$ mm za pogoj $a_p > 8d_v$ enačbe odpornosti proti preboju; stolpci prikazujejo obtežne kombinacije, vrstice prikazujejo različne vrednosti koeficienta natezne armature; barve prikazujejo vrednosti obtežnega faktorja χ_2, velikost oznake na grafu prikazuje vrednost uteži; horizontalna polna črta prikazuje ciljni indeks zanesljivosti (4.7). 43

4.18 Indeksi zanesljivosti β kot funkcija obtežnega faktorja χ_1 pri $d = 500$ mm za pogoj $a_p > 8d_v$ enačbe odpornosti proti preboju; stolpci prikazujejo obtežne kombinacije, vrstice prikazujejo različne vrednosti koeficienta natezne armature; barve prikazujejo vrednosti obtežnega faktorja χ_2, velikost oznake na grafu prikazuje vrednost uteži; horizontalna polna črta prikazuje ciljni indeks zanesljivosti (4.7). 44

B.1 Faktorji občutljivosti α^2, ki ustrezajo pogoju $a_{cs} \geq 4d$ enačbe strižne odpornosti za obtežno kombinacijo sneg-koristna obtežba in projektne vrednosti višine prereza d: (a) 150 mm, (b) 520 mm, (c) 890 mm. 1

B.2 Faktorji občutljivosti α^2, ki ustrezajo pogoju $a_{cs} \geq 4d$ enačbe strižne odpornosti za obtežno kombinacijo sneg-koristna obtežba in projektne vrednosti višine prereza d: (a) 1260 mm, (b) 1630 mm, (c) 2000 mm. 2

B.3 Faktorji občutljivosti α^2, ki ustrezajo pogoju $a_{cs} \geq 4d$ enačbe strižne odpornosti za obtežno kombinacijo veter-koristna obtežba in projektne vrednosti višine prereza d: (a) 150 mm, (b) 520 mm, (c) 890 mm. 3

B.4 Faktorji občutljivosti α^2, ki ustrezajo pogoju $a_{cs} \geq 4d$ enačbe strižne odpornosti za obtežno kombinacijo veter-koristna obtežba in projektne vrednosti višine prereza d: (a) 1260 mm, (b) 1630 mm, (c) 2000 mm. 4

B.5 Indeksi zanesljivosti β kot funkcija obtežnega faktorja χ_1 pri $d = 520$ mm za pogoj $a_{cs} \geq 4d$ enačbe strižne odpornosti; stolpci prikazujejo obtežne kombinacije, vrstice prikazujejo različne vrednosti koeficienta natezne armature; barve prikazujejo vrednosti obtežnega faktorja χ_2, velikost oznake na grafu prikazuje vrednost uteži; horizontalna polna črta prikazuje ciljni indeks zanesljivosti (4.7). 5

B.6 Indeksi zanesljivosti β kot funkcija obtežnega faktorja χ_1 pri $d = 890$ mm za pogoj $a_{cs} \geq 4d$ enačbe strižne odpornosti; stolpci prikazujejo obtežne kombinacije, vrstice prikazujejo različne vrednosti koeficienta natezne armature; barve prikazujejo vrednosti obtežnega faktorja χ_2, velikost oznake na grafu prikazuje vrednost uteži; horizontalna polna črta prikazuje ciljni indeks zanesljivosti (4.7). 6

B.7 Indeksi zanesljivosti β kot funkcija obtežnega faktorja χ_1 pri $d = 1260$ mm za pogoj $a_{cs} \geq 4d$ enačbe strižne odpornosti; stolpci prikazujejo obtežne kombinacije, vrstice prikazujejo različne vrednosti koeficienta natezne armature; barve prikazujejo vrednosti obtežnega faktorja χ_2, velikost oznake na grafu prikazuje vrednost uteži; horizontalna polna črta prikazuje ciljni indeks zanesljivosti (4.7). 7

B.8 Indeksi zanesljivosti β kot funkcija obtežnega faktorja χ_1 pri $d = 1630$ mm za pogoj $a_{cs} \geq 4d$ enačbe strižne odpornosti; stolpci prikazujejo obtežne kombinacije, vrstice prikazujejo različne vrednosti koeficienta natezne armature; barve prikazujejo vrednosti obtežnega faktorja χ_2, velikost oznake na grafu prikazuje vrednost uteži; horizontalna polna črta prikazuje ciljni indeks zanesljivosti (4.7). 8

B.9 Faktorji občutljivosti α^2, ki ustrezajo pogoju $a_{cs} < 4d$ enačbe strižne odpornosti za obtežno kombinacijo sneg-koristna obtežba in projektne vrednosti višine prereza d: (a) 150 mm, (b) 520 mm, (c) 890 mm. 9

B.10 Faktorji občutljivosti α^2, ki ustrezajo pogoju $a_{cs} < 4d$ enačbe strižne odpornosti za obtežno kombinacijo sneg-koristna obtežba in projektne vrednosti višine prereza d: (a) 1260 mm, (b) 1630 mm, (c) 2000 mm. 10

B.11 Faktorji občutljivosti α^2, ki ustrezajo pogoju $a_{cs} < 4d$ enačbe strižne odpornosti za obtežno kombinacijo veter-koristna obtežba in projektne vrednosti višine prereza d: (a) 150 mm, (b) 520 mm, (c) 890 mm. 11

B.12 Faktorji občutljivosti α^2, ki ustrezajo pogoju $a_{cs} < 4d$ enačbe strižne odpornosti za obtežno kombinacijo veter-koristna obtežba in projektne vrednosti višine prereza d: (a) 1260 mm, (b) 1630 mm, (c) 2000 mm. 12

B.13 Indeksi zanesljivosti β kot funkcija obtežnega faktorja χ_1 pri $d = 520$ mm za pogoj $a_{cs} < 4d$ enačbe strižne odpornosti; stolpci prikazujejo obtežne kombinacije, vrstice prikazujejo različne vrednosti koeficienta natezne armature; barve prikazujejo vrednosti obtežnega faktorja χ_2, velikost oznake na grafu prikazuje vrednost uteži; horizontalna polna črta prikazuje ciljni indeks zanesljivosti (4.7). 13

B.14 Indeksi zanesljivosti β kot funkcija obtežnega faktorja χ_1 pri $d = 890$ mm za pogoj $a_{cs} < 4d$ enačbe strižne odpornosti; stolpci prikazujejo obtežne kombinacije, vrstice prikazujejo različne vrednosti koeficienta natezne armature; barve prikazujejo vrednosti obtežnega faktorja χ_2, velikost oznake na grafu prikazuje vrednost uteži; horizontalna polna črta prikazuje ciljni indeks zanesljivosti (4.7). 14

B.15 Indeksi zanesljivosti β kot funkcija obtežnega faktorja χ_1 pri $d = 1260$ mm za pogoj $a_{cs} < 4d$ enačbe strižne odpornosti; stolpci prikazujejo obtežne kombinacije, vrstice prikazujejo različne vrednosti koeficienta natezne armature; barve prikazujejo vrednosti obtežnega faktorja χ_2, velikost oznake na grafu prikazuje vrednost uteži; horizontalna polna črta prikazuje ciljni indeks zanesljivosti (4.7). 15

B.16 Indeksi zanesljivosti β kot funkcija obtežnega faktorja χ_1 pri $d = 1630$ mm za pogoj $a_{cs} < 4d$ enačbe strižne odpornosti; stolpci prikazujejo obtežne kombinacije, vrstice prikazujejo različne vrednosti koeficienta natezne armature; barve prikazujejo vrednosti obtežnega faktorja χ_2, velikost oznake na grafu prikazuje vrednost uteži; horizontalna polna črta prikazuje ciljni indeks zanesljivosti (4.7). 16

B.17 Faktorji občutljivosti α^2, ki ustrezajo pogoju $a_p \leq 8d_v$ enačbe odpornosti proti preboju za obtežno kombinacijo sneg-koristna obtežba in projektne vrednosti višine prereza d: (a) 150 mm, (b) 300 mm, (c) 400 mm, (d) 500 mm. 17

B.18 Faktorji občutljivosti α^2, ki ustrezajo pogoju $a_p \leq 8d_v$ enačbe odpornosti proti preboju za obtežno kombinacijo veter-koristna obtežba in projektne vrednosti višine prereza d: (a) 150 mm, (b) 300 mm, (c) 400 mm, (d) 500 mm. 18

B.19 Indeksi zanesljivosti β kot funkcija obtežnega faktorja χ_1 pri $d = 300$ mm za pogoj $a_p \leq 8d_v$ enačbe odpornosti proti preboju; stolpci prikazujejo obtežne kombinacije, vrstice prikazujejo različne vrednosti koeficienta natezne armature; barve prikazujejo vrednosti obtežnega faktorja χ_2, velikost oznake na grafu prikazuje vrednost uteži; horizontalna polna črta prikazuje ciljni indeks zanesljivosti (4.7). 19

B.20 Indeksi zanesljivosti β kot funkcija obtežnega faktorja χ_1 pri $d = 400$ mm za pogoj $a_p \leq 8d_v$ enačbe odpornosti proti preboju; stolpci prikazujejo obtežne kombinacije, vrstice prikazujejo različne vrednosti koeficienta natezne armature; barve prikazujejo vrednosti obtežnega faktorja χ_2, velikost oznake na grafu prikazuje vrednost uteži; horizontalna polna črta prikazuje ciljni indeks zanesljivosti (4.7). 20

B.21 Faktorji občutljivosti α^2, ki ustrezajo pogoju $a_p > 8d_v$ enačbe odpornosti proti preboju za obtežno kombinacijo sneg-koristna obtežba in projektne vrednosti višine prereza d: (a) 150 mm, (b) 300 mm, (c) 400 mm, (d) 500 mm. 21

B.22 Faktorji občutljivosti α^2, ki ustrezajo pogoju $a_p > 8d_v$ enačbe odpornosti proti preboju za obtežno kombinacijo veter-koristna obtežba in projektne vrednosti višine prereza d: (a) 150 mm, (b) 300 mm, (c) 400 mm, (d) 500 mm. 22

B.23 Indeksi zanesljivosti β kot funkcija obtežnega faktorja χ_1 pri $d = 300$ mm za pogoj $a_p > 8d_v$ enačbe odpornosti proti preboju; stolpci prikazujejo obtežne kombinacije, vrstice prikazujejo različne vrednosti koeficienta natezne armature; barve prikazujejo vrednosti obtežnega faktorja χ_2, velikost oznake na grafu prikazuje vrednost uteži; horizontalna polna črta prikazuje ciljni indeks zanesljivosti (4.7). 23

B.24 Indeksi zanesljivosti β kot funkcija obtežnega faktorja χ_1 pri $d = 400$ mm za pogoj $a_p > 8d_v$ enačbe odpornosti proti preboju; stolpci prikazujejo obtežne kombinacije, vrstice prikazujejo različne vrednosti koeficienta natezne armature; barve prikazujejo vrednosti obtežnega faktorja χ_2, velikost oznake na grafu prikazuje vrednost uteži; horizontalna polna črta prikazuje ciljni indeks zanesljivosti (4.7). 24

SEZNAM TABEL

3.1 Vrednosti uteži, uporabljenih v kalibracijah. 9

3.2 Število generiranih projektnih scenarijev za kalibracijo enačb mejnih stanj. 10

4.1 Primerava ocenjenih parametrov za zajem modelne negotovosti v primerjavi s trenutnimi vrednostmi za enačbo mejnega stanja strižne odpornosti armiranobetonskih elementov. 13

4.2 Diskretne vrednosti parametrov projektnih scenarijev, ki so bili uporabljeni za kalibracijo enačbe strižne odpornosti. 16

4.3 Parametri porazdelitev slučajnih spremenljivk modela strižne odpornosti. 17

4.4 Parametri porazdelitev slučajnih spremenljivk za model stalne obtežbe, ki je bil uporabljen za kalibracijo enačbe strižne odpornosti. 17

4.5 Parametri porazdelitev slučajnih spremenljivk za model koristne obtežbe, ki je bil uporabljen za kalibracijo enačbe strižne odpornosti. 18

4.6 Parametri porazdelitev slučajnih spremenljivk za model prometne obtežbe, ki je bil uporabljen za kalibracijo enačbe strižne odpornosti. 19

4.7 Parametri porazdelitev slučajnih spremenljivk za model snežne obtežbe, ki je bil uporabljen za kalibracijo enačbe strižne odpornosti. 20

4.8 Parametri porazdelitev slučajnih spremenljivk za model vetrovne obtežbe, ki je bil uporabljen za kalibracijo enačbe strižne odpornosti. 21

4.9 Izračunani varnostni faktorji za beton za enačbo mejnega stanja strižne odpornosti. . . 22

4.10 Primerava ocenjenih parametrov za zajem modelne negotovosti v primerjavi s trenutnimi vrednostmi za enačbo mejnega stanja odpornosti proti preboju armiranobetonskih elementov. 34

4.11 Vrednosti parametrov projektnih scenarijev, uporabljenih za kalibracijo enačbe odpornosti proti preboju. 36

4.12 Parametri porazdelitev slučajnih spremenljivk modela odpornosti proti preboju. 37

4.13 Izračunani varnostni faktorji za beton za enačbo mejnega stanja odpornosti proti preboju. 38

1 INTRODUCTION

1.1 Motivation

Structural design codes provide engineers with a set of standardized instructions that helps with their day-to-day work. A common basis for design in modern design codes is the verification of limit states which follows the main principle as to ensure an adequate level of safety, such that the failure probability is lower than a specified target failure probability.

The Eurocodes are a set of harmonized standards that specify the rules for structural design in the European Union and beyond. The requirements for minimum structural safety are specified in EN 1990:2002 (Eurocode 0). EN 1990:2002 enables the designers to assess the reliability of a structural member with either probabilistic or semi-probabilistic approaches. Regarding the semi-probabilistic approach, EN 1990:2002 adopts the partial safety factor method.

Ideally, the partial factors should be chosen on the basis of probabilistic calibrations, which consider a wide range of design scenarios and the uncertainties of design parameters. In reality, however, the currently available partial factors in Eurocodes were chosen mainly based on expert judgment and past experiences. This leads to unbalanced design codes with a large scatter of reliability levels when using the same partial factors for different design scenarios and resistance formulas [1]. The exact reliability level is consequently unknown.

The described deficiencies provide a motivation for performing probabilistic calibrations that produce partial safety factors tailored to the resistance formulas. In this way, it is possible to ensure the reliability levels of structural members to be as close as possible to the predefined target levels in a wide range of design situations.

1.2 Problem statement

The rules for designing concrete structures according to the Eurocode are given in EN 1992-1 [2]. During the time period of preparing this thesis, a major revision of this code is under preparation. Among others, a new one-way shear and punching shear expressions based on different theoretical background have been proposed. The two expressions are semi-empirical and thus need to be calibrated with experimental data. Additionally, as both expressions are elementary design expressions that will be widely applied in design of concrete structures, the Eurocode committee is seeking to have a reliability-based calibration of the partial safety factors for both expressions, in addition to the semi-probabilistic calibration based on the EN 1990:2002 Annex D. Therefore, the main research question of this thesis is:

What are the partial safety factors for concrete for the one-way shear and the design punching shear expression in EN 1992-1:2018 D4 obtained by performing a reliability-based code calibration?

Before answering that question we attempted to summarize the probabilistic code calibration procedure that we used by asking the following question:

What are the key steps that we need to take to use the implemented reliability-based calibration procedure on a specific structural design code?

1.3 Approach

In the process of preparing this thesis, we reviewed relevant structural reliability literature. This included the study of proposals for performing design code calibration from a reliability-based perspective, such as those by Ellingwood [3], Thoft-Christensen and Baker [4] and Sørensen [5]. Different implementations of reliability-based code calibrations were also studied, for example those by Nowak and Szerzsen [6], and Nadolski et al. [7]. In this study a MATLAB implementation of reliability-based code calibration mainly based on the proposal of Ellingwood [3] and developed by researchers at TNO and TU Delft is used. The functionality of this implementation was studied and summarized in key steps. The implementation considers the model uncertainty of the resistance design formula as an additional random variable. Consequently, a pre-existing method of inferring parameters of the resistance model uncertainty based on experimental databases was introduced. The databases included parameters and exhibited resistances of relevant experimental test specimens. The implementation of the reliability-based calibration procedure was then demonstrated on the proposed design one-way shear resistance without shear reinforcement and design punching shear without shear reinforcement expression, where the partial safety factors for concrete were calculated.

1.4 Scope and limitations

In this thesis the probabilistic calibration procedure is used to determine the partial safety factors for concrete for only two design expressions in Eurocode 2. With small modifications the procedure could be used for design provisions of different material in the Eurocodes as well. This procedure focuses on the determination of the partial safety factor for the resistance model, therefore, the partial safety factors for loads are fixed and not considered. Additionally, the weights that are used for the calibration currently signify only the importance of particular load levels, while the prevalence of any particular structural design, the class of the structure, as well as the importance of any particular load combination on the calibration are not considered.

1.5 Outline of the thesis

This thesis is divided into six chapters. In Chapter 1, an introduction is presented along with the motivation and the goals of the thesis. Relevant literature regarding reliability-based code calibrations is reviewed in Chapter 2. In Chapter 3, the proposed implementation of the reliability-based calibration procedure is presented and summarized in key steps. Chapter 4 presents two examples of the implemented calibration approach: the partial safety factors for concrete of two design expressions from EN

1992-1:2018 Draft 4 are calculated. In Chapter 5 the results are discussed. Finally, in Chapter 6 conclusions, recommendations, and an outlook are given.

2 LITERATURE REVIEW

2.1 Code calibration approaches

Semi-probabilistic design codes use partial safety factors for the verification of limit states and consequently define the level of reliability. They can be selected based on [7]: expert judgment, non-probabilistic calibration to established design practices, statistical measures for determining design values, probabilistic methods, which use reliability as the objective for calibration, and cost optimization methods [8].

One of the first papers on developing design codes by using methods of structural reliability for deriving partial safety factors has been put forward by Lind in 1972 [9]. Even earlier in 1959, Brinch Hansen [10] applied the principles of partial safety factor approach in code formulation, which was developed in Denmark in 1950s. One of the first guidelines for performing probabilistic code calibrations was the technical report by Ellingwood et al. [3] in 1980. They proposed a procedure for determining the partial factors for loads and materials on the basis of estimating the level of reliability of ACI, AISC and NASI design standards that were in use in the United States at the time. Since then, several authors have outlined similar approaches to calibrating design codes process for different design formats: Ditlevsen and Madsen [11], Melchers [12], and others.

Most of the subsequent work on optimization of existing structural design codes consequently followed Ellingwood's example. Foster et al. [13] applied a similar principle of code calibration on the Australian standard AS3600, dealing with design expressions for reinforced concrete beams, slabs, and columns to provide updated partial factors. They drew attention to the point that design codes should be frequently updated since improvements in production quality of materials over time can lead to overdesign. Nowak and Szerzsen [6] analyzed the American standard ACI 318-99, which also deals with reinforced concrete structures. Specifically, they calibrated material partial factors for design expressions for eccentrically loaded columns, slabs, and foundation beams. Partial factors for loads and their probabilistic models were not assessed in this study.

2.2 The Eurocodes

Several authors have shown that the partial safety factors that are currently in use are not calibrated. Kohler et al. [1] examined present semi-probabilistic design codes, specifically Eurocodes, where they focused on calibrating the partial safety factors for loads. By assessing the reliability level of design expressions in the Eurocodes they observed a high scatter of the reliability level when considering the same material, while the average yearly reliability level was in most cases lower than the prescribed target level. Nadolski et al. [7] studied design expression for steel structures in EN 1991-3:2004. They also made the distinction of separating partial factors for variable action effects (wind, imposed, and snow load). Similarly to Kohler [1], they noticed that current partial factors result in a lower reliability level than the target, attributing this to hidden safety, i.e. a model bias due to an implicit introduction of

the uncertainties of material parameters.

EN 1990:2002 gives a simplified reliability-based approach for calibrating partial safety factors. However, the resulting partial safety factor are in many cases under- or over-conservative. Studies show that the reliability levels obtained on the basis of this method are in some cases much larger than the target one [14], or much smaller [15].

2.3 Concluding remarks

Most of the reviewed literature takes a narrow look at calibrating design codes from a reliability-based perspective; the calibrations are performed on a limited scale, where in most cases either load or material partial safety factors are calculated. In all cases, the calibration protocol follows the procedure, instigated by Ellingwood [3], that requires optimization to a certain target reliability level. The authors studying the Eurocodes found that the partial safety factor method with the current values of the partial factors often leads to unbalanced design provisions.

3 RELIABILITY-BASED CODE CALIBRATION IMPLEMENTATION

3.1 Overview

This chapter describes the adopted approach that is used in this work to perform calibrations of selected design formulas, which are presented in Sections 4.1 and 4.2. The description is based on a MATLAB implementation of a probabilistic code calibration procedure that is jointly developed by researchers at TNO and TU Delft.

In this thesis, the described approach is used for the calibration of existing design formulas in the Eurocodes. More specifically, the result of this calibration approach is the resistance partial factor, which takes into account uncertainty of the resistance model and of the geometric and material variables. We use the definition of the Eurocode for the representative values of the defined random variables wherever possible. The partial safety factors for the loads are not calibrated. They are taken from the Eurocode and are kept unchanged.

In order to perform the calibration the following five main steps are taken:

1. Definition of calculation input;
2. Quantification of model uncertainty;
3. Definition of the limit state function and selection of random variables;
4. Generation of design scenarios;
5. Reliability analysis and optimization of the objective function to obtain the partial factor.

In the following subsection the listed steps are described in a general way. Chapter 4 provides the details for each of the considered design formulas.

3.2 Calibration procedure

The main objective of the calibration procedure is to calculate an optimal partial safety factor for the resistance model that satisfies on average the limit state function for all design scenarios that are intended to be covered by the design formula.

Step 1 – Definition of calculation input

The first step is to define the design resistance formula that needs to be calibrated. The target reliability β_{target}, which is related to the target probability of failure ($P_{\mathrm{f,target}} = \Phi(-\beta_{\mathrm{target}})$) is defined, in addition to the load combinations that are to be considered for the calibration, as well as the weights of prevalence. For the considered calculation we use a target reliability of 4.7, corresponding to a 1-year reference period and RC2 consequence class, as defined in EN 1990:2002 [16].

Step 2 – Quantification of model uncertainty

One of the key parameters in the limit state function is the model uncertainty, which is a result of incomplete knowledge regarding a physical phenomena that is being modelled. It stems from missing variables and/or mismatch in the mathematical model compared to reality [17]. In the case of resistance models of structural members, this usually occurs due to simplified assumptions and boundary conditions, as well as unknown interactions between variables. The model uncertainty is usually defined by θ in the following way [18]:

$$\theta = \frac{R_{\text{exp}}}{R_{\text{mod}}}, \tag{3.1}$$

where:
R_{exp} is the experimentally obtained value of the value of resistance and
R_{mod} is the model prediction of the value of resistance.

In this thesis, the considered design formulas addresses the model uncertainty by means of a multiplicative regression factor $1/C_{\text{c}}$. The model uncertainty is usually assumed to be log-normally distributed, hence:

$$C_{\text{c}} \sim LN(\mu_{ln_{C_{\text{c}}}}, \sigma_{ln_{C_{\text{c}}}}), \tag{3.2}$$

where:
$\mu_{ln_{C_{\text{c}}}}$ and $\sigma_{ln_{C_{\text{c}}}}$ are the mean and standard deviation of the underlying normal distribution.

In this work we estimate model uncertainty of resistance models on the basis of collected sets of experimental results. These contain the parameters and values of the observed resistances for a large number of specimens. By using the parameters of the tests we calculate R_{mod} and evaluate Equation (3.1). Next, the maximum likelihood method is used to estimate the distribution function parameters of C_{c}.

Step 3 – Definition of the limit state function and selection of random variables

The failure probability is approximated on the basis of a linear limit-state function g, which is defined as:

$$g = R - E, \tag{3.3}$$

where:
R is the resistance of the structural member and
E is the load effect on the structural member.

This definition assumes that the resistance and load effect models are separable. The values of R and E depend on their parameters, which can be considered either as deterministic or random variables. In this work, the resistance parameters and loads are treated as random variables. In order to describe the random variable we need to specify their probabilistic distributions and the corresponding distribution parameters. Our choices in this respect are mostly based on literature or on expert judgment. In the Eurocodes the representative values of some parameters are defined with their characteristic values corresponding to certain fractiles, which represent the probability of obtaining a more unfavorable value. Consequently, for such random variables this probability is an input parameter and needs to be specified in order to link the characteristic values to the probabilistic models.

Step 4 – Generation of design scenarios

The design formula is calibrated for a certain domain of application. In this step the ranges of the parameter values in the loads and the resistance formula are specified. Based on these ranges, a discrete set of parameters is defined that sufficiently covers the intended application domain. The calibration includes all possible combinations within this set. A combination is denoted as a design scenario.

The usual approach for designing structural members according to the Eurocode is to first determine the load effect on a structural member and then to calculate the critical cross-section. Afterwards, the resistance variables are varied so that the design requirement $R_\mathrm{d} \geq E_\mathrm{d}$ is satisfied at all cross-sections. In the reliability-based calibration this design approach is not convenient: It can easily happen that the design requirement would lead to unrealistic values of design parameters in certain design scenarios. To filter these unrealistic designs, a manual check would be needed, which is a laborious task. Therefore, an alternative design approach is used in this calibration procedure, which is easy to automate. This approach is based on the principle of inverse design, in which the scenarios are designed to full utilization of the design resistance by modifying the loading side and keeping the resistance-side fixed. The modification of the loads is done at the level of the probabilistic models for the loads, by changing their mean values while still respecting the connection between the representative values and the probabilistic models.

The task in the inverse design is defined as such: for each design scenario i, which includes the level of variable load j, find the characteristic values of the permanent load $G_{\mathrm{k},i}$ and variable load $Q_{j,\mathrm{k},i}$ such that the design condition is fulfilled: $R_{\mathrm{d},j} = E_{\mathrm{d},j}$. The load effect $E_{\mathrm{d},j}$ is calculated for various load types and load ratios $\chi_{j,i}$. The $\chi_{j,i}$-values are defined by:

$$\chi_{j,i} = \frac{Q_{j,k,i}}{Q_{j,k,i} + G_{k,i}}. \tag{3.4}$$

By rewriting Equation (3.4) to show the relationship between variable load and the load ratio, we obtain:

$$Q_{j,k,i} = G_{k,j} \frac{\chi_{i,j}}{1 - \chi_{i,j}}. \tag{3.5}$$

The variable load for each design scenario can be determined by using the corresponding load ratio and the permanent load. By again considering the design requirement, we can observe that the Equation (3.3) is now a function of the fixed resistance parameters, as well as of the permanent load and load ratio. To obtain the value of the characteristic permanent load $G_{k,i}$ for the i-th design scenario, the following problem must be solved:

$$f(G_{k,i}) = R_{d,j} - E_{d,j}(G_{k,i}) = 0. \tag{3.6}$$

With the characteristic values of the permanent and variable loads known, we can establish the relation between the design scenarios and the probabilistic models. This is done by using the specified fractiles belonging to the characteristic values, which are used to obtain the mean values of the loads.

Step 6 – Reliability analysis and optimization of the objective function

The reliability analysis is performed using the FORM (First Order Reliability Method) procedure with which the reliability level is estimated for each design scenario. A brief description of FORM is given in Annex A. The partial safety factor can be seen as a free parameter in the calibration procedure. Its optimal

value is calculated for a given objective function. To solve the optimization problem, an initial value for the partial factor is taken. Based on that value of the partial factor, all considered design scenarios are designed such that they satisfy $R_{\mathrm{d},j} = E_{\mathrm{d},j}$. Next, for each of the design scenarios a reliability analysis is performed and the reliability index β_i is obtained. The objective function is then evaluated and the process is repeated until the optimum criteria is satisfied. In this thesis we use a symmetric objective function as defined in ISO 2394:2015:

$$O(\gamma) = \sum_{i=1}^{n} w_i \cdot \left(\beta_{\mathrm{target}} - \beta_i(\gamma)\right)^2, \tag{3.7}$$

where:
γ is the vector (in our case a scalar) of free parameters (partial factors) to be calculated, n is the number of design scenarios, w_i is the weight of prevalence for i-th design scenario. The used weights of prevalence are the same for all considered load combinations. They are based on expert judgment and on the study by Ellingwood [3]. They do not incorporate structural characteristics or the prevalence of certain designs over others. Rather, they represent our judgment regarding the possibility of having certain values of load ratios applied to structures in engineering practice. For example, the value of the weight function when $\chi = 0.1$ is zero, meaning that we believe that the chance of having a structure with a load effect composed of 90 % static load and 10 % live load is very low. Similarly, the chance of having a structure which carries 90 % of live load and only 10 % of static load is also very low.

Table 3.1: Values of weights of prevalence used in the presented calibrations.

Preglednica 3.1: Vrednosti uteži, uporabljenih v kalibracijah.

Load ratio χ	0.1	0.2	0.3	0.4	0.5	0.6	0.7	0.8	0.9
Weight w [%]	0	8	28	31	23	8	2	0	0

3.3 Software engineering

The workflow of the implemented probabilistic code calibration procedure is shown in Figure 3.1. In Table 3.2 we show the number of used design scenarios in each of the calibrations, which were performed on a computer with the following specifications: Intel Xeon(R) E5-2620 v3 @ 2.40 GHz CPU, 128 GB RAM, Windows 10 65-bit OS. We can see that there is a needed for a considerable computation effort due to the large scale of the problem and due to the fact that we evaluate the objective function in parallel for several values of the trial partial safety factors.

Table 3.2: Number of design scenarios that were used in the calibration of the considerd design formulas.

Preglednica 3.2: Število generiranih projektnih scenarijev za kalibracijo enačb mejnih stanj.

Design formula	Subset	Number of design scenarios	Computation time [hours] *
One-way shear	$a_{cs} < 4\,d_v$	18144	13
	$a_{cs} \geq 4\,d_v$	18144	13
Punching shear	$a_p \leq 8\,d_v$	36288	25
	$a_p > 8\,d_v$	36288	25

* Rough estimation of the computational run time.

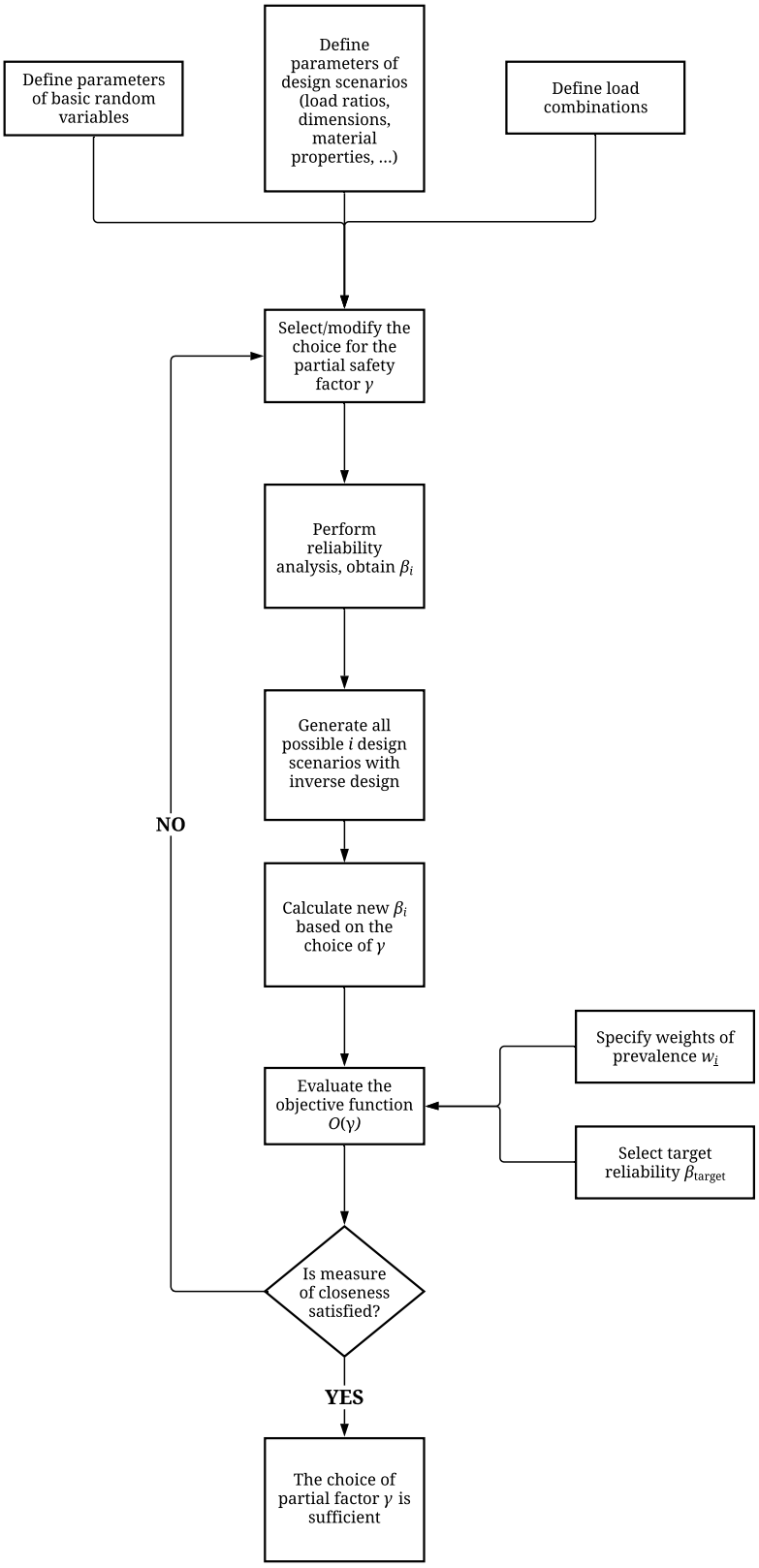

Figure 3.1: Flowchart of the probabilistic calibration procedure that was used in this thesis.

Slika 3.1: Diagram poteka procedure probabilistične kalibracije, uporabljene v tej magistrski nalogi.

4 DEMONSTRATION OF THE PROPOSED CALIBRATION APPROACH ON THE REVISED EUROCODE 2 DESIGN EQUATIONS

4.1 One-way shear resistance of reinforced concrete members without shear reinforcement

The design value of the one-way shear resistance for members not requiring shear reinforcement proposed by by EN 1992-1:2018 Draft 4 in [MPa] is:

$$\tau_{\mathrm{Rd,c}} = \frac{0.66}{\gamma_{\mathrm{C}}} \left(100\,\rho_{\mathrm{l}}\, f_{\mathrm{ck}}\, \frac{d_{\mathrm{dg}}}{d}\right)^{1/3}, \tag{4.1}$$

where:
γ_{C} is the material partial safety factor for concrete; 1.5 in the current proposal,
ρ_{l} is the ratio of longitudinal reinforcement and the cross-section of the member,
f_{ck} is the characteristic compressive strength of concrete in [MPa],
$d_{\mathrm{dg}}$is the critical shear crack roughness in [mm],
d is the effective depth of the structural member in [mm].
In those cases when $a_{\mathrm{cs}} < 4\,d$, the value of d in equation (4.1) may be replaced by a_{v}:

$$a_{\mathrm{v}} = \sqrt{\frac{a_{\mathrm{cs}}}{4}\, d}. \tag{4.2}$$

For members where no axial force is present, the effective shear span a_{cs} may be calculated as:

$$a_{\mathrm{cs}} = \left|\frac{M_{\mathrm{Ed}}}{V_{\mathrm{Ed}}}\right| \geq d, \tag{4.3}$$

where:
M_{Ed} is the design value of the bending moment and
V_{Ed} is the design value of the shear force acting on the member.

4.1.1 Model uncertainty inference

Based on Equation (4.2) we can observe that the design resistance equation may be considered for two cases of assumption on the basis of the effective shear span a_{cs}. We quantified the model uncertainty of the resistance based on the database of experiments compiled from literature [19], where the authors studied shear resistance of reinforced concrete beams without shear reinforcement. The databases thus contain the measured shear resistances and the design parameters for each of the test subjects. We separated the test results into two subsets based on the effective shear span according to Equation (4.3). For each subsets, the model uncertainties for the resistance were determined.

We derive the model uncertainty from the assumption that it is a log-normally distributed random variable, defined as a ratio between the experimental and the predicted (model) value of the resistance. This

is in line with the definition in Step 2 of Section 3.2. The maximum likelihood method is then used to estimate the parameters of the distribution, namely the mean value and the coefficient of variation.

In Table 4.1 we present some results of the model uncertainty inference. In the table, C_{EC2} denotes the current values of the model uncertainty factor, while C_{R} and CoV_{CR} represent the mean value and the coefficient of variation of the estimated model uncertainty, respectively. Several statistical measures of goodness-of-fit are also presented: MAE represents the mean absolute error, MEDAE is the median absolute error, RMSD the root-mean square deviation and ρ_{c} is the Pearson correlation factor. We can see that the estimated mean values of the resistance model uncertainty is similar to the present value for both subsets. In Figure 4.1 and 4.2 we show the relationship between the theoretical (model) and experimental values of the one-way shear resistance. In Figure 4.1a and Figure 4.2a we can see that for lower values, the experimental and model shear resistance tend to be similar. The increase of the model shear resistance seems to lead to a larger deviation from the experimental value. From Figure 4.1b and Figure 4.2b we can conclude that despite the larger scatter most of data fits the 95% confidence interval. The value of the calculated Pearson coefficients also indicate that the model is a good capture of the experimental results.

Table 4.1: Estimated model uncertainty parameters of the design one-way shear resistance expression in comparison to the present value used for representing resistance model uncertainty.

Preglednica 4.1: Primerava ocenjenih parametrov za zajem modelne negotovosti v primerjavi s trenutnimi vrednostmi za enačbo mejnega stanja strižne odpornosti armiranobetonskih elementov.

Subset	C_{EC2}	C_{R}	CoV_{CR}	MAE	MEDAE	RMSD	ρ_{c}
$a_{\mathrm{cs}} \geq 4d$	0.66	0.72	0.19	14.30	7.22	31.44	0.97
$a_{\mathrm{cs}} < 4d$	0.66	0.74	0.21	14.67	7.90	32.73	0.97

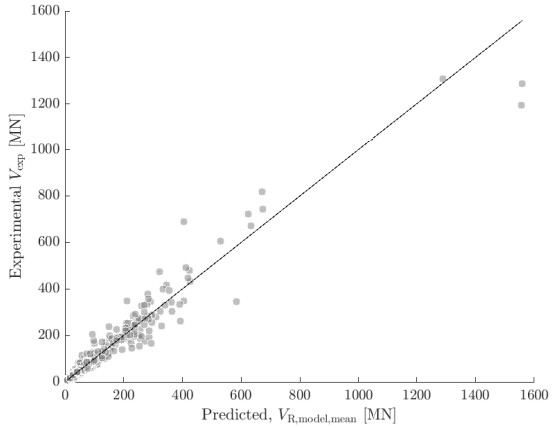

(a) Ratio between experimental and model one-way shear resistance.
Razmerje med eksperimentalno in modelno strižno odpornostjo.

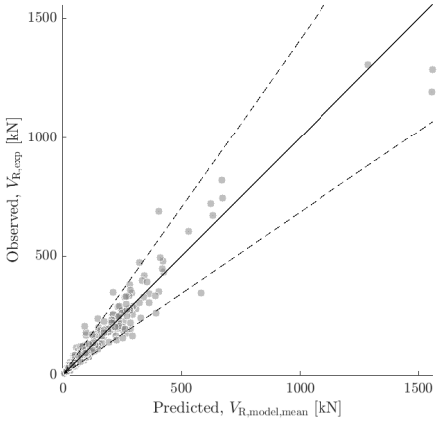

(b) Razmerje med eksperimentalno in napovedano strižno odpornostjo na intervalu 95% zaupanja (označen črtkano).
Ratios between experimental and calibrated model one-way shear resistance values within the 95% confidence interval. The range is denoted with dashed lines.

Figure 4.1: Relationship between experimental and model one-way shear resistance values for subset $a_{\mathrm{cs}} \geq 4\,d$; the solid black line represents perfect model prediction; circles denote individual data points from the experimental database.
Slika 4.1: Razmerje med eksperimentalnimi in modelnimi vrednostmi strižne odpornosti za pogoj $a_{\mathrm{cs}} \geq 4\,d$; neprekinjena črta prikazuje idealno modelno napoved; krožne oznake prikazujo posamezne vrednosti iz nabora eksperimentov.

4.1.2 Definition of design scenarios

We perform a calibration for each subset of the design one-way shear resistance expression. In the calibration of the one-way shear equation we used the same values of the design scenario parameters for both subsets. Design scenarios are constructed by covering all possible combinations of the parameters of the model one-way shear resistance equation. The parameters that are used for design scenarios are presented in Table 4.2. If the parameters are considered as random variables, the values in Table 4.2 represent mean values of their probabilistic models.

Load combination rules for the calibration presented in this thesis are constructed according to Equation 6.10 in section 6.4.3.2 of EN 1990:2002 [16], which stipulates that loads should be combined the following way:

$$E_{\mathrm{d}} = \max \begin{cases} \sum_{j\geq 1} \gamma_{\mathrm{G},j} G_{\mathrm{k},j} \text{"}+\text{"} \gamma_{\mathrm{P}} P \text{"}+\text{"} \gamma_{\mathrm{Q},1}\psi_{\mathrm{Q},1} Q_{\mathrm{k},1} \text{"}+\text{"} \sum_{i>1} \gamma_{\mathrm{Q},,i}\psi_{\mathrm{Q},i} Q_{\mathrm{k},i}, \\ \sum_{j\geq 1} \xi_j \gamma_{\mathrm{G},j} G_{\mathrm{k},j} \text{"}+\text{"} \gamma_{\mathrm{P}} P \text{"}+\text{"} \gamma_{\mathrm{Q},1}\psi_{\mathrm{Q},1} Q_{\mathrm{k},1} \text{"}+\text{"} \sum_{i>1} \gamma_{\mathrm{Q},,i}\psi_{\mathrm{Q},i} Q_{\mathrm{k},i}, \end{cases} \tag{4.4}$$

where:

ξ_j is a reduction factor for unfavorable permanent actions $G_{\mathrm{k},j}$,

$\psi_{\mathrm{Q},1}$ is the load combination factor for the leading variable action Q_1,

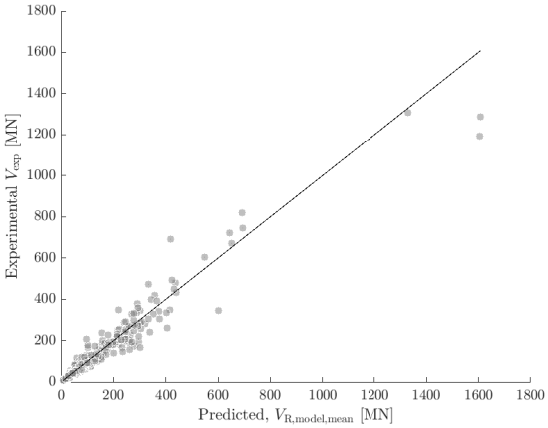

(a) Ratio between experimental and model one-way shear resistance.
Razmerje med eksperimentalno in modelno strižno odpornostjo.

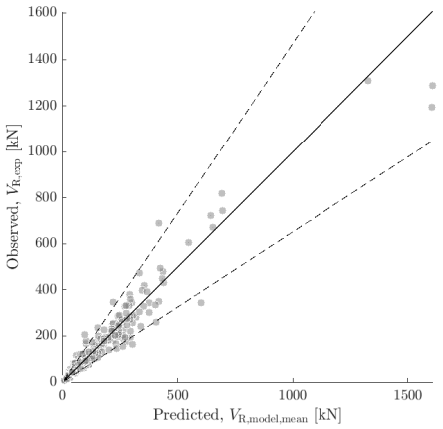

(b) Razmerje med eksperimentalno in napovedano strižno odpornostjo na intervalu 95% zaupanja (označen črtkano).
Ratios between experimental and calibrated model one-way shear resistance values within the 95% confidence interval. The range is denoted with dashed lines.

Figure 4.2: Relationship between experimental and model one-way shear resistance values for subset $a_{\mathrm{cs}} \geq 4\,d$; the solid black line represents perfect model prediction; circles denote individual data points from the experimental database.
Slika 4.2: Razmerje med eksperimentalnimi in modelnimi vrednostmi strižne odpornosti za pogoj $a_{\mathrm{cs}} < 4\,d$; neprekinjena črta prikazuje idealno modelno napoved; krožne oznake prikazujo posamezne vrednosti iz nabora eksperimentov.

$\psi_{\mathrm{Q,i}}$ is the load combination factor for the accompanying variable action $Q_{\mathrm{k},i}$,

γ_{P} is the partial factor for the prestressing action P,

$\gamma_{\mathrm{Q},j}$ is the partial factor for the variable action $Q_{\mathrm{k},j}$.

We performed the calibration based on four load combinations defined in EN 1990 [16], they are named as following: traffic, wind-imposed, snow-imposed, and snow-wind load combination. The first part of the name in the load combination indicates the leading action and the second part of the name the accompanying one. For example: in the case of the snow-wind load combination, the snow load is the leading variable action, while the wind load is the accompanying variable action.

4.1.3 Probabilistic description of resistance and load models for the calibration of one-way shear resistance expression

In this section, we introduce the probabilistic description of the resistance and load models in the calibration of the one-way shear resistance expression. For each model we: specify the parameters that were treated as random variables, list their probabilistic description, and mention the references for the used values. In the designation of distributions *N* represents the normal distribution, *L-N* the log-normal distribution, *GUM* the Gumbel distribution, and *DET* a deterministic variable.

Table 4.2: Design scenario parameters and their discrete values that were used in the calibration of the one-way shear design expression.

Preglednica 4.2: Diskretne vrednosti parametrov projektnih scenarijev, ki so bili uporabljeni za kalibracijo enačbe strižne odpornosti.

Design scenario parameter	Value(s)[1]
d[mm]	150, 520, 890, 1260, 1630, 2000
f_c[MPa]	20, 40, 60, 80
χ_1[−]	0.1, 0.2, 0.3, 0.4, 0.5, 0.6, 0.7, 0.8, 0.9
χ_2[−]	0.1, 0.2, 0.3, 0.4, 0.5, 0.6, 0.7, 0.8, 0.9
ρ_l[−]	0.005, 0.010, 0.015
b[mm]	100
d_{dg}[mm]	16

[1] When design scenario parameters are considered as random variables in the calibration procedure, the values represent the mean values of their probabilistic distributions. Otherwise, they represent fixed values.

Resistance model

The design value of the one-way shear resistance force is based on Equation (4.13):

$$V_{Rd,d} = \frac{0.66}{\gamma_C}\left(100\,\rho_l f_{ck}\frac{d_{dg}}{d}\right)^{1/3} b\,d, \tag{4.5}$$

The probabilistic value can be written as follows:

$$V_{R,c} = \theta_R\left(100\,\rho_l f_c\frac{d_{dg}}{d}\right)^{1/3} b\,d. \tag{4.6}$$

where:
θ_R is the resistance model uncertainty,
$\rho_l = A_{sl}/b\,d$ is the longitudinal reinforcement ratio,
A_{sl} is the longitudinal reinforcement ratio,
f_c is the compressive strength of concrete,
d is the effective depth of the member,
b is the width of the member and
d_{dg} is the shear crack roughness.
The parameters of the resistance model are presented in Table 4.3.

Table 4.3: Probabilistic description of random variables in the one-way shear resistance model.

Preglednica 4.3: Parametri porazdelitev slučajnih spremenljivk modela strižne odpornosti.

Random variable	Description	Dist.	Mean	CoV	P_{char}	Source
θ_{R}	Model uncertainty of the resistance [-]	L-N	0.72[1] 0.74[2]	0.19 0.21	- -	exp. database exp. database
d	Effective beam depth in [mm]	N	d_{mean}[3]	0.10	-	Probabilistic Model Code [20]
f_{c}	Compressive concrete strength in [MPa]	N	$f_{\text{c,mean}}$[3]	0.06	0.05	Probabilistic Model Code [20]
A_{sl}	Longitudinal reinforcement cross-section in [mm^2]	N	$0.01 \cdot b_{\text{mean}} \cdot d_{\text{mean}}$	0.02	-	Probabilistic Model Code [20]
b	Beam width in [mm]	N	100	0.05	-	-

[1] For the calibration of the expression corresponding to $a_{\text{cs}} \geq 4d$.
[2] For the calibration of the expression corresponding to $a_{\text{cs}} < 4d$.
[3] Mean values for these variables are obtained from design scenario parameters.

Loads and load effects

Here we present the loads that were used in the calibration of the one-way shear resistance equation. For each of the loads we show their design expressions that are defined by the characteristic values of their parameters. We further specify the probabilistic models of these parameters, from which the characteristic values are calculated on the basis of the probability of non-exceedance P_{char}.

Permanent load

We include self-weight and permanent loads in the calibration protocol as a single action. The parameters of this action model that we use in the calibration are presented in Table 4.4.

Table 4.4: Parameters of random variables used in the permanent load model for the one-way shear expression.

Preglednica 4.4: Parametri porazdelitev slučajnih spremenljivk za model stalne obtežbe, ki je bil uporabljen za kalibracijo enačbe strižne odpornosti.

Random variable	Description	Dist.	Mean	CoV	P_{char}	Source
G	RC self-weight and imposed permanent load	N	20	0.10	-	fib Bulletin 80 [21]
θ_G	Model uncertainty factor for permanent loads	L-N	1.0	0.05	-	expert knowledge
ξ	Reduction factor for unfavourable permanent loads	DET	0.85	0	-	EN 1990 [16]

Imposed load

The design value of the imposed load is defined as:

$$Q_{\mathrm{I,d}} = \gamma_{\mathrm{Q}}\, q_{\mathrm{equ,k}}\, A, \tag{4.7}$$

where:
γ_{Q} is the partial factor for variable loads presently equal to 1.5,
$q_{\mathrm{equ,k}}$ is the characteristic value of the time-dependent equivalent value of the imposed load,
A is a geometric property, representing the area on which the load is applied.
Probabilistic value of the imposed load can be written as:

$$Q_{\mathrm{I}} = \theta_{\mathrm{Q,I}}\, q_{\mathrm{equ}}\, A, \tag{4.8}$$

where:
$\theta_{\mathrm{Q,I}}$ represents the model uncertainty of the time-dependent part of the imposed load model.
The parameters of these imposed load model parameters are presented in Table 4.5

Table 4.5: Probabilistic description of random variables in the imposed load model for the one-way shear formula.

Preglednica 4.5: Parametri porazdelitev slučajnih spremenljivk za model koristne obtežbe, ki je bil uporabljen za kalibracijo enačbe strižne odpornosti.

Random variable	Description	Dist.	Mean	CoV	P_{char}	Source
$\theta_{\mathrm{Q,I}}$	Model uncertainty factor for time dependent part of imposed loads	L-N	1.0	0.10	-	expert knowledge
q_{equ}	1-year time-dependent equivalent value of the imposed load	GUM	1.0	0.53	0.98	Probabilistic Model Code [22]
ψ_{I}	Load combination factor	DET	0.7	0	-	EN 1990 [16]

Traffic load

The traffic load value is constructed according to the specification in EN 1991-2. The parameters of the traffic load model are shown in Table 4.6.

Table 4.6: Probabilistic description of random variables in the traffic load model for the one-way shear formula.

Preglednica 4.6: Parametri porazdelitev slučajnih spremenljivk za model prometne obtežbe, ki je bil uporabljen za kalibracijo enačbe strižne odpornosti.

Random variable	Description	Dist.	Mean	CoV	P_{char}	Source
$\theta_{\text{Q,T}}$	Model uncertainty factor for the traffic load	L-N	1.0	0.15	-	Slobbe et al. [23]
q_{equ}	Value of the traffic load	GUM	1.0	0.0858	0.99	-
ψ_{T}	Load combination factor	DET	0.8	0	-	EN 1990 [16]

Snow load

The design value of the snow load is determined based on the specifications in EN 1991-3 [24] as:

$$Q_{S,\mathrm{d}} = \gamma_Q \, s_{\mathrm{k,k}} \, C_{\mathrm{e,k}} \, C_{\mathrm{t,k}} \, \mu_{\mathrm{t,k}} \, A, \tag{4.9}$$

where:
γ_{Q} is the partial factor for variable loads presently equal to 1.5,
$s_{\mathrm{k,k}}$ is the characteristic value of the snow load on the ground,
$C_{\mathrm{e,k}}$ is the characteristic value of the exposure coefficient,
$C_{\mathrm{t,k}}$ is the characteristic value of the heat coefficient,
$\mu_{\mathrm{i,k}}$ is the characteristic value of the load shape coefficient,
A is a geometric property, representing the area on which the snow load is applied.

The probabilistic value of the snow load can be written as follows:

$$Q_{\mathrm{S}} = \theta_{\mathrm{Q,S}} \, s_{\mathrm{k}} \, C_{\mathrm{e}} \, C_{\mathrm{t}} \, \mu_{\mathrm{i}} \, A, \tag{4.10}$$

where:
$\theta_{\mathrm{Q,S}}$ represents the time-independent model uncertainty factor of the snow load model.
The parameters of the snow load model are presented in Table 4.7.

Table 4.7: Probabilistic descriptions of random variables in the snow load model for the one-way shear resistance formula.

Preglednica 4.7: Parametri porazdelitev slučajnih spremenljivk za model snežne obtežbe, ki je bil uporabljen za kalibracijo enačbe strižne odpornosti.

Random variable	Description	Dist.	Mean	CoV	P_{char}	Source
$\theta_{\mathrm{Q,S}}$	Time-independent model uncertainty factor	L-N	1.0	0.10	-	expert knowledge
s_{k}	1-year extreme value of the snow load on the ground	GUM	1.0	0.60	0.98	Meinen et al. [15]
C_{e}	Load shape coefficient for a uniform snow load on the whole roof, multiplied with the exposure coefficient	GUM	0.8	0.17	0.50	Ellingwood and O'Rourke [25]
ψ_{S}	Load combination factor	DET	0.7	0	-	EN 1990 [16]

Wind load

The design value of the wind load is constructed based on the specifications in EN 1991-4 [26] as:

$$Q_{\mathrm{W,d}} = \gamma_{\mathrm{Q}} \, q_{\mathrm{ref,k}} \, C_{\mathrm{e,k}} \, C_{\mathrm{p,k}} \, C_{\mathrm{s,k}} \, C_{\mathrm{d,k}} \, A, \tag{4.11}$$

where:
γ_{Q} is the partial safety factor for variable loads presently equal to 1.5,

$q_{\mathrm{ref,k}}$ is the characteristic value of the annual extreme hourly-mean wind pressure at a reference height and reference terrain roughness,
$C_{\mathrm{e,k}}$ is the characteristic value of the exposure factor,
$C_{\mathrm{p,k}}$ is the characteristic value of hourly extreme pressure coefficient,
$C_{\mathrm{s,k}}$ is the characteristic value of the size coefficient,
$C_{\mathrm{d,k}}$ is the characteristic value of the dynamic factor,
A is the area of the loaded element.

The probabilistic value of the wind load can be expressed as follows:

$$Q_{\mathrm{W}} = \theta_{\mathrm{Q,W}}\, q_{\mathrm{ref}}\, C_{\mathrm{e}}\, C_{\mathrm{p}}\, C_{\mathrm{s}}\, C_{\mathrm{d}}\, A, \tag{4.12}$$

where:
$\theta_{\mathrm{Q,W}}$ represents the time-independent model uncertainty of the wind load model.
The parameters of their probabilistic models are presented in Table 4.8.

Table 4.8: Parameters of random variables used in the wind load model for the one-way shear resistance equation calibration.

Preglednica 4.8: Parametri porazdelitev slučajnih spremenljivk za model vetrovne obtežbe, ki je bil uporabljen za kalibracijo enačbe strižne odpornosti.

Random variable	Description	Dist.	Mean	CoV	P_{char}	Source
$\theta_{\mathrm{Q,W}}$	Time-independent model uncertainty factor	L-N	1.0	0.10	-	expert knowledge
q_{ref}	1-year extreme hourly mean wind pressure	GUM	1,0	0.27	0.98	expert knowledge
c_{e}	Exposure factor	L-N	1.0	0.15	0.94	Probabilistic Model Code [22]
c_{p}	Hourly extreme pressure coefficient	GUM	1.0	0.20	0.78	Meinen et al. [15]
c_{s}	Size coefficient	DET	1.0	-	-	-
c_{d}	Dynamic factor	L-N	1.0	0.15	0.50	Probabilistic Model Code [22]
ψ_{W}	Load combination factor	DET	0.6	0	-	EN 1990 [16]

4.1.4 Results

In this section we present the results of the calibration of the design one-way shear equation. The calibrations for the two subsets of the model equation were performed separately, hence the results are presented separately as well. First, we present the calculated partial safety factors in Table 4.9, which were estimated so that the target reliability level is on average met for all considered design scenarios.

In the figures we show two types of results: the squared sensitivity factors α^2 and reliability indices β. The α^2 factors are calculated for each random variable and tell us the influence of that random variable on the β. Below, we show only the calculated α^2 values for the snow-wind load combination in Figures 4.3 and 4.4 for the subset corresponding to $a_{cs} \geq 4d$ and in Figures 4.7 and 4.8 for the subset corresponding to $a_{cs} < 4d$, respectively. The calculated factors for other load combinations are highly similar and are consequently presented in Appendix B.

In Figures 4.6 and B.8 we present selected results of β values for the subset corresponding to $a_{cs} \geq 4d$, while the chosen results of β for the subset $a_{cs} < 4d$ are shown in Figures 4.9 and 4.10. The calculated reliability indices for other combinations of design parameters are similar to the presented and are thus shown in Appendix B.

In the figures we show the relationship between α^2 or β and χ_1, which represents the leading variable load Q_1 of a load combination. In the case of β values, the plot is split into a matrix of sub figures, where the rows corresponds to different values of the reinforcement ratio ρ_l and columns represent different load combinations.

Table 4.9: Calculated partial safety factors for concrete for the design one-way shear resistance expression.

Preglednica 4.9: Izračunani varnostni faktorji za beton za enačbo mejnega stanja strižne odpornosti.

Design expression subset	Calibrated partial factor γ_C
$a_{cs} < 4d$	1.54
$a_{cs} \geq 4d$	1.46

Figures for subset $a_{cs} \geq 4d$

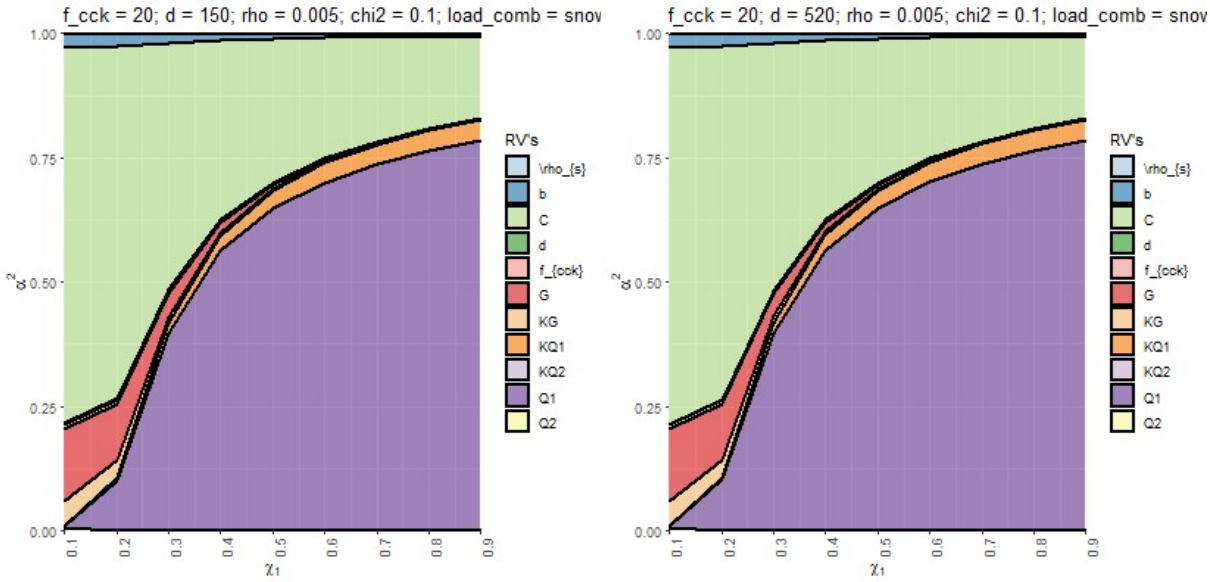

(a) (b)

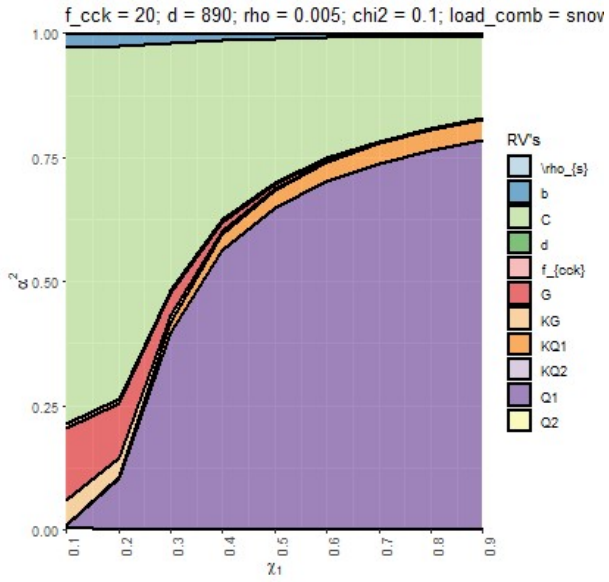

(c)

Figure 4.3: Sensitivity factors α^2 corresponding to subset $a_{cs} \geq 4d$ of the one-way shear resistance equation with the snow-wind load combination and with different effective depth d: a) 150 mm, (b) 520 mm, (c) 890 mm.

Slika 4.3: Faktorji občutljivosti α^2, ki ustrezajo pogoju $a_{cs} \geq 4d$ enačbe strižne odpornosti za obtežno kombinacijo sneg-veter in projektne vrednosti višine prereza d: a) 150 mm, (b) 520 mm, (c) 890 mm.

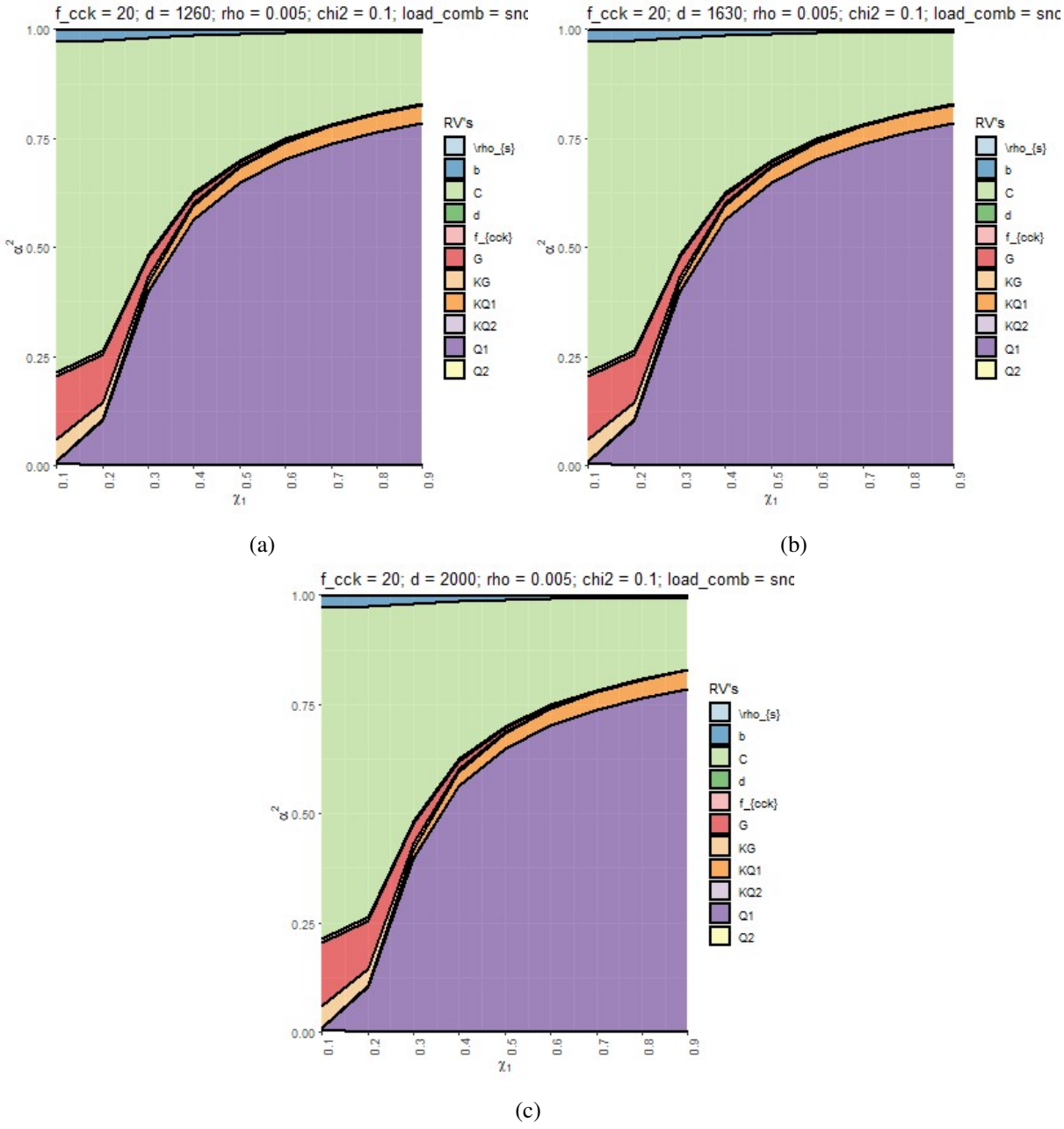

(a) (b)

(c)

Figure 4.4: Sensitivity factors α^2 corresponding to subset $a_{cs} \geq 4d$ of the one-way shear resistance equation with the snow-wind load combination and with different effective depth d: (a) 1260 mm, (b) 1630 mm, (c) 2000 mm.

Slika 4.4: Faktorji občutljivosti α^2, ki ustrezajo pogoju $a_{cs} \geq 4d$ enačbe strižne odpornosti za obtežno kombinacijo sneg-veter in projektne vrednosti višine prereza d: (a) 1260 mm, (b) 1630 mm, (c) 2000 mm.

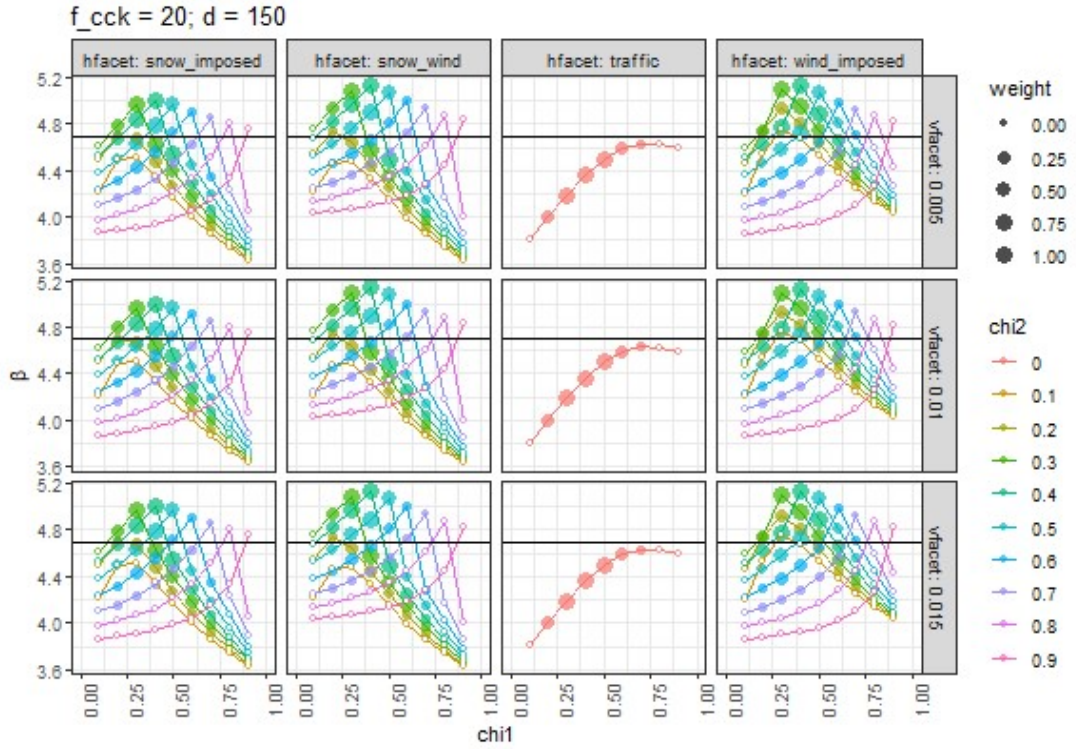

Figure 4.5: Reliability indices β as a function of load ratio χ_1 with $d = 150$ mm for the subset $a_{cs} \geq 4d$ corresponding to the one-way shear resistance formula. Columns present different load combinations, while rows different value of longitudinal reinforcement ratios. Colors represent different values of χ_2 load ratios, while the marker size shows the magnitude of the weight of prevalence. The black horizontal line indicates the target reliability (4.7).

Slika 4.5: Indeksi zanesljivosti β kot funkcija obtežnega faktorja χ_1 pri $d = 150$mm za pogoj $a_{cs} \geq 4d$ enačbe strižne odpornosti; stolpci prikazujejo obtežne kombinacije, vrstice prikazujejo različne vrednosti koeficienta natezne armature; barve prikazujejo vrednosti obtežnega faktorja χ_2, velikost oznake na grafu prikazuje vrednost uteži; horizontalna polna črta prikazuje ciljni indeks zanesljivosti (4.7).

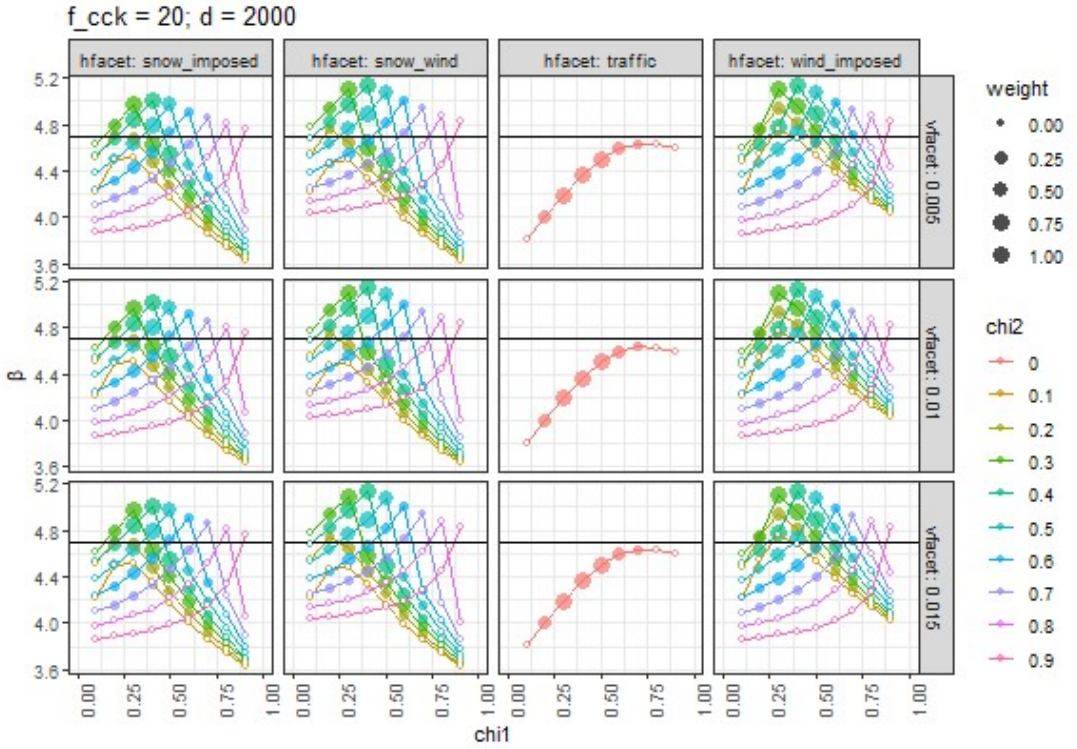

Figure 4.6: Reliability indices β as a function of load ratio χ_1 with $d = 2000$ mm for the subset $a_{cs} \geq 4\,d$ corresponding to the one-way shear resistance formula. Columns present different load combinations, while rows different value of longitudinal reinforcement ratios. Colors represent different values of χ_2 load ratios, while the marker size shows the magnitude of the weight of prevalence. The black horizontal line indicates the target reliability (4.7).

Slika 4.6: Indeksi zanesljivosti β kot funkcija obtežnega faktorja χ_1 pri $d = 2000$ mm za pogoj $a_{cs} \geq 4\,d$ enačbe strižne odpornosti; stolpci prikazujejo obtežne kombinacije, vrstice prikazujejo različne vrednosti koeficienta natezne armature; barve prikazujejo vrednosti obtežnega faktorja χ_2, velikost oznake na grafu prikazuje vrednost uteži; horizontalna polna črta prikazuje ciljni indeks zanesljivosti (4.7).

Figures for subset $a_{cs} < 4d$

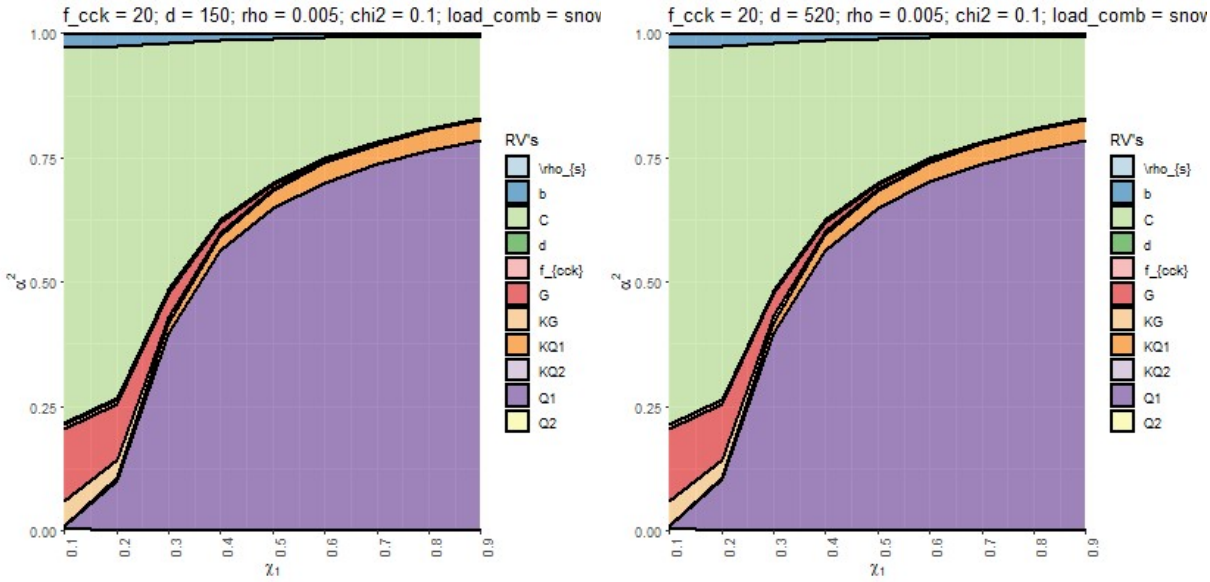

(a) (b)

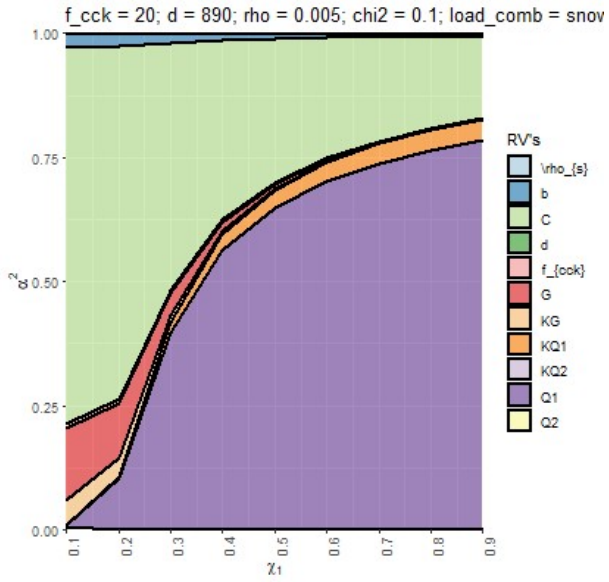

(c)

Figure 4.7: Sensitivity factors α^2 corresponding to subset $a_{cs} < 4d$ of the one-way shear resistance equation with the snow-wind load combination and with different effective depth d: (a) 150 mm, (b) 520 mm, (c) 890 mm.

Slika 4.7: Faktorji občutljivosti α^2, ki ustrezajo pogoju $a_{cs} < 4d$ enačbe strižne odpornosti za obtežno kombinacijo sneg-veter in projektne vrednosti višine prereza d: (a) 150 mm, (b) 520 mm, (c) 890 mm.

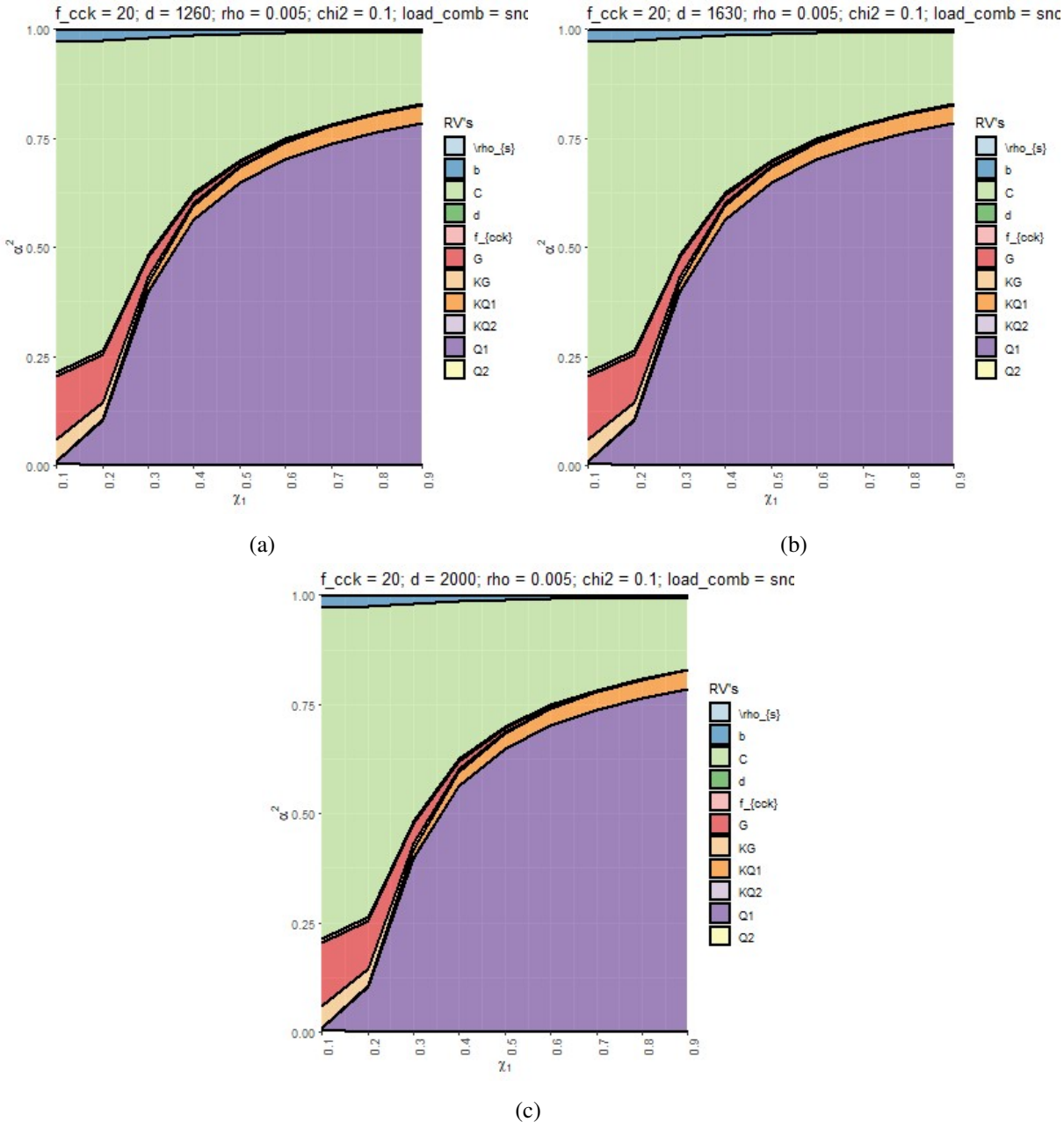

(a) (b)

(c)

Figure 4.8: Sensitivity factors α^2 corresponding to subset $a_{cs} < 4d$ of the one-way shear resistance equation with the snow-wind load combination and with different effective depth d: (a) 1260 mm, (b) 1630 mm, (c) 2000 mm.

Slika 4.8: Faktorji občutljivosti α^2, ki ustrezajo pogoju $a_{cs} < 4d$ enačbe strižne odpornosti za obtežno kombinacijo sneg-veter in projektne vrednosti višine prereza d: (a) 1260 mm, (b) 1630 mm, (c) 2000 mm.

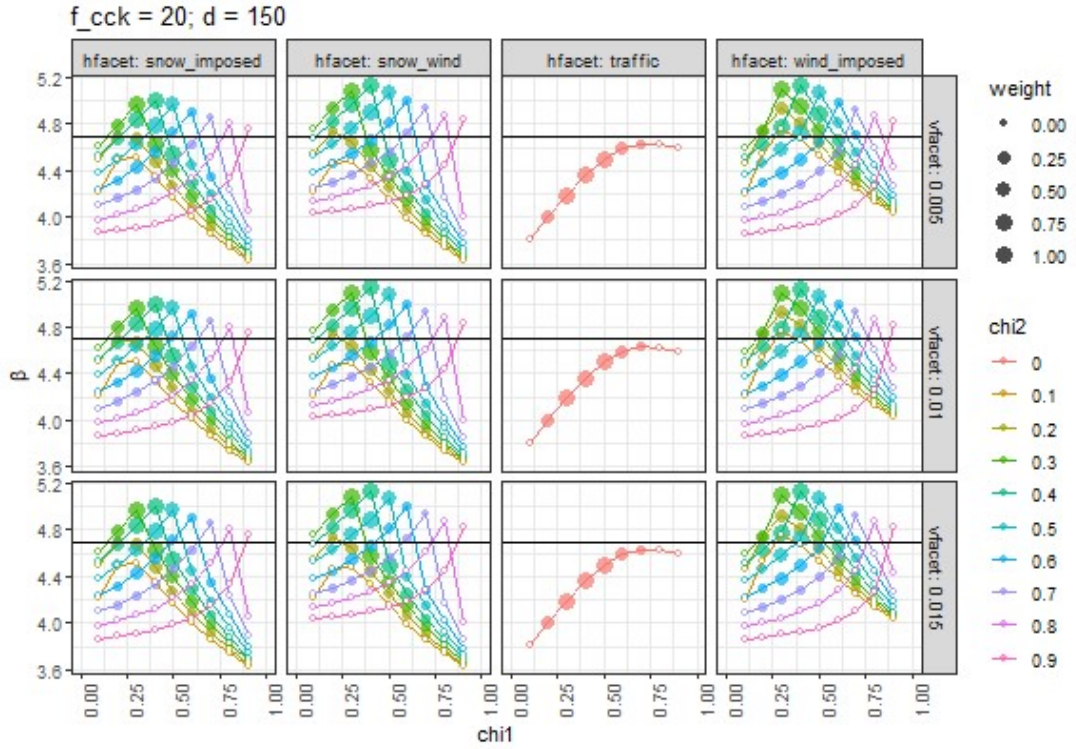

Figure 4.9: Reliability indices β as a function of load ratio χ_1 with $d = 150$ mm for the subset $a_{cs} < 4\,d$ corresponding to the one-way shear resistance formula. Columns present different load combinations, while rows different value of longitudinal reinforcement ratios. Colors represent different values of χ_2 load ratios, while the marker size shows the magnitude of the weight of prevalence. The black horizontal line indicates the target reliability (4.7).

Slika 4.9: Indeksi zanesljivosti β kot funkcija obtežnega faktorja χ_1 pri $d = 150$ mm za pogoj $a_{cs} < 4\,d$ enačbe strižne odpornosti; stolpci prikazujejo obtežne kombinacije, vrstice prikazujejo različne vrednosti koeficienta natezne armature; barve prikazujejo vrednosti obtežnega faktorja χ_2, velikost oznake na grafu prikazuje vrednost uteži; horizontalna polna črta prikazuje ciljni indeks zanesljivosti (4.7).

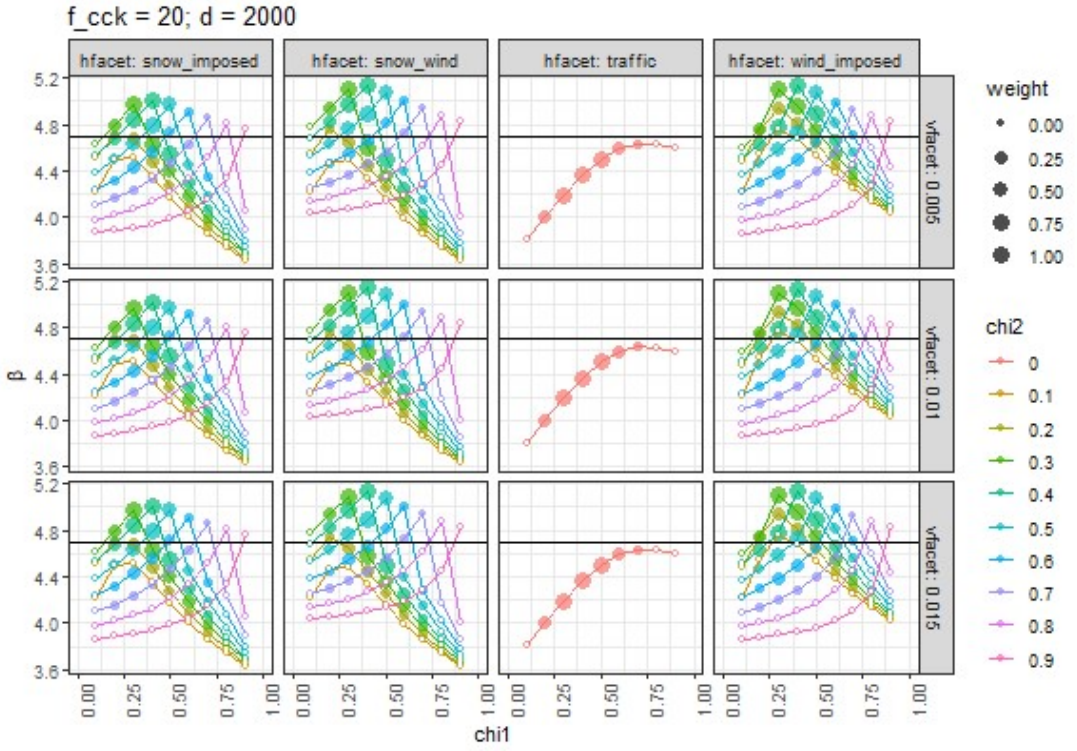

Figure 4.10: Reliability indices β as a function of load ratio χ_1 with $d = 2000$ mm for the subset $a_{cs} < 4\,d$ corresponding to the one-way shear resistance formula. Columns present different load combinations, while rows different value of longitudinal reinforcement ratios. Colors represent different values of χ_2 load ratios, while the marker size shows the magnitude of the weight of prevalence. The black horizontal line indicates the target reliability (4.7).

Slika 4.10: Indeksi zanesljivosti β kot funkcija obtežnega faktorja χ_1 pri $d = 2000$ mm za pogoj $a_{cs} < 4\,d$ enačbe strižne odpornosti; stolpci prikazujejo obtežne kombinacije, vrstice prikazujejo različne vrednosti koeficienta natezne armature; barve prikazujejo vrednosti obtežnega faktorja χ_2, velikost oznake na grafu prikazuje vrednost uteži; horizontalna polna črta prikazuje ciljni indeks zanesljivosti (4.7).

Analysis of the results

The main observations from the results of the calibration of the design one-way shear resistance formula are summarized:

- Based on Table 4.9, we can see that the calibrated partial factors for both considered subsets of the model equation are close to the present value of the partial safety factor for concrete $\gamma_C = 1.5$.
- Sensitivity factors α^2 for the two subsets are highly similar. The same is observable for the reliability indices β – a fact, which is reflected in similar values of the calibrated partial factors for the two subsets. There is almost no observable change in α^2 or β values as different design scenario parameters are used.
- Model uncertainty is the most important among random variables on the resistance side. The calculated α^2 values corresponding to the model uncertainty is between 0.4 and 0.7 for design situations where the permanent load is dominant ($\chi_1 = 0.1 - 0.3$). The influence of resistance-side variables diminishes as variable loads increase. In design scenarios where variable load is dominant ($\chi_1 = 0.7 - 0.9$) the α^2 for the model uncertainty variale is between 0.15 and 0.25. Other resistance-side random variables show considerably small α^2 values compared to the model uncertainty variable.
- The snow-wind, wind-imposed and snow-imposed load combinations show similar β values with values ranging between 3.6 and 5.2. The traffic load combination shows considerably different behavior with values between 3.5 and 4.7. Thus for this load combination the reliability level is lower than β_{target} for almost all design scenarios.

4.2 Punching shear resistance of reinforced concrete members without shear reinforcement

The punching shear resistance expression for slabs without shear reinforcement is given in EN 1992-1:2018 Draft 4 in [MPa] as:

$$\tau_{\mathrm{Rd,c}} = \frac{0.6}{\gamma_{\mathrm{C}}} k_{\mathrm{pb}} \left(100 \rho_{\mathrm{l}} f_{\mathrm{ck}} \frac{d_{\mathrm{dg}}}{a_{\mathrm{pd}}}\right)^{1/3} \leq \frac{0.6}{\gamma_{\mathrm{C}}}, \tag{4.13}$$

where:
γ_{C} is the material partial safety factor for concrete; 1.5 in the current proposal,
k_{pb} is the punching shear gradient, defined as: $k_{\mathrm{pb}} = \sqrt{5\,\mu_{\mathrm{p}} \frac{d_{\mathrm{v}}}{b_0}}$,
μ_{p} is a factor, taking into account the shear force gradient and bending moments in the region of control perimeter,
d_{v} is the effective slab depth in [mm],
b_0 is the control perimeter size in [mm], calculated at a distance $0.5\,d_{\mathrm{v}}$ from the edge of the column,
d_{dg} is the roughness of the critical shear crack in [mm], calculated as:

$$d_{\mathrm{dg}} = d_{\mathrm{g}} + d_{\mathrm{g0}} \min\left\{\left(\frac{60}{f_{\mathrm{ck}}}\right)^2; 1\right\} \leq 40 \text{ mm}, \tag{4.14}$$

where:
$d_{\mathrm{g0}} = 16$ mm and d_{g} is the maximum aggregate size,
f_{ck} is the characteristic compressive strength of concrete in [MPa].

According to EN 1992-1:2018 Draft 4, when: $a_{\mathrm{p}} \leq 8\,d_{\mathrm{v}}$, we can replace a_{pd} in equation (4.13) with: $a_{\mathrm{pd}} = \sqrt{a_{\mathrm{p}}/8 \cdot d_{\mathrm{v}}}$, where a_{p} is calculated using the following formula: $a_{\mathrm{p}} = \sqrt{a_{\mathrm{p,x}} \cdot a_{\mathrm{p,y}}} \geq d_{\mathrm{v}}$ and $a_{\mathrm{p,x}}$ and $a_{\mathrm{p,y}}$ are the distances from the centre of the control perimeter to the point of zero bending moment in each slab direction. Hence, $a_{\mathrm{p,x}}$ and $a_{\mathrm{p,y}}$ outline the location of hogging moments zone in the slab around the internal column.

The calculation of a_{p} can be contentious since:

- the size of the hogging moments zone depends on several factors, such as loads, boundary conditions, as well as slab and column geometries,
- the redistribution of stresses due to cracking of the slab appears to change the size of the hogging moment zone when it is statically indeterminate.

In this thesis, depending on the expected boundary conditions of the member, we used two different means of calculating a_{p}:

1. While evaluating the resistance model uncertainty using lab test data, we use the formula $a_{\mathrm{p}} = 0.5\,L$ proposed by Muttoni [27], with L being the slab depth. Because in most lab tests, the slabs were simply supported.
2. In the calibration procedure, we used the following formula, as proposed in the revised Eurocode

2, because the expression is typically applied to continuous slabs:

$$a_{\mathrm{p,x}} = 0.22 L_{\mathrm{x}}, \tag{4.15}$$

$$a_{\mathrm{p,y}} = 0.22 L_{\mathrm{y}}, \tag{4.16}$$

$$a_{\mathrm{p}} = \sqrt{a_{\mathrm{p,x}} \cdot a_{\mathrm{p,y}}}. \tag{4.17}$$

This equation is limited by the geometry of the slab, specifically by the ratio of the slab side lengths $L_{\mathrm{x}}/L_{\mathrm{y}}$: $0.5 \leq L_{\mathrm{x}}/L_{\mathrm{y}} \leq 2$. This difference in consideration of a_{p} was driven by the desire to derive the parameters of the resistance equation consistently according to Eurocode 2. This choice was also motivated by the judgment that a_{p} will not have a large influence on the design punching shear resistance. Consequently, for determining the range of a_{p} we use the slab length L.

In the calibration phase we narrow the scope of the design resistance equation on slabs with internal columns and without nearby openings. The eccentricity of the resultant shear force acting on the slab can thus be neglected and a shear gradient factor value μ_{p} can be adopted according to Draft 4 of EC2. Furthermore, the design punching shear resistance expression can be split into two subset equations and rewritten in the following form:

$$V_{\mathrm{Rd,c}} = \begin{cases} \dfrac{24.91}{\gamma_{\mathrm{C}}} d_{\mathrm{v}}^{4/3} b_0^{1/2} \rho_1^{1/3} f_{\mathrm{ck}}^{1/3} d_{\mathrm{dg}}^{1/3} a_{\mathrm{p}}^{1/6} & a_{\mathrm{p}} \leq 8 d_{\mathrm{v}}\,, \quad (4.18) \\ \dfrac{17.61}{\gamma_{\mathrm{C}}} d_{\mathrm{v}}^{4/3} b_0^{1/2} \rho_1^{1/3} f_{\mathrm{ck}}^{1/3} d_{\mathrm{dg}}^{1/3} & a_{\mathrm{p}} > 8 d_{\mathrm{v}}. \quad (4.19) \end{cases}$$

We can observe that Equation (4.18) is the general version which takes into account the effect of the slab slenderness explicitly, while Equation (4.19) is a simplified version of Equation (4.18), which gives a conservative estimation of the punching shear capacity without having to consider the slab slenderness explicitly.

4.2.1 Model uncertainty inference

We used a database of 121 experimental test to quantify the resistance model uncertainty. This is the identical database to the one used by Muttoni [28], which is a joint effort of researchers from EPFL and RWTH Aachen. The database was subdivided based on a_{p}, resulting in 82 tests that were used for evaluating by Equation (4.18) and 39 tests were used for evaluating Equation (4.19). Seven specimens were removed due to a high longitudinal reinforcement ratio that exceeded the perceived range of applicability.

Model uncertainty was derived based on the concepts, described in Step 2 of Section 3.2. We assumed that the model uncertainty is a log-normal distributed random variable defined as a ratio between the experimentally obtained and the model predicted punching shear resistance values. The parameters of this distribution were then obtained using the maximum likelihood method. In Table 4.10 we present the the evaluated parameters model uncertainty random variable. In the table, C_{EC2} denotes the theoretical values of the model uncertainty factor for each of the subset equations, while C_{R} and CoV_{CR} represent the mean value and the coefficient of variation of the model uncertainty random variable. We also calculated several statistical measures of goodness-of-fit: MAE represents the mean absolute error, MEDAE is the median absolute error, RMSD is the root-mean square deviation and ρ_{c} is the Pearson correlation factor. In Figure 4.11 and 4.12 we present the results of the resistance model uncertainty for model

Table 4.10: Estimated model uncertainty parameters of the design punching shear resistance expression in comparison to the present value used for representing resistance model uncertainty.

Preglednica 4.10: Primerava ocenjenih parametrov za zajem modelne negotovosti v primerjavi s trenutnimi vrednostmi za enačbo mejnega stanja odpornosti proti preboju armiranobetonskih elementov.

Subset	C_{EC2}	C_R	CoV_{CR}	MAE	MEDAE	RMSD	ρ_c
$a_p \leq 8\,d_v$	24.91	24.42	0.18	0.128	0.091	0.184	0.94
$a_p > 8\,d_v$	17.61	17.34	0.14	0.043	0.047	0.051	0.94

Equations (4.18) and (4.19), respectively. We can observe that the model predictions of the punching shear resistance closely approximate the experimental test results for the lower value and that the results mostly fit the interval range corresponding to a 95 % confidence level. We can observe that the evaluation

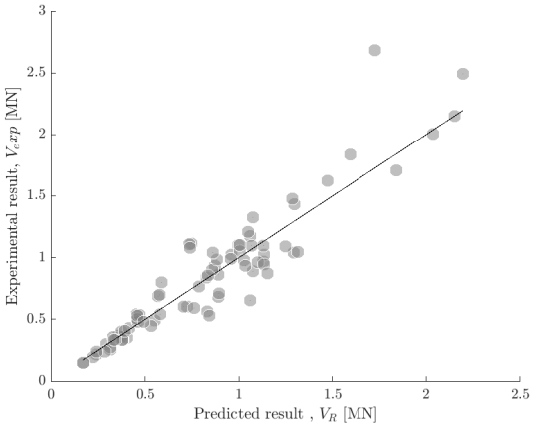

(a) Ratio between experimental and calibrated model one-way shear resistance.
Razmerje med eksperimentalno in modelno strižno odpornostjo.

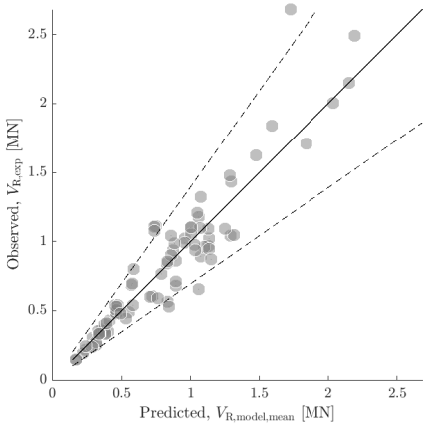

(b) Razmerje med eksperimentalno in napovedano odpornostjo proti preboju na intervalu 95% zaupanja (označen črtkano).
Ratios between experimental and calibrated model punching shear resistance values within the 95% confidence interval. The range is denoted with dashed lines.

Figure 4.11: Relationship between experimental and model punching shear resistance values for subset $a_p \leq 8\,d_v$; the solid black line represents perfect model prediction; circles denote individual data points from the experimental database.
Slika 4.11: Razmerje med eksperimentalnimi in modelnimi vrednostmi odpornosti proti preboju za pogoj $a_p \leq 8\,d_v$; neprekinjena črta prikazuje idealno modelno napoved; krožne oznake prikazujo posamezne vrednosti iz nabora eksperimentov.

of the model uncertainty seems to yield a mean value, which is represented as a regression factor, similar in comparison with the presently established value. This holds for both subsets of the model punching shear resistance equation.

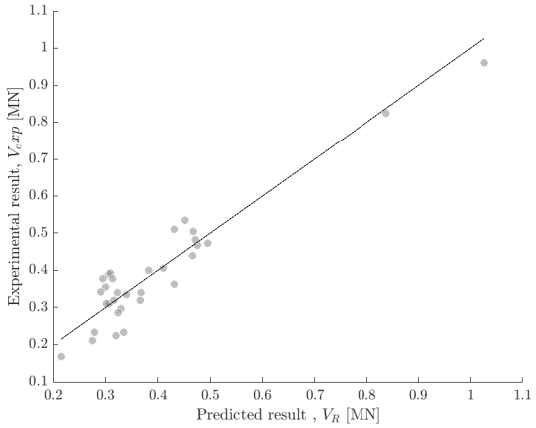

(a) Ratio between experimental and calibrated model one-way shear resistance.
Razmerje med eksperimentalno in modelno strižno odpornostjo.

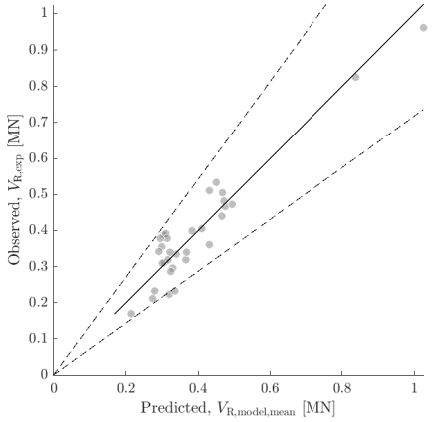

(b) Razmerje med eksperimentalno in napovedano odpornostjo proti preboju na intervalu 95% zaupanja (označen črtkano).
Ratios between experimental and calibrated model punching shear resistance values within the 95% confidence interval. The range is denoted with dashed lines.

Figure 4.12: Relationship between experimental and model punching shear resistance values for subset $a_\mathrm{p} > 8\,d_\mathrm{v}$; the solid black line represents perfect model prediction; circles denote individual data points from the experimental database.
Slika 4.12: Razmerje med eksperimentalnimi in modelnimi vrednostmi odpornosti proti preboju za pogoj $a_\mathrm{p} > 8\,d_\mathrm{v}$; neprekinjena črta prikazuje idealno modelno napoved; krožne oznake prikazujo posamezne vrednosti iz nabora eksperimentov.

4.2.2 Definition of design scenarios

While setting up design scenarios, the following parameters are varied: effective slab depth d_v, compressive strength of concrete f_c, longitudal reinforcement ratio ρ_l, load ratios χ_1 and χ_2 representing variable loads Q_1 and Q_2, slab span L, and column size (either side length or diameter) c. Load combinations are set up according to EN 1990:2002 and are presented in Equation (4.4). We include L and c as design scenario parameters in the calibration procedure, because they are the design parameters that can be directly applied in design practice. They are used to provide an indication of the range of the parameter. In the actual calibration procedure, we considered a_p and b_0 directly as deterministic variables and calculate them from L and c as:

$$a_\mathrm{p} = 0.22\,L, \tag{4.20}$$

$$b_0 = \frac{c}{2} + 2\pi c. \tag{4.21}$$

As described, we treat the resistance expression in two subset formulas, for which we perform calibrations separately. Due to different applicability of the subset formulas for different ranges of a_p the design scenarios differ. They are presented in Table 4.11. For the parameters that are considered as random variables the discrete values in Table 4.11 represent their mean values.

Table 4.11: Design scenario parameters and their discrete values that were used in the calibration of the punching shear design expression.

Preglednica 4.11: Vrednosti parametrov projektnih scenarijev, uporabljenih za kalibracijo enačbe odpornosti proti preboju.

Design scenario parameter	Value(s)[1]
d_v [mm]	150, 300, 400, 500
f_c [MPa]	30, 60, 80
χ_1 [-]	0.1, 0.2, 0.3, 0.4, 0.5, 0.6, 0.7, 0.8, 0.9
χ_2 [-]	0.1, 0.2, 0.3, 0.4, 0.5, 0.6, 0.7, 0.8, 0.9
ρ_l [-]	0.0025, 0.005, 0.0075
L [mm]	4000, 7000[2] 7000, 9000[3]
c [mm]	200, 350
d_{dg} [mm]	16

[1] When design scenario parameters are considered as random variables in the calibration procedure, the values represent the mean values of their probabilistic distributions. Otherwise, they represent fixed values.
[2] For the calibration of subset Equation (4.18).
[3] For the calibration of subset Equation (4.19).

4.2.3 Probabilistic description of resistance and load models for the calibration of punching shear resistance expression

In this section, we introduce the probabilistic description of the resistance and load models in the calibration of the punching shear resistance expression. For each of the models, we: specify the parameters that were treated as random variables, list the parameters of their probabilistic models, and mention the sources for the values. In the designation of distributions *N* represents the normal distribution, *L-N* the log-normal distribution, *GUM* the Gumbel distribution, and *DET* a deterministic variable.

Resistance model

The design punching shear stress resistance formula, defined in Equation (4.13) can be seen as a general formula for the design punching shear stress resistance. By applying the model assumptions described in Section 4.2, we obtain the formula for the design punching shear resistance force, which is defined for two subsets of a_p in Equations (4.18) and (4.19). The probabilistic models of these design equations can be stated as follows:

$$V_{Rd,c} = \begin{cases} \theta_R \, d_v^{4/3} \, b_0^{1/2} \, \rho_l^{1/3} \, f_c^{1/3} \, d_{dg}^{1/3} \, a_p^{1/6}, & a_p \leq 8\, d_v \,, \quad (4.22) \\ \theta_R \, d_v^{5/6} \, b_0^{1/2} \, \rho_l^{1/3} \, f_c^{1/3} \, d_{dg}^{1/3} & a_p > 8\, d_v. \quad (4.23) \end{cases}$$

The parameters of the resistance model are shown Table 4.12.

Table 4.12: Probabilistic description of random variables in the punching shear resistance model.

Preglednica 4.12: Parametri porazdelitev slučajnih spremenljivk modela odpornosti proti preboju.

Random variable	Description	Dist.	Mean	CoV	P_{char}	Source
θ_R	Model uncertainty of the resistance [-]	L-N	24.42[1]	0.18	-	exp. database
			19.74[2]	0.21	-	exp. database
d_v	Effective slab depth in [mm]	N	$d_{v,mean}$[3]	0.10	-	Probabilistic Model Code [20]
f_c	Compressive concrete strength in [MPa]	N	$f_{c,mean}$[3]	0.06	0,05	Probabilistic Model Code [20]
A_{sl}	Longitudal reinf. area in [mm^2]	N	$0.01 \cdot b \cdot d_{mean}$	0.02	-	Probabilistic Model Code [20]
b	Slab width in [mm]	DET	1000	-	-	-

[1] For the calibration of subset Equation (4.18).
[2] For the calibration of subset Equation (4.19).
[3] Mean values for these variables are obtained from design scenario parameters.

Loads and load effects

The load models that are used in the calibration of the design punching shear equation are the same as the models used for the calibration of the design one-way shear formula. In Table 4.4 the parameter of the permanent load model are presented. Table 4.5 shows the parameters of the imposed load model, Table 4.6 shows the parameters for the traffic load model, Table 4.7 presents the parameters of the snow load model, and Table 4.8 the parameters for the wind load model.

4.2.4 Results

In this section we present the results of the calibration of the design punching shear equation. We present the results of the calibrations separately for the two subsets of the model equation. We present the partial safety factors for concrete in Table 4.13. These partial factors were estimated so that the target reliability level is on average met for all considered design scenarios.

In the figures we show two types of results: the squared sensitivity factors α^2 and reliability indices β. The α^2 are calculated for each random variable and tell us the influence of that random variable on the β. Similarily to the results of the calibration for the one-way shear resistance formula, we observed that the calculated values are almost identical for all of the load combinations. Consequently, we present only the results of the snow-wind load combination. These are shown in Figure 4.13 for the subset corresponding to $a_\mathrm{p} \leq 8\,d_\mathrm{v}$ and in Figure 4.16 for the subset corresponding to $a_\mathrm{p} > 8\,d_\mathrm{v}$. The calculated α^2 values are for other load combinations are shown in Appendix B. The calculated β values for the selected combinations of the design parameters are shown in Figure 4.14 and 4.15 for the subset $a_\mathrm{p} \leq 8\,d_\mathrm{v}$, and in Figures 4.17 and 4.18 for the subset $a_\mathrm{p} > 8\,d_\mathrm{v}$. Again, we observed that the β values for other combinatios of design parameters are highly similar. They are thus shown in Annex B.

In the figures we show the relationship between α^2 or β and χ_1, which represents the leading variable load Q_1 of a load combination. In the case of β values, the plot is split into a matrix of sub figures, where the rows corresponds to different values of the reinforcement ratio ρ_l and columns represent different load combinations.

Table 4.13: Calculated partial safety factors for concrete for the design punching shear resistance expression.

Preglednica 4.13: Izračunani varnostni faktorji za beton za enačbo mejnega stanja odpornosti proti preboju.

Design expression subset	Calibrated partial factor γ_C
$a_\mathrm{p} \leq 8\,d_\mathrm{v}$	1.61
$a_\mathrm{p} > 8\,d_\mathrm{v}$	1.45

Figures corresponding to subset $a_p \leq 8\,d_v$

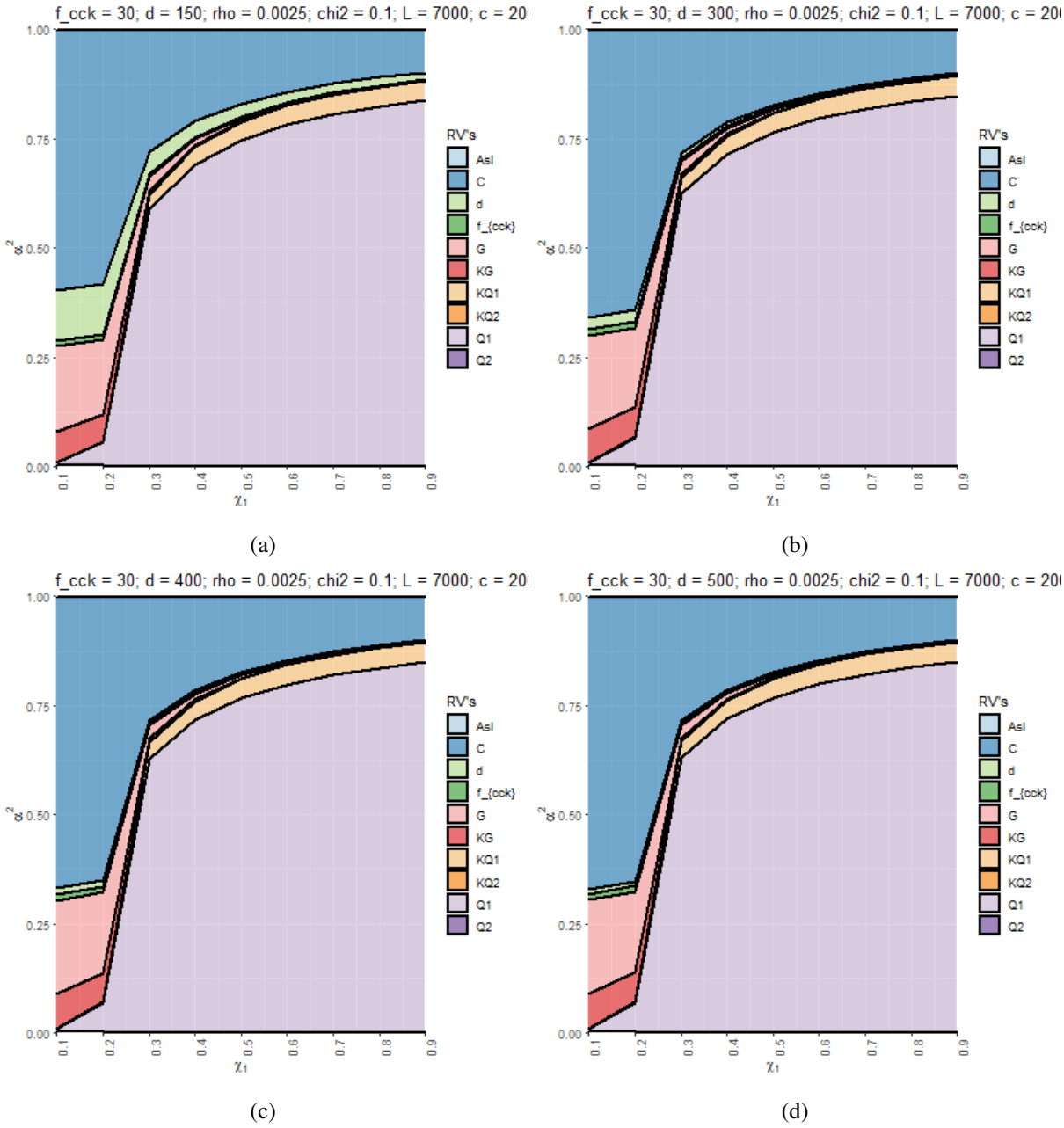

Figure 4.13: Sensitivity factors α^2 corresponding to subset $a_p \leq 8\,d_v$ of the punching shear resistance equation with the snow-wind load combination and with different effective depth d: (a) 150 mm, (b) 300 mm, (c) 400 mm, (d) 500 mm.

Slika 4.13: Faktorji občutljivosti α^2, ki ustrezajo pogoju $a_p \leq 8\,d_v$ enačbe odpornosti proti preboju za obtežno kombinacijo sneg-veter in projektne vrednosti višine prereza d: (a) 150 mm, (b) 300 mm, (c) 400 mm, (d) 500 mm.

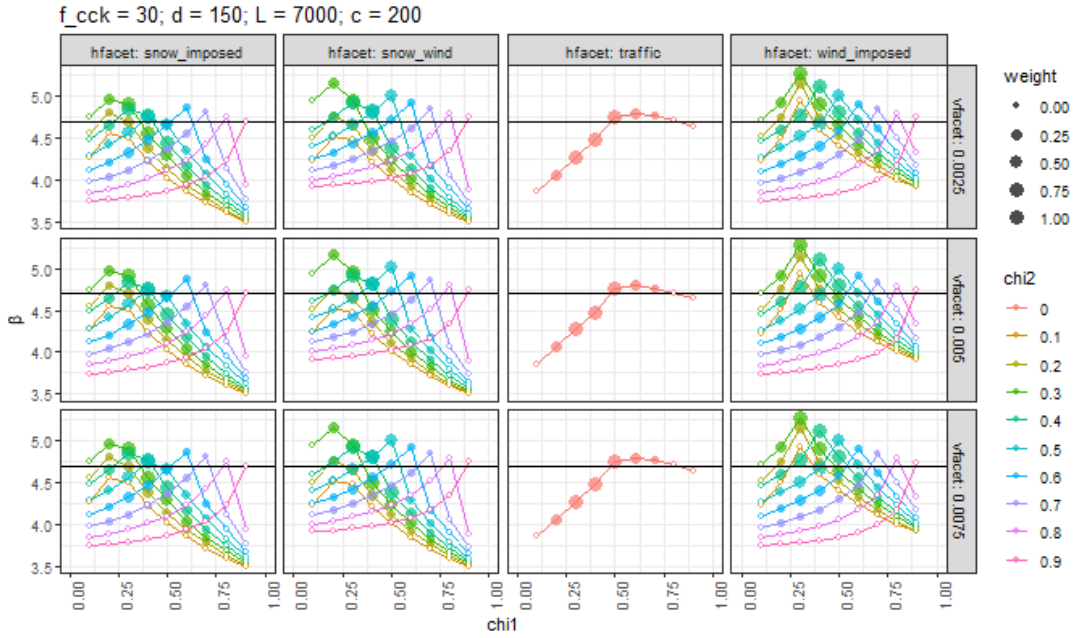

Figure 4.14: Reliability indices β as a function of load ratio χ_1 with $d = 150$ mm for the subset $a_p \leq 8\,d_v$ corresponding to the punching shear resistance formula. Columns present different load combinations, while rows different value of longitudinal reinforcement ratios. Colors represent different values of χ_2 load ratios, while the marker size shows the magnitude of the weight of prevalence. The black horizontal line indicates the target reliability (4.7).

Slika 4.14: Indeksi zanesljivosti β kot funkcija obtežnega faktorja χ_1 pri $d = 150$ mm za pogoj $a_p \leq 8\,d_v$ enačbe odpornosti proti preboju; stolpci prikazujejo obtežne kombinacije, vrstice prikazujejo različne vrednosti koeficienta natezne armature; barve prikazujejo vrednosti obtežnega faktorja χ_2, velikost oznake na grafu prikazuje vrednost uteži; horizontalna polna črta prikazuje ciljni indeks zanesljivosti (4.7).

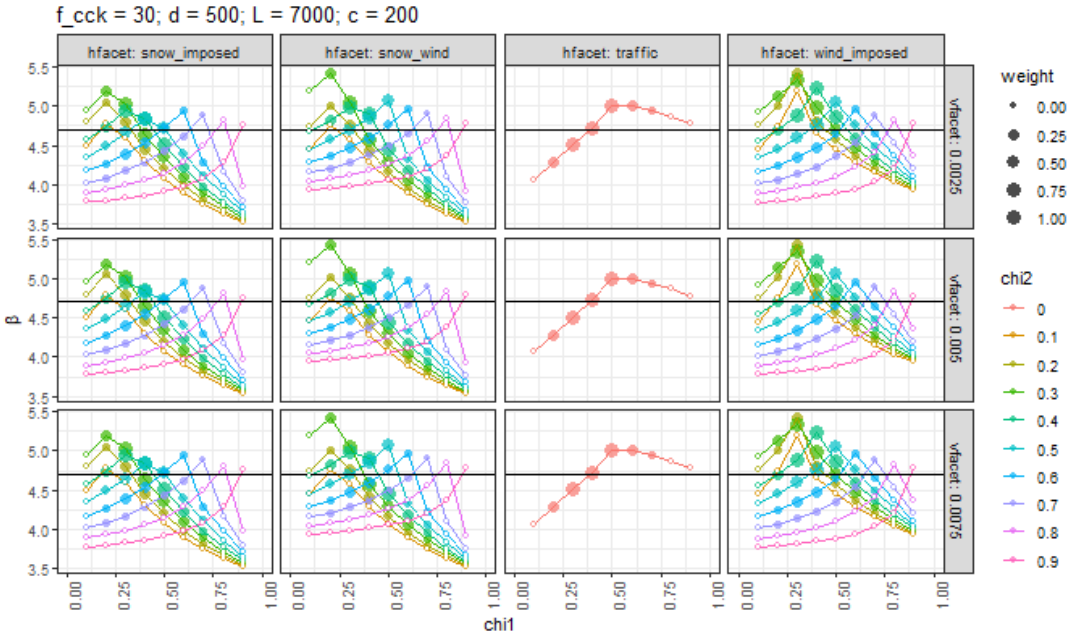

Figure 4.15: Reliability indices β as a function of load ratio χ_1 with $d = 500$ mm for the subset $a_p \leq 8\,d_v$ corresponding to the punching shear resistance formula. Columns present different load combinations, while rows different value of longitudinal reinforcement ratios. Colors represent different values of χ_2 load ratios, while the marker size shows the magnitude of the weight of prevalence. The black horizontal line indicates the target reliability (4.7).

Slika 4.15: Indeksi zanesljivosti β kot funkcija obtežnega faktorja χ_1 pri $d = 500$ mm za pogoj $a_p \leq 8\,d_v$ enačbe odpornosti proti preboju; stolpci prikazujejo obtežne kombinacije, vrstice prikazujejo različne vrednosti koeficienta natezne armature; barve prikazujejo vrednosti obtežnega faktorja χ_2, velikost oznake na grafu prikazuje vrednost uteži; horizontalna polna črta prikazuje ciljni indeks zanesljivosti (4.7).

Figures corresponding to subset $a_p > 8\,d_v$

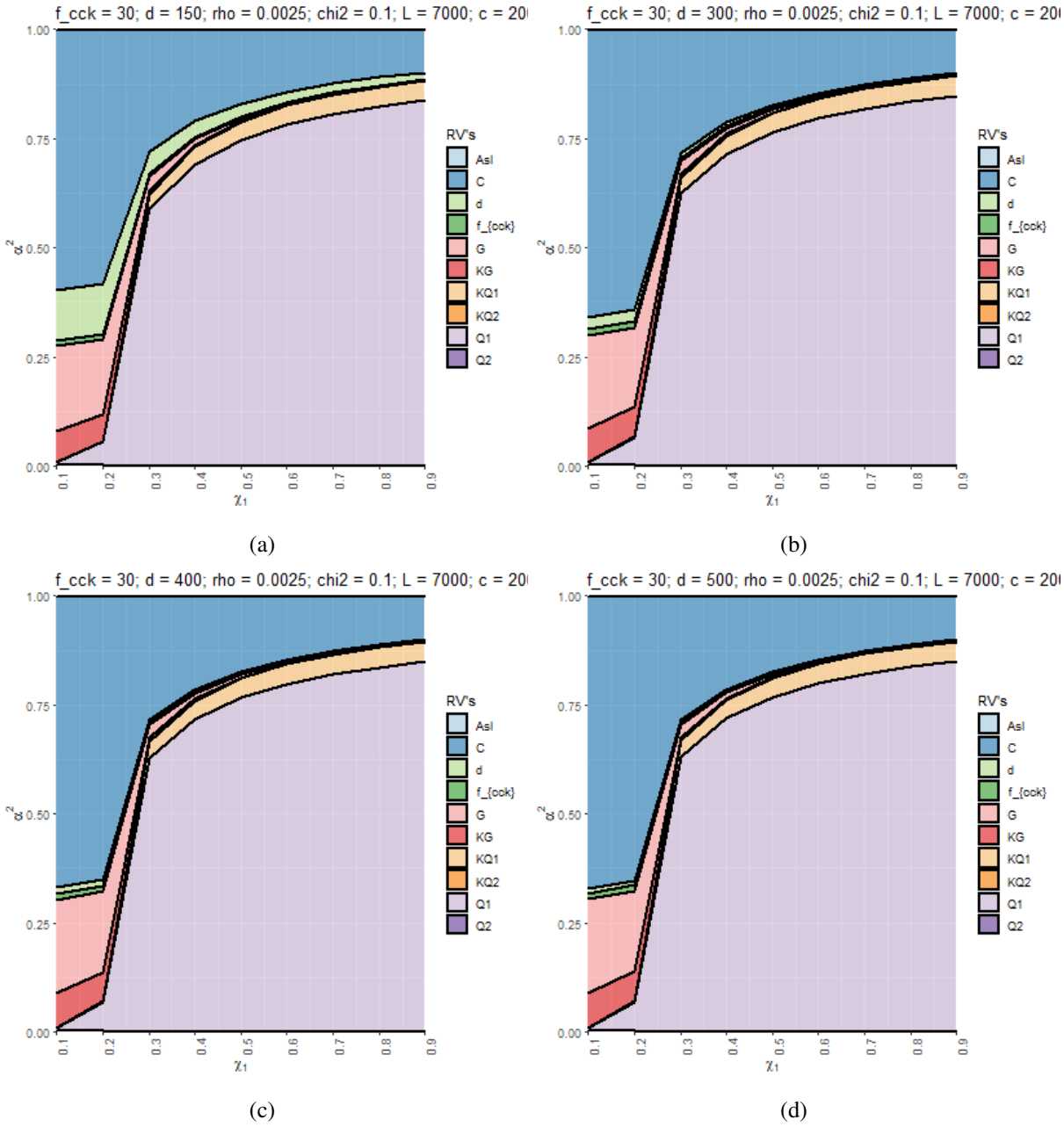

Figure 4.16: Sensitivity factors α^2 corresponding to subset $a_p > 8\,d_v$ of the punching shear resistance equation with the snow-wind load combination and with different effective depth d: (a) 150 mm, (b) 300 mm, (c) 400 mm, (d) 500 mm.

Slika 4.16: Faktorji občutljivosti α^2, ki ustrezajo pogoju $a_p > 8\,d_v$ enačbe odpornosti proti preboju za obtežno kombinacijo sneg-veter in projektne vrednosti višine prereza d: (a) 150 mm, (b) 300 mm, (c) 400 mm, (d) 500 mm.

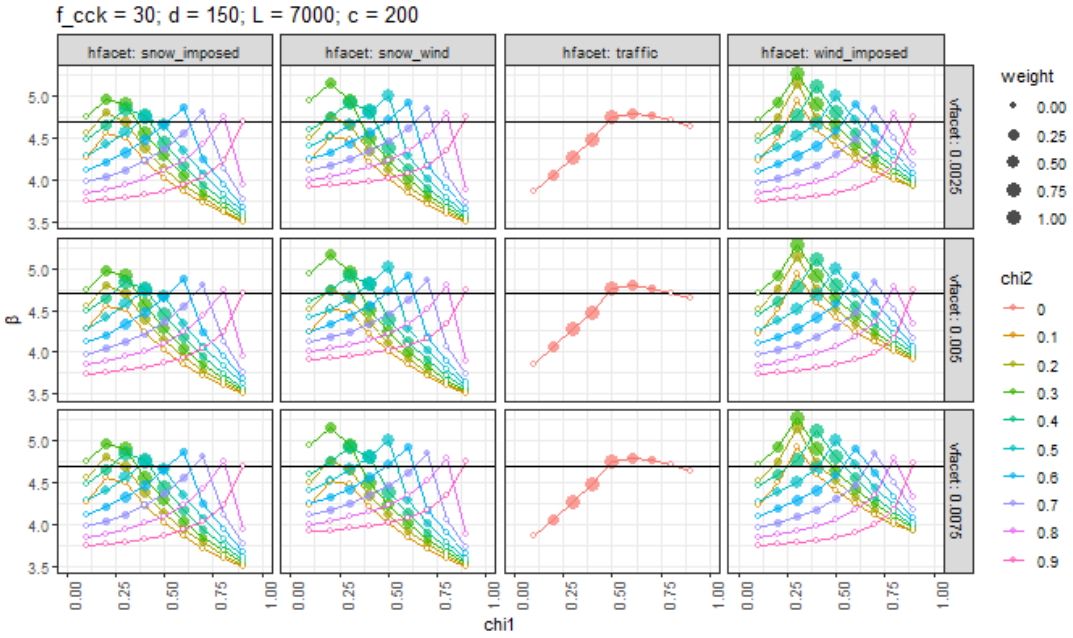

Figure 4.17: Reliability indices β as a function of load ratio χ_1 with $d = 150$ mm for the subset $a_p > 8\,d_v$ corresponding to the punching shear resistance formula. Columns present different load combinations, while rows different value of longitudinal reinforcement ratios. Colors represent different values of χ_2 load ratios, while the marker size shows the magnitude of the weight of prevalence. The black horizontal line indicates the target reliability (4.7).

Slika 4.17: Indeksi zanesljivosti β kot funkcija obtežnega faktorja χ_1 pri $d = 150$ mm za pogoj $a_p > 8\,d_v$ enačbe odpornosti proti preboju; stolpci prikazujejo obtežne kombinacije, vrstice prikazujejo različne vrednosti koeficienta natezne armature; barve prikazujejo vrednosti obtežnega faktorja χ_2, velikost oznake na grafu prikazuje vrednost uteži; horizontalna polna črta prikazuje ciljni indeks zanesljivosti (4.7).

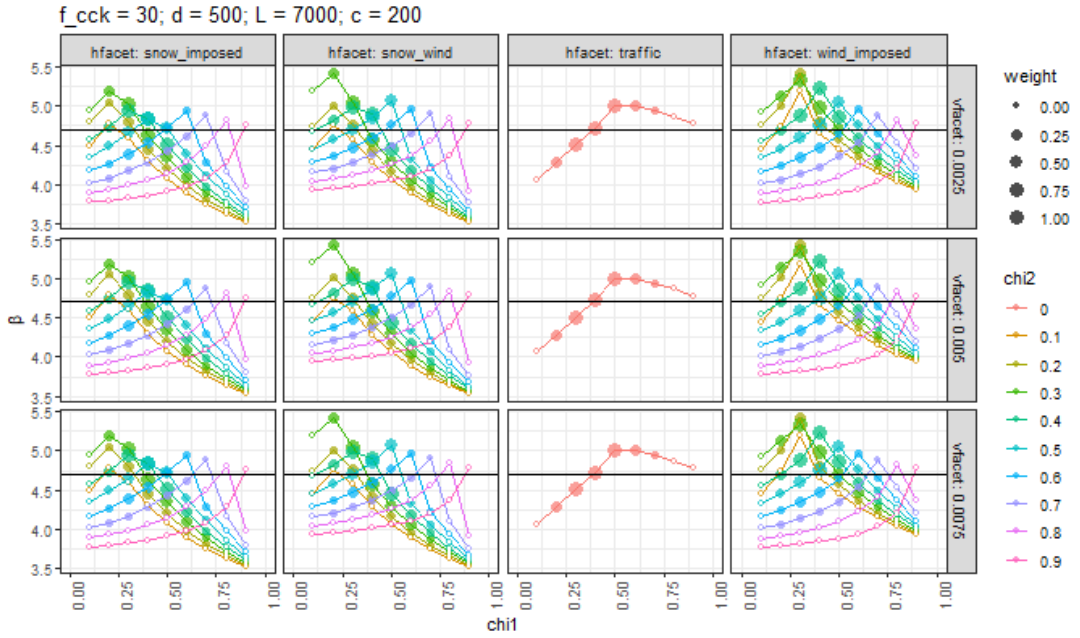

Figure 4.18: Reliability indices β as a function of load ratio χ_1 with $d = 500$ mm for the subset $a_p > 8\,d_v$ corresponding to the punching shear resistance formula. Columns present different load combinations, while rows different value of longitudinal reinforcement ratios. Colors represent different values of χ_2 load ratios, while the marker size shows the magnitude of the weight of prevalence. The black horizontal line indicates the target reliability (4.7).

Slika 4.18: Indeksi zanesljivosti β kot funkcija obtežnega faktorja χ_1 pri $d = 500$ mm za pogoj $a_p > 8\,d_v$ enačbe odpornosti proti preboju; stolpci prikazujejo obtežne kombinacije, vrstice prikazujejo različne vrednosti koeficienta natezne armature; barve prikazujejo vrednosti obtežnega faktorja χ_2, velikost oznake na grafu prikazuje vrednost uteži; horizontalna polna črta prikazuje ciljni indeks zanesljivosti (4.7).

Analysis of the results

The main observations of the results of calibration of the design punching shear formula are:

- The resistance partial safety factors for the punching shear equation were calculated as 1.61 and 1.45. Comparing to the present value of 1.5, the offsets of partial safety factors for punching shear are slightly larger than for the one-way shear resistance formula.
- While observing the sensitivity factors α^2 we can see that the values for the resistance-side random variables are the largest for those design cases where the permanent load is predominant ($\chi_1 = 0.1 - 0.3$). As the variable load increases, the sensitivity factors for the load-side random variables increase and the resistance-side values decrease.
- The model uncertainty variable has the largest α^2 value among the resistance-related random variables. This ranges between 0.5 and 0.7 for lower and between 0.1 and 0.25 for higher values of the variable load Q_1. Therefore, the assumed α value suggested by the simplified approach in Eurocode 0, annex D seems to be a safe approximation.
- For those design scenarios where the used slab depth is smaller, there appears to be a noticeable α^2 value for that random variable, which ranges between 0.1 and 0.2. As the value of the slab depth in the design scenario is increased, the α^2 for that random variable decreases.This is due to the assumption that the standard deviation of d is constant.
- As resistance-related parameters in design scenarios are changed, we can observe that there is almost no change in the calculated results. There is also almost no observable difference between the α^2 values for the snow-wind, wind-imposed and snow-imposed load combinations.
- There is a noticeable difference between the β values for the two considered subsets of the calibrated design equation. The snow-wind, snow-imposed and wind-imposed load combinations show results ranging between 3.5 and 5.5, while the values for the traffic load combination range between 4.0 and 5.0.
- Behavior of α^2 values in relation to the load ratios χ_1 or χ_2 is similar for all load combinations, except for traffic. For this load combination, most of the design scenarios show inadequate reliability level.

5 DISCUSSION

On the basis of the calculated sensitivity factors α^2 we can see that these values change as the variable loads Q_1 and Q_2 are increased via load ratios χ_1 and χ_2, respectively. The change in α^2 values are in line with what we can expect: for the design scenarios, in which the permanent load G is larger than the variable load, we obtain larger α^2 values for the random variables that are related to the permanent load and the resistance. That means that in such design scenarios the failure probability is significantly more governed by the resistance-related variables and by the permanent load. As variable load increases, the α^2 factors for the random variables that belong to that load increase as well. Most of the random variables, representing the parameters of the resistance equation show small α^2 values, with the exception being the model uncertainty variable and (for the punching shear formula) the effective slab depth. The sum of α^2 values for the resistance-side variables for the one-way shear equation is between 0.5 and 0.80 at lower χ_1 values (from 0.1 to 0.3), while it is between 0.20 and 0.30 for higher χ_1 values (from 0.7 to 0.9). For the punching shear equation they are between 0.40 to 0.80 for lower load ratios and between 0.20 and 0.30 for higher load ratios. A reason for this could be given by looking at how the resistance models are constructed. We can see in Equations (4.18) and (4.19), for example, that most of the parameters of the punching shear resistance force model have very small exponents, meaning that a change in their values should not significantly influence the value of the resistance force. This reasoning applies to the one-way shear equation as well. In comparison, the simplified reliability method for calculating a corrected material partial factor in the Eurocodes defines the resistance sensitivity factor for $\beta_{\text{target}} = 3.8$ as a constant value $\alpha_{\text{R}} = 0.8$.

As expected, the β values can change considerably depending on the design scenarios. The change of β in terms of increasing variable load seems to be highly similar for all of the used load combinations, with the exception of the traffic load. The scenarios belonging to this load resulted in calculated reliability levels that rarely achieved the target β_{target}, which could indicate that the present value of the partial safety factor for concrete is undervalued for structures subjected to traffic load. In fact, when performing a calibration for design scenarios with the traffic load involved only, we obtain larger partial factors than the current ones, ranging from 1.60 to 1.69 for the one-way shear resistance equation. Hence, the calibrated partial safety factor would be lower if the traffic load would be excluded from the set of considered design scenarios in the calibration.

The calculated partial factors differ depending on the subsets of the considered design formulas. For both of the calibrated expressions, the narrower case corresponds to a higher partial safety factor. This may be due to the use of two version of the same formula - one is a more general case, which should give more accurate results for different ranges of applications, while the other is defined for a more narrow case with additional assumptions.

For both of calibrated design expressions we appear to obtain values of partial factors that are similar to the presently used value of the partial safety factor for concrete $\gamma_{\text{C}} = 1.50$.

6 CONCLUSIONS AND RECOMMENDATIONS

6.1 Conclusions

In the thesis, the implementation of a reliability-based code calibration procedure was used on two design expressions in EN 1992-1:2018 Draft 4: the one-way shear resistance equation without shear reinforcement and the punching shear resistance equation without shear reinforcement. The main research question of this work is:

What are the partial safety factors for concrete for Eurocode 2 design expressions obtained by performing a reliability-based code calibration?

This question is answered in the remainder of this section.

For the first case study, where the calibration of the design resistance expression of one-way shear was performed, the partial safety factors for concrete were calculated to be:

- $\gamma_C = 1.54$ for the subset, corresponding to $a_{cs} < 4d$,
- $\gamma_C = 1.46$ for the subset, corresponding to $a_{cs} \geq 4d$.

The partial safety factors for concrete of the design punching shear equation were calculated to be:

- $\gamma_C = 1.61$ for the subset, corresponding to $a_p \leq 8d_v$,
- $\gamma_C = 1.45$ for the subset, corresponding to $a_p > 8d_v$.

Based on these results, we can conclude that the calculated values of the partial safety factors for concrete are close to the presently used value $\gamma_C = 1.50$. By coming to this conclusion on the basis of a probabilistic calibration, we can confirm that use of the present value of the partial safety factor for concrete leads to reasonable levels of reliability for the design one-way shear and design punching shear resistance formulas.

Given that we identified traffic load as potentially problematic in terms of ensuring adequate reliability, we performed additional calibrations for this load combination only. For the design one-way shear formula, the calibrations resulted in the following values of the partial factors: $\gamma_C = 1.60$ and $\gamma_C = 1.69$, while the calibration for the design punching shear expression resulted in: $\gamma_C = 1.46$ and $\gamma_C = 1.73$.

6.2 Recommendations

In this final section, we propose recommendations for future research based on the observations from the results of this thesis.

We have seen that for both case studies the calculated partial factors lead to low reliability indices (as low as 3.5) in design scenarios where either the permanent load dominates (i.e. for low load ratios) or where the variable load dominates (i.e. for high load ratios). This is especially the case for the traffic load combination, which exhibits reliability levels that are mostly lower than the target reliability level, meaning that designs based on the traffic load combinations could yield structural members that achieve unsatisfactory reliability levels according to EN 1990. It is therefore recommended that a further study of reliability based on traffic load design is conducted.

The calibrated partial factors presented here are based on a single value of the target reliability. EN 1990:2002 recommends calibration to two target reliability levels corresponding to the same consequence class. Further calibrations should be performed for different consequence classes in order to study how the material partial factor changes. In this thesis we also use a single set of weights of prevalence for design scenario for all load combinations. We have observed that the calculated reliability levels tend to be considerably smaller than the target reliability for design scenarios in which the variable load is either significantly smaller or higher than the permanent load. In those design scenarios small weights of prevalence are assigned. Additionally, the weights are currently based only on the frequency of occurrence of the load ratios. In further development, it would make sense to base the weights on the basis of information regarding the frequency of occurrence of certain dominant resistance-related parameters as well.

Through the study of sensitivity factors, we observe that the majority of resistance-side random variables have in most cases a limited effect on the reliability of both of the considered case studies ($\alpha^2 < 0.2$). In all calibrations, the predominant parameter among resistance variables seems to be the resistance model uncertainty ($\alpha^2 = 0.5 - 0.7$). The random variables corresponding to the loads appear to have the largest influence – this is even more pronounced in design scenarios where the variable loads are significantly higher than the permanent load. This opens a question if the number of resistance related random variables could not be reduced in the calculation. A sensitivity analysis should be performed in order to study the influence of any particular random variables on the value of calibrated resistance partial factors.

The inconsistency among different parts of the Eurocode in terms of partial safety factors should be highlighted. In EN 1990, γ_M is the material partial factor, constructed from γ_{Rd}, which takes into account the model uncertainty of the resistance model, and γ_m, which considers uncertainty of the material. In EN 1992, a single partial safety factor γ_C, which is named the partial factor for concrete is used. The naming in EN 1992-1:2004 insinuates that the partial factor only covers uncertainty of the concrete material; however, as demonstrated in this thesis, it in fact covers both the model and material uncertainties. Consequently, we suggest that in future versions of EN 1992 more clarity is given with regards to what kind of uncertainties are covered by certain partial safety factors. This could in part be completed by providing partial safety factors in line with the definition in EN 1990:2002.

POVZETEK

Uvod

Pravilniki za projektiraje gradbenih konstrukcij uporabnikom ponujajo zbirko standardiziranih navodil za njihovo vsakodnevno delo. Večina modernih gradbenih standardov temelji na zagotavljanju zadostne varnosti projektiranega elementa, kar je zagotovljeno s preverjanjem mejnih stanj. Njihov cilj je zasnovati konstrukcijske elemente z verjetnostjo porušitve, ki je manjša od mejne vrednosti, določene za izbrano projektno življensko dobo.

Evrokodi so harmonizirani standardi, ki določajo pravila za projektiranje gradbenih konstrukcij za države Evropske unije in drugod. EN 1990:2002 (Evrokod 0) določa osnovna pravila za projektiranje in zahteve glede zanesljivosti projektiranih elementov. Za zagotavljanje varnosti dovoljuje uporabo probabilističnih ali delno probabilističnih metod, ena izmed teh je znana kot metoda delnih faktorjev. V sklopu le-teh se zagotavlja varnost na podlagi izbire tolikšnih delnih varnostih faktorjev, da je verjetnost, da je mejno stanje preseženo dovolj majhna. Postopek izbora delnih varnostnih faktorjev, ki izpolnjujejo določene zahteve po varnosti, imenujemo kalibracija ali optimizacija pravilnikov.

V idealnem primeru so delni faktorji izbrani na podlagi probabilistične kalibracije, ki temelji na širokem izboru projektnih scenarijev in z upoštevanjem modelnih negotovosti. Dejansko pa so bile trenutne vrednosti izbrane na podlagi primerjave s starejšimi, že uveljavljenimi gradbenimi standardi ali na podlagi izkušenj inženirjev, ki so jih pripravljali. Posledično trenutne enačbe mejnih stanj sledijo k različnim nivojem zanesljivosti glede na izbiro projektnih scenarijev. Posledično je nemogoče govoriti o natančnem nivoju zanseljivosti. V Dodatku D standarda EN 1990:2002 je ponujena metoda za izračun popravljenega materialnega varnostnega faktorja, ki poenostavljeno zajema metodo zanesljivosti prvega reda. To predstavlja motivacijo za obravnavo naslednjega problema.

Standard EN 1992-1:2004 (Evrokod 2) določa pravila za projektiranje betonskih konstrukcij v sklopu Evrokodov. Trenutni osnutek prenovljene verzije tega standarda EN 1992-1:2018 D4 predstavlja številne popravke enačb mejnih stanj. Po našem vedenju probabilistična kalibracija enačb iz tega standarda še ni bila opravljena. Cilj te magistrske naloge je tako izračun delnega varnostnega faktorja za beton za enačbo projektne strižne odpornosti armiranobetonskih elementov brez strižne armature ter projektne strižne odpornosti proti preboju z uporabo probabilistične kalibracije.

Procedura za probabilistično kalibracijo enačb mejnih stanj

Za kalibracijo delnih faktorjev uporabimo proceduro, ki temelji na pristopu, ki ga je predstavil Ellingwood [3] in, ki je bila razvita v sodelovanju organizacije TNO in Tehniške univerze v Delftu. Ta procedura neposredno zajema modelno negotovost kot eno izmed slučajnih spremenljivk. Za to uporabimo metodo največjega verjetja, s katero ocenimo parametre porazdelitve, pripravljene na podlagi zbranih eksperimentalnih podatkov. Rezultat izračuna je optimalni delni faktor za odpornost, ki zajema

negotovosti materiala in računskega modela, ter v povprečju (gledano za vse projektne scenarije) dosega kriterij zanesljivosti. Postopek kalibracije poteka v naslednjih ključnih korakih:

1. Definicija vhodnih podatkov;
2. Določitev parametrov porazdelitve modelne negotovosti;
3. Izbor slučajnih spremenljivk in funkcije mejnega stanja;
4. Generiranje projektnih scenarijev;
5. Analiza zanesljivosti in reševanje optimizacijskega problema;

V prvem koraku sta definirana računski model odpornosti in kriterij zanesljivosti. Slednji je podan v obliki ciljnega indeksa zanesljivosti β_{target}, ki je povezan s ciljno (mejno) verjetnostjo porušitve ($P_{\text{f,target}} = \Phi(-\beta_{\text{target}})$). Prav tako so podane obtežne kombinacije, ki so uporabljene za generiranje projektnih scenarijev, ter utežna funkcija, potrebna za optimizacijo. V tej magistrski nalogi uporabimo $\beta_{\text{target}} = 4.7$, ki po EN 1990:2002 ustreza enoletnemu referenčnemu obdobju in razredu zanesljivosti RC2.

V drugem koraku so določeni parametri porazdelitve modelne negotovosti, ki je eden izmed ključnih parametrov odpornostnega modela in je rezultat nepopolnega poznavanja fizikalnega pojava, ki ga model zajema. Odraža se kot razmerje med vrednostjo odpornosti, ki jo napove računski model in dejansko, eksperimentalno dobljeno vrednostjo. V primeru modelov odpornosti gradbenih konstrukcijah so vzrok za modelno negotovost večinoma preveč poenostavljene predpostavke glede robnih pogojev in odvisnosti med osnovnimi spremenljivkami, ki jih model ne zajema. Slučajna spremenljivka modelne negotovosti θ je tako definirana v enačbi (3.1). V obravnavanih kalibracijah v tej magistrski nalogi je zajeta kot multiplikativni regresijski faktor $1/C_{\text{c}}$. Ponavadi je θ obravnavana kot logaritemsko normalna slučajna spremenljivka; posledično velja enako za C_{c}. Parametre porazdelitve te slučajne spremenljivke ocenimo na podlagi velike količine eksperimentalnih podatkov za obravnavani mejni stanji. Na podlagi parametrov eksperimentalnih vzorcev določimo modelno odpornost in uporabimo eksperimentalno dobljeno vrednost odpornosti, da določimo θ. Z metodo največjega verjetja nato ocenimo parametre te porazdelitve.

V tretjem koraku sledi izbor parametrov modela odpornosti R in učinka vplivov E, ki so lahko slučajne ali deterministične spremenljivke. Za uporabo slučajnih spremenljivk v proceduri moramo poznati parametre njihovih porazdelitev, to so: pričakovane vrednosti in koeficienti variacije. V pripravljenih kalibracijah uporabimo parametre, ki večinoma temeljijo na lastni presoji ali na podlagi podatkov iz literature. Nekateri parametri so v Evrokodu definirani tako, da so njihove reprezentativne vrednosti podane s karakterističnimi vrednostmi, ki odražajo določen percentil njihovih porazdelitev. Za take parametre mora torej biti podan tudi percentil, ki povezuje probabilistični model s karakteristično vrednostjo.

Enačbe mejnih stanj so kalibrirane za določeno domeno vrednosti parametrov odpornosti in vplivov. Diskretne kombinacije vrednosti parametrov iz te domene predstavljajo projektne scenarije. V tem koraku opravimo generiranje projektnih scenarijev. Postopek projektiranja običajno poteka tako, da so najprej določeni učinki vplivov za konstrukcijski element ter nato njegov kritični prerez. Parametri odpornosti se nato spreminjajo tako, da je izpolnjeno pogoju mejnega stanja. Tak pristop je težko uporabiti za veliko število projektnih scenarijev, hkrati pa lahko pripelje do nerealističnih vrednostih parametrov. Zato v tej

magistrski nalogi predlagamo alternativen pristop, ki je enostaven za implementacijo znotraj avtomatizirane procedure. To je t. i. inverzni pristop, ki temelji na popolnem izkoristku kritičnega prereza, kjer je mejnemu stanju identično zadoščeno. Tako se spreminjajo samo parametri na strani vplivov, ki so vpeljani z obtežnimi faktorji χ, s katerimi predstavljamo delež spremenljive obtežbe glede na skupno obtežbo.

V zadnjem koraku je opravljena analiza zanesljivosti, kjer so na podlagi funkcije mejnega stanja $g = R - S$ za posamezni projektni scenarij izračunani indeksi zanesljivosti. Sledi kalibracija, katero lahko obravnavamo kot optimizacijski problem, v katerem iskani delni faktor nastopa kot prosta spremenljivka. Problem je definiran s ciljno funkcijo, ki meri skupno odstopanje indeksov zanesljivosti od ciljne zanesljivosti, hkrati pa upošteva ocenjeno pomembnost posameznih projektnih scenarijev z utežmi, ki so predstavljene v preglednici 3.1. Ta ne predstavlja merila, s katerim presodimo o verjetnosti pojava posameznega projektnega scenarija, temveč predstavlja našo presojo glede pojava določenih kombinacij vplivov. Na primer: vrednost utežne funkcije je 0, ko je $\chi = 0.1$. To pomeni, da je možnost pojava projektnega stanja, ko 90% skupne obtežbe predstavljajo stalni vplivi in 10% spremenljivi vplivi, po našem mnenju zanemarljiva. Cilj optimizacijskega problema je torej poiskati tisto vrednost delnega varnostnega faktorja, ki minimizira vrednost ciljne funkcije.

Opisani postopek je grafično prikazan z delotokom na sliki 3.1.

Rezultati demonstriranih kalibracij

V predstavitvi kalibriranih enačb in rezultatov večinoma sledimo opisanemu postopku.

Enačba mejnega stanja za račun strižne odpornosti armiranobetonskih elementov brez strižne armature po EN 1992-1:2018 D4 je podana v enačbi (4.1). Kalibracijo enačbe opravimo za dva pogoja, na podlagi parametra učinkovitega efektivnega razpona a_{cs}, predstavljenega v enačbi (4.3). Tako je tudi izračun parametrov porazdelitve slučajne spremenljivke regresijskega koeficienta, s katerim zajamemo modelno negotovost razdeljen na dva dela. Rezultati so prikazani v preglednici 4.1. Ugotovimo lahko, da je izračunana vrednost dober približek obstoječe vrednosti regresijskega koeficienta ter da ni bistvene razlike med obema pogojema. Projektni scenariji so generirani na podlagi diskretnih vrednosti spremenljivk, definiranih v preglednici 4.2. Vhodni podatki za probabilistične modele odpornosti in vplivov, so predstavljeni v poglavju 4.1.3.

Rezultati kalibracije so predstavljeni v preglednici 4.9. Kalibrirani delni faktorji znašajo $\gamma_C = 1.54$ za pogoj $a_{cs} < 4d$ ter $\gamma_C = 1.46$ za pogoj $a_{cs} \geq 4d$. Iz analize zanesljivosti dobimo faktorje občutljivosti α^2 in indekse zanesljivosti β za posamezni projektni scenarij. Razberemo lahko, da je regresijski koeficient, s katerim zajamemo modelno negotovost edina slučajna spremenljivka na strani odpornosti z znatnimi vrednostmi faktorjev občutljivosti. Te vrednosti znašajo med 0.4 in 0.7 za projektne scenarije, kjer je stalna obtežba dominantna ($\chi_1 = 0.1 - 0.3$), s povečevanjem spremenljive obtežbe pa α^2 za to slučajno spremenljivko pada, kot tudi za ostale slučajne spremenljivke na strani odpornosti. S spreminjanjem vrednosti parametrov projektnih scenarijev lahko opazimo, da se izračunane vrednosti α^2 in β skoraj ne spreminjajo. Indeksi zanesljivosti so za obtežne kombinacije sneg-veter, sneg-koristna obtežba in veter-koristna obtežba podobni; vrednosti znašajo med 3.6 in 5.2. To ne velja za obtežno kombinacijo za promet, ki izkazuje vrednosti indeksov zanesljivosti med 3.5 in 4.7. V tej kombinaciji je ciljna

zanesljivost β_{target} dosežena le v redkih primerih.

Enačba mejnega stanja za račun odpornosti proti preboju armiranobetonskih elementov brez strižne armature po EN 1992-1:2018 D4 je podana v enačbi (4.13). Kalibrirano enačbo razdelimo glede na dva različna pogoja, v tem primeru glede na vrednosti parametra a_{p}, ki predstavlja velikost območja v okolici naleganja elementa na steber, kjer prihaja do negativnih upogibnih momentov. Razdeljena enačba mejnega stanja, ki je uporabljena za kalibracijo, je predstavljena v enačbah (4.18) in (4.19). Rezultati približnega izračuna parametrov porazdelitve regresijskega koeficienta, s katerim zajamemo modelno negotovost modela odpornosti so prikazani v preglednici 4.10. Tudi v tem primeru lahko ocenimo, da sta izračunani srednji vrednosti podobni obstoječima vrednostima regresijskega koeficienta. Parametri projektnih scenarijev so prikazani v preglednici 4.11. V primeru kalibracije te enačbe so projektni scenariji odvisni od nekaterih parametrov (a_{p} in b_0), za katere je težko določiti razpon njihovih vrednosti, ki se pojavlja v praksi. Zato ta parametra v projektnih scenarijih upoštevamo posredno z izračunom iz geometrijskih parametrov, za katere smo lahko z večjo gotovostjo prepričani, da se bodo v praksi pojavili. Gre za dolžino elementa L in dolžino stranice c. Vhodni podatki za probabilistične modele odpornosti in vplivov so enaki kot za kalibracijo enačbe strižne odpornosti. Predstavljeni so v poglavju 4.2.3.

Rezultate kalibracije enačbe mejnega stanja odpornosti proti preboju brez strižne armature predstavljamo v preglednici 4.13. Kalibrirani delni faktorji znašajo $\gamma_{\text{C}} = 1.61$ za pogoj $a_{\text{p}} \leq 8\,d_{\text{v}}$ ter $\gamma_{\text{C}} = 1.45$ za pogoj $a_{\text{p}} > 8\,d_{\text{v}}$. Tudi v tem primeru lahko opazimo, da sta izračunani vrednosti blizu obstoječe vrednosti delnega varnostnega faktorja, ki znaša 1.5, je pa razlika med pogojema v primerjavi s prvim primerom kalibracije večja. Iz rezultatov analize zanesljivosti lahko opazimo, da so vrednosti faktorjev občutljivosti α^2 za slučajne spremenljivke na strani odpornosti največje v projektnih scenarijih, kjer stalna obtežba predstavlja večino celotne obtežbe ($\chi_1 = 0.1 - 0.3$). S povečevanjem koristne obtežbe se vrednosti α^2 za omenjene slučajne spremenljivke zmanjšujejo. Slučajna spremenljivka z največjimi vrednostmi (med 0.5 in 0.7) α^2 je parameter s katerim zajamemo modelno negotovost. V projektnih scenarijih, kjer je uporabljena manjša vrednost parametra višine prereza elementa, je opazno, da je vrednost α^2 te slučajne spremenljivke (med 0.1 in 0.2) znatna v primerjava z vrednostmi za ostale spremenljivke. Opazimo lahko znatno razliko med izračunanimi vrednostmi indeksov zanesljivosti β za uporabljena pogoja kalibrirane enačbe. Vrednosti za obtežne kombinacije sneg-veter, veter-koristna obtežba in sneg-koristna obtežba znašajo med 3.5 in 5.5, medtem ko obtežna kombinacija za promet ponovno izkazuje vrednosti β, ki redko presežejo ciljni indeks zanesljivosti β_{target}.

Komentar in zaključek

Na podlagi izračunanih vrednosti faktorjev občutljivosti α^2 lahko ocenimo vpliv posamezne slučajne spremenljivke na izračun indeksa zanesljivosti. Na strani odpornosti v veliki večini opazimo, da ima samo regresijski koeficient za modelno negotovost odpornosti, znatne vrednosti. Razlog temu so lahko sami matematični modeli, v katerih imajo parametri, katere zajamemo v kalibracijski proceduri s slučajnimi spremenljivkami, majhne potenčne faktorje. Sprememba njihovih vrednosti tako ne prinaša bistvene spremembe vrednosti. Drug razlog je lahko izbira parametrov porazdelitev. V našem primeru smo uporabili majhne koeficiente variacije, kar lahko privede do majhnih vrednosti α^2.

Dobljene vrednosti indeksov zanesljivosti večinoma ustrezajo pričakovanju. Za vse obtežne kombinacije,

razen prometne kombinacije, so si vrednosti podobne in v povprečju izpolnjujejo nivo ciljne zanesljivosti. Nasprotno velja za obtežno kombinacijo za promet, ki le v redkih primerih dosega ciljni indeks zanesljivosti. To lahko potrdimo s kalibracijo na podlagi samo te obtežne kombinacije: za enačbo strižne odpornosti znašata delna varnostna faktorja 1.60 in 1.69. To nakazuje tudi na to, da bi v primeru, da izključimo to obtežno kombinacijo iz kalibracije, dobili manjšo vrednost kalibriranega delnega faktorja.

Iz navedenih razlogov priporočamo dodatne študije delnih varnostnih faktorjev na podlagi principa zanesljivosti. Smiselno bi bilo pripraviti občutljivostno študijo, s katero bi lahko natančneje kot v tej magistrski nalogi ocenili vpliv zajema parametrov v obliki slučajnih ali deterministčnih spremenljivk na izračunan delni varnostni faktor. S tem bi lahko zmanjšali število potrebnih projektnih scenarijev in tako tudi reducirali računsko zahtevnost tega problema. Prav tako bi bile potrebne dodatne analize obtežne kombinacije za promet, ki se kaže kot problematična.

Omeniti je potrebno še nedoslednost, ki se pojavlja v Evrokodih glede delnih varnostnih faktorjev. Po EN 1990:2002 je materialni varnosti faktor γ_M sestavljen iz delnega faktorja γ_{R_d}, ki zajema modelno negotovost, ter iz delnega faktorja γ_m, ki zajema negotovost materiala. V EN 1992-1:2004 se uporablja izključno materialni varnostni faktor za beton γ_C, za katerega ni obrazloženo, katere negotovosti zajema. Za prihajajoče vrednosti tega standarda zato predlagamo, da se delne varnostne faktorje uporablja tako kot to priporoča EN 1990:2002.

REFERENCES

[1] Köhler, J., Sørensen, J., Baravalle, M. 2019. Calibration of existing semi-probabilistic design codes. Procceedings of the 13th International Conference on Applications of Statistics and Probability in Civil Engineering, ICASP13 in Seoul, South Korea, May 26–30, 2019.

[2] EN 1992-1-1: 2004. Eurocode 2: Design of concrete structures – Part 1-1: General rules and rules for buildings. Brussels, European Committee for Standardisation.

[3] Ellingwood, B., Galambos, T. V., MacGregor, J. G., Cornell, C. A. 1980. Development of a Probability Based Load Criterion for American National Standard A58, National Bureau of Standards, US Departement of Commerce.

[4] Thoft-Christensen, P., Baker, M. J. 1982. Structural Reliability Theory and Its Applications. Berlin, Springer-Verlag: 266 p.

[5] Sørensen, J., Kroon, I., Faber, M. 1994. Optimal reliability-based code calibration. Structural Safety 15: 197 – 208.

[6] Nowak, A. S., Szerszen, M. M. 2004. Reliability-Based Calibration for Structural Concrete, Phase 2. Ann Arbor, University of Michigan.

[7] Nadolski, V., Rózsás, Á., Sýkora, M. 2019. Calibrating Partial Factors – Methodology, Input Data and Case Study of Steel Structures. Periodica Polytechnica Civil Engineering 63: 222–242.

[8] Rackwitz, R. 2000. Optimization – the basis of code-making and reliability verification. Structural Safety 22: 27 – 60.

[9] Lind, N. C. 1972. The Design of Structural Design Norms. Journal of Struct. Mechanics 1: 357–370.

[10] Hansen, J. B. 1959. Definition und Grosse der Sicherheitsgrades im Erd- und Grundbau. Der Bauingenieur .

[11] Ditlevsen, O., Madsen, H. O. 2007. Structural Reliability Methods. Chichester, John Wiley and Sons: 373 p.

[12] Melchers, R. E. 2002. Structural Reliability Analysis and Prediction. Chichester, John Wiley and Sons: 356 p.

[13] Foster, S. J., Stewart, M. G., Loo, M., Ahammed, M., Sirivivatnanon, V. 2016. Calibration of Australian Standard AS3600 Concrete Structures: part I statistical analysis of material properties and model error. Australian Journal of Structural Engineering .

[14] Holický, M., Retief, J. 2005. Reliability assessment of alternative Eurocode and South African load combination schemes for structural design. Journal of the South African Institution of Civil Engineering. 47: 15–20.

[15] Meinen, N. E., Steenbergen, R. D. J. M. 2018. Reliability levels obtained by eurocode partial factor design - a discussion on current and future reliability levels. HERON 63.

[16] EN 1990: 2002. Eurocode – Basis of structural design. Brussels, European Committee for Standardisation.

[17] Holický, M., Retief, J. V., Sýkora, M. 2016. Assessment of model uncertainties for structural resistance. Probabilistic Engineering Mechanics 45: 188 – 197.

[18] Sýkora, M., Krejsa, J., Mlcoch, J., Prieto, M., Tanner, P. 2018. Uncertainty in shear resistance models of reinforced concrete beams according to fib MC2010. Structural Concrete 19: 284–295.

[19] Reineck, K.-H., Bentz, E., Fitik, B., Kuchma, D., Bayrak, O. 2014. ACI-DAfStb databases for Shear Tests on Slender Reinforced Concrete Beams with Stirrups. ACI Structural Journal 111.

[20] JCSS 2000. Probabilistic Model Code. Part III – Resistance Models. Accesed: 04-09-2020.

[21] CEB-FIB 2016. Fib Bulletin 80: Partial factor methods for existing concrete structures.

[22] JCSS 2001. Probabilistic Model Code. Part II – Load Models. Accesed: 04-09-2020.

[23] Slobbe, A., Rózsás, Á., Allaix, D., Bigaj-van Vliet, A. 2019. On the value of a reliability-based nonlinear finite element analysis approach in the assessment of concrete structures. Structural Concrete .

[24] EN 1991-1-3: 2003. Eurocode 1: Actions on structures – Part 1-3: General actions - Snow loads. Brussels, European Committee for Standardisation.

[25] Ellingwood, B., O'Rourke, M. 1985. Probabilistic models of snow loads on structures. Structural Safety 2: 291 – 299.

[26] EN 1991-1-4: 2004. Eurocode 1: Actions on structures - Part 1-4: General actions - Wind actions. Brussels, European Committee for Standardisation.

[27] Muttoni, A., Fernandez Ruiz, M., Simões, J. T. 2018. The theoretical principles of the critical shear crack theory for punching shear failures and derivation of consistent closed-form design expressions. Structural Concrete 19: 174–190.

[28] Muttoni, A. 2008. Punching Shear Strength of Reinforced Concrete Slabs without Transverse Reinforcement. ACI Structural Journal 105.

LIST OF APPENDICES

A: RELIABILITY ANALYSIS

B: CALIBRATION RESULTS

A RELIABILITY ANALYSIS

Structural reliability deals with the probabilistic analysis of engineering structures. Specifically, this means that one of its goals is the calculation of the failure of probability of a structure that has uncertain properties and is subjected to uncertain actions. The problem is defined using the limit state concept, which specifies the boundary between the safe and failure domains. This concept is characterized with the performance function $g(X)$ and its particular value $g(X) = 0$ separates the safe and failure regions. The failure probability P_f can be calculated by integrating the joint probability density function of random variables $f_\mathbf{X}(\mathbf{x})$ over the failure domain:

$$P_\mathrm{f} = P\big[g(\mathbf{X}) < 0\big] = \int_{g(\mathbf{X})<0} f_\mathrm{X}(\mathbf{x})\,\mathrm{d}.\mathbf{x} \tag{A.1}$$

A convenient expression of structural reliability is in terms of a reliability index, which is obtained as a transformation of the failure probability:

$$\beta = \Phi^{-1}(P_\mathrm{f}), \tag{A.2}$$

where $\Phi(\cdot)$ is the standardized normal cumulative distribution function.

Since the random vector describing the problem is usually high-dimensional, the calculation of the integral can be challenging. The value of the integral can be approximated using various numerical techniques, such as the First Order Reliability Method, which is designed to find the most probable (design) point over the limit state function $g(X) = 0$. The problem of calculating the failure probability is then restated as a search for minimum distance by transforming it into the space of uncorrelated standard random variables — the so-called U space. In this space, the design point is the one that is the closest to the origin. From a mathematical viewpoint this constrained optimization problem is easier to solve and is defined as:

$$\begin{aligned} &\beta = \min(||\mathbf{u}||) = \min\big(\sqrt{\Sigma_{i=1}^{n} u_i^2}\big), \\ &\text{while } g(\mathbf{X}) = 0. \end{aligned} \tag{A.3}$$

After finding the design point the failure probability is approximated as the integral behind the tangent hyperplane in the design point. This approximated value is usually adequate due to that failure probabilities of engineering structures are usually small, i.e. the design point is relatively far from the origin.

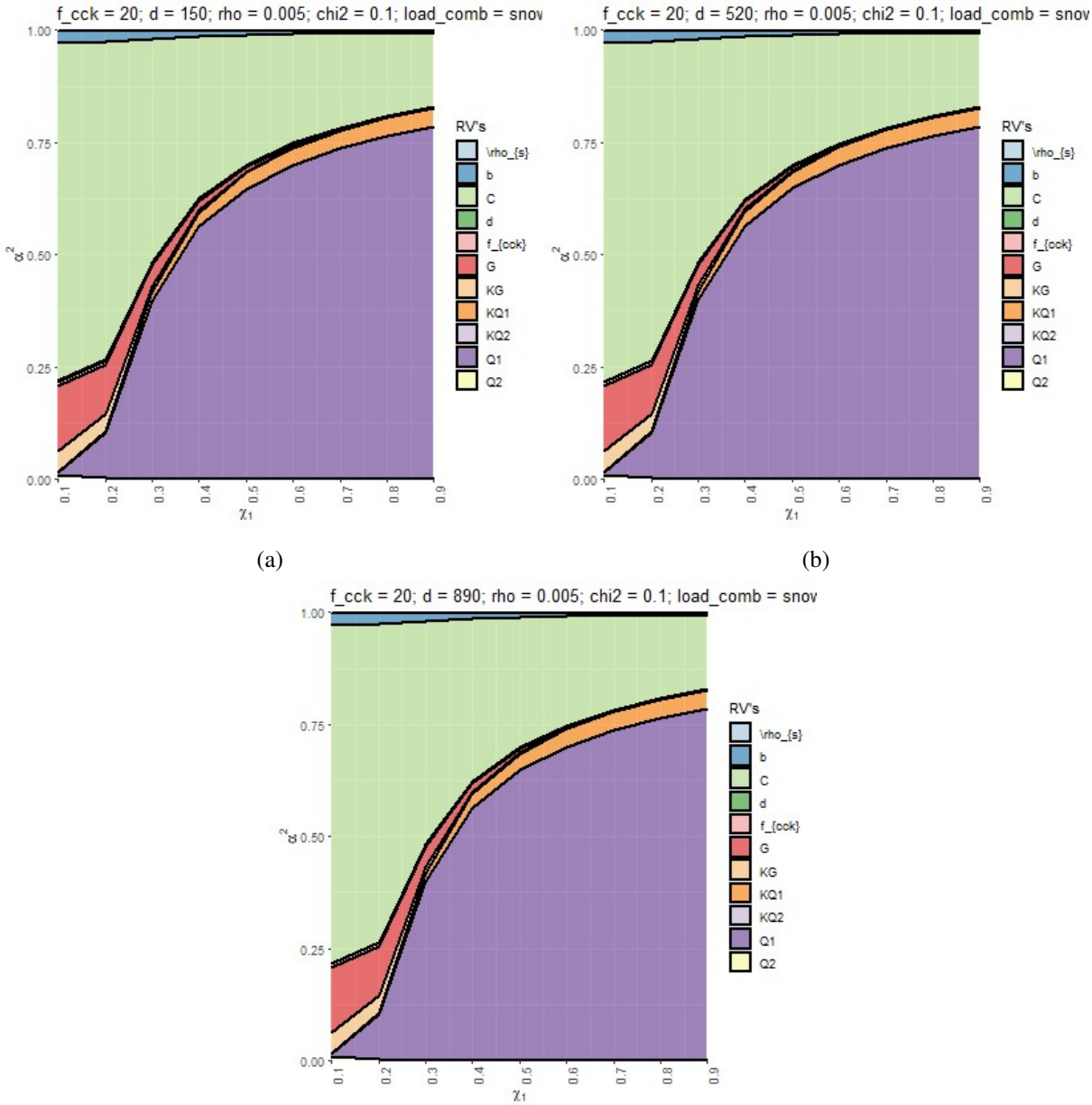

(a) (b)

(c)

Figure B.1: Sensitivity factors α^2 corresponding to subset $a_{cs} \geq 4d$ of the one-way shear resistance equation with the snow-imposed load combination and with different effective depth d: (a) 150 mm, (b) 520 mm, (c) 890 mm

Slika B.1: Faktorji občutljivosti α^2, ki ustrezajo pogoju $a_{cs} \geq 4d$ enačbe strižne odpornosti za obtežno kombinacijo sneg-koristna obtežba in projektne vrednosti višine prereza d: (a) 150 mm, (b) 520 mm, (c) 890 mm.

B CALIBRATION RESULTS

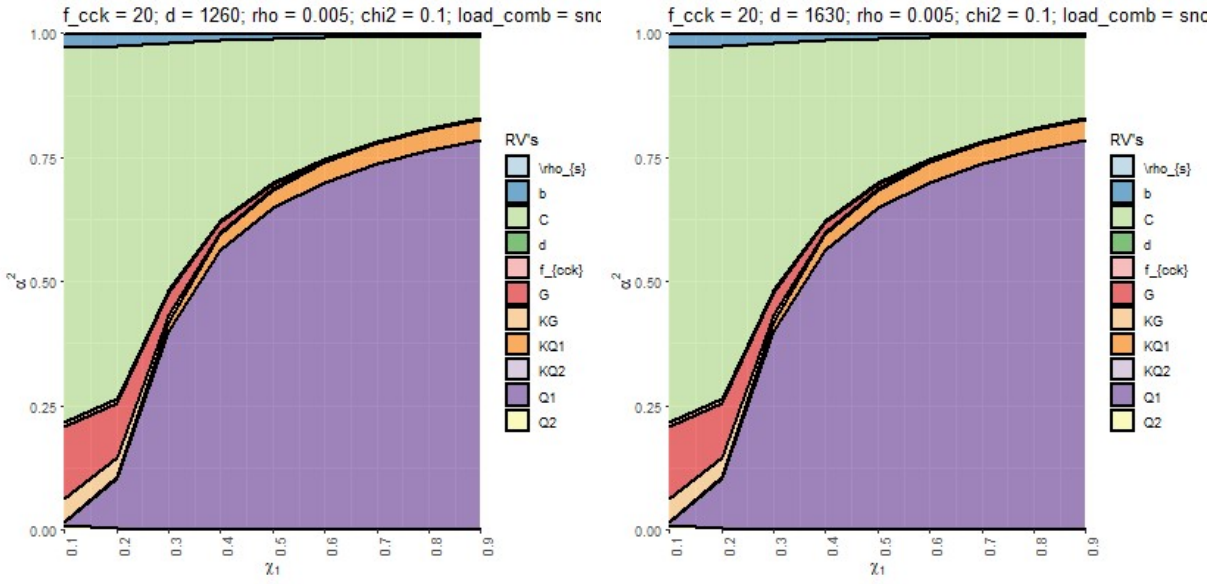

(a) (b)

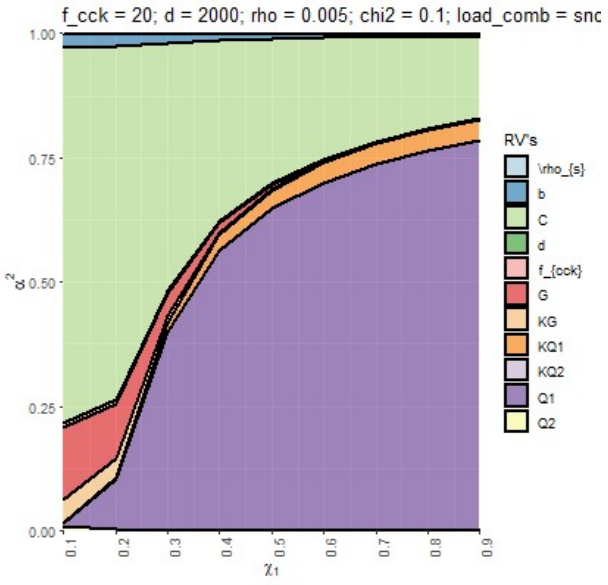

(c)

Figure B.2: Sensitivity factors α^2 corresponding to subset $a_{cs} \geq 4d$ of the one-way shear resistance equation with the snow-imposed load combination and with different effective depth d: (a) 1260 mm, (b) 1630 mm, (c) 2000 mm.

Slika B.2: Faktorji občutljivosti α^2, ki ustrezajo pogoju $a_{cs} \geq 4d$ enačbe strižne odpornosti za obtežno kombinacijo sneg-koristna obtežba in projektne vrednosti višine prereza d: (a) 1260 mm, (b) 1630 mm, (c) 2000 mm.

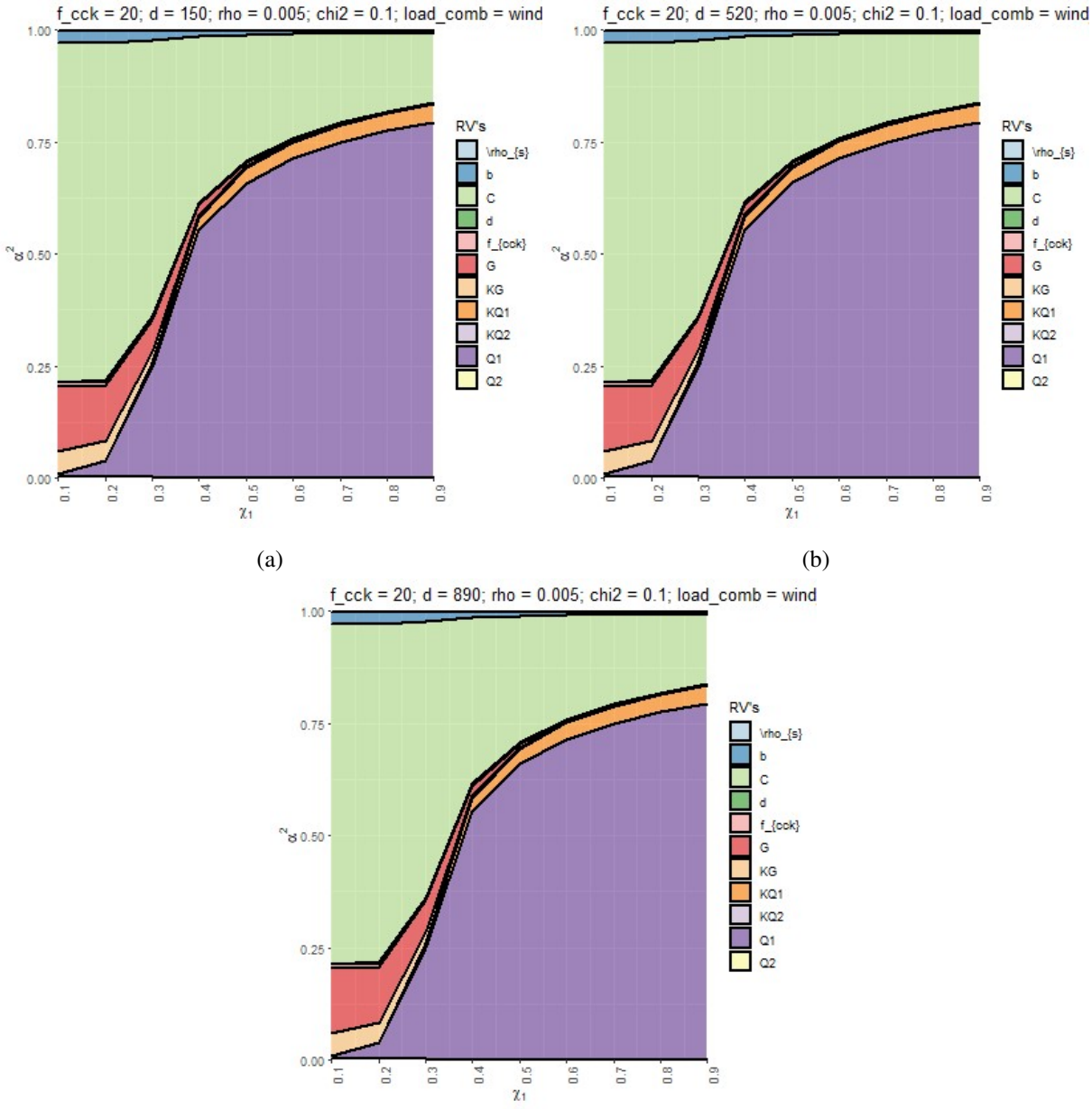

(a) (b)

(c)

Figure B.3: Sensitivity factors α^2 corresponding to subset $a_{cs} \geq 4d$ of the one-way shear resistance equation with the wind-imposed load combination and with different effective depth d: (a) 150 mm, (b) 520 mm, (c) 890 mm.

Slika B.3: Faktorji občutljivosti α^2, ki ustrezajo pogoju $a_{cs} \geq 4d$ enačbe strižne odpornosti za obtežno kombinacijo veter-koristna obtežba in projektne vrednosti višine prereza d: (a) 150 mm, (b) 520 mm, (c) 890 mm.

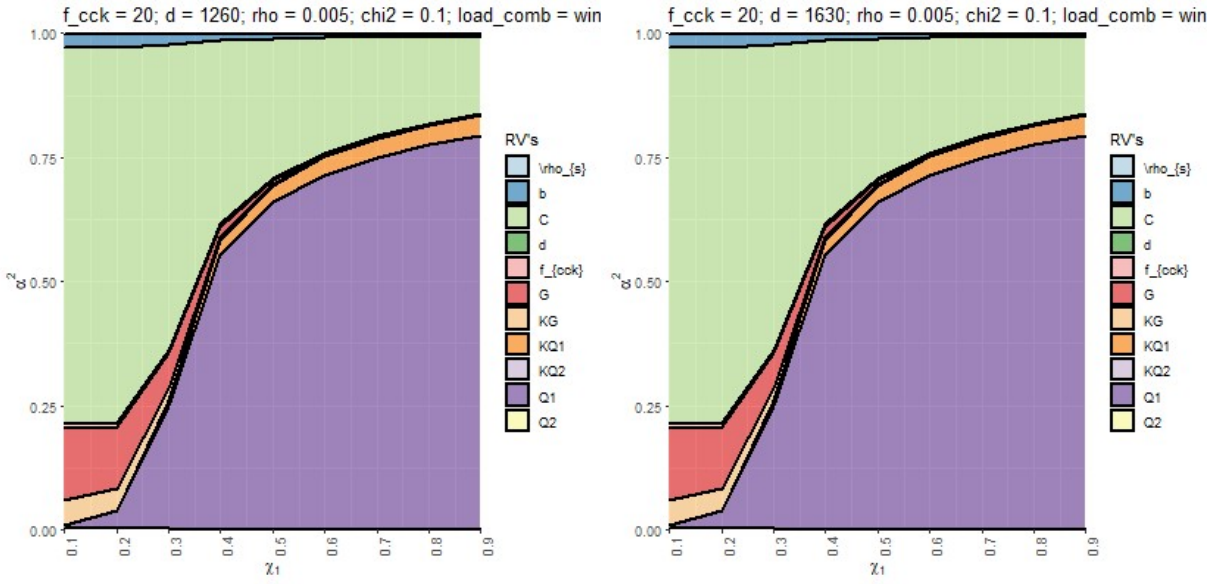

(a) (b)

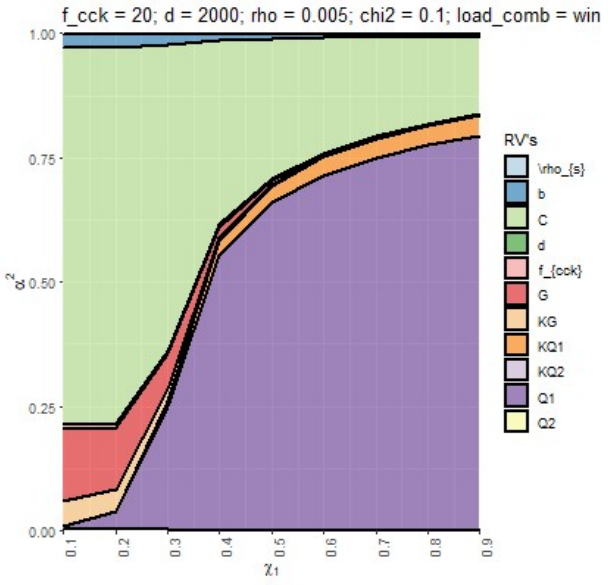

(c)

Figure B.4: Sensitivity factors α^2 corresponding to subset $a_{cs} \geq 4d$ of the one-way shear resistance equation with the wind-imposed load combination and with different effective depth d: (a) 1260 mm, (b) 1630 mm, (c) 2000 mm.

Slika B.4: Faktorji občutljivosti α^2, ki ustrezajo pogoju $a_{cs} \geq 4d$ enačbe strižne odpornosti za obtežno kombinacijo veter-koristna obtežba in projektne vrednosti višine prereza d: (a) 1260 mm, (b) 1630 mm, (c) 2000 mm.

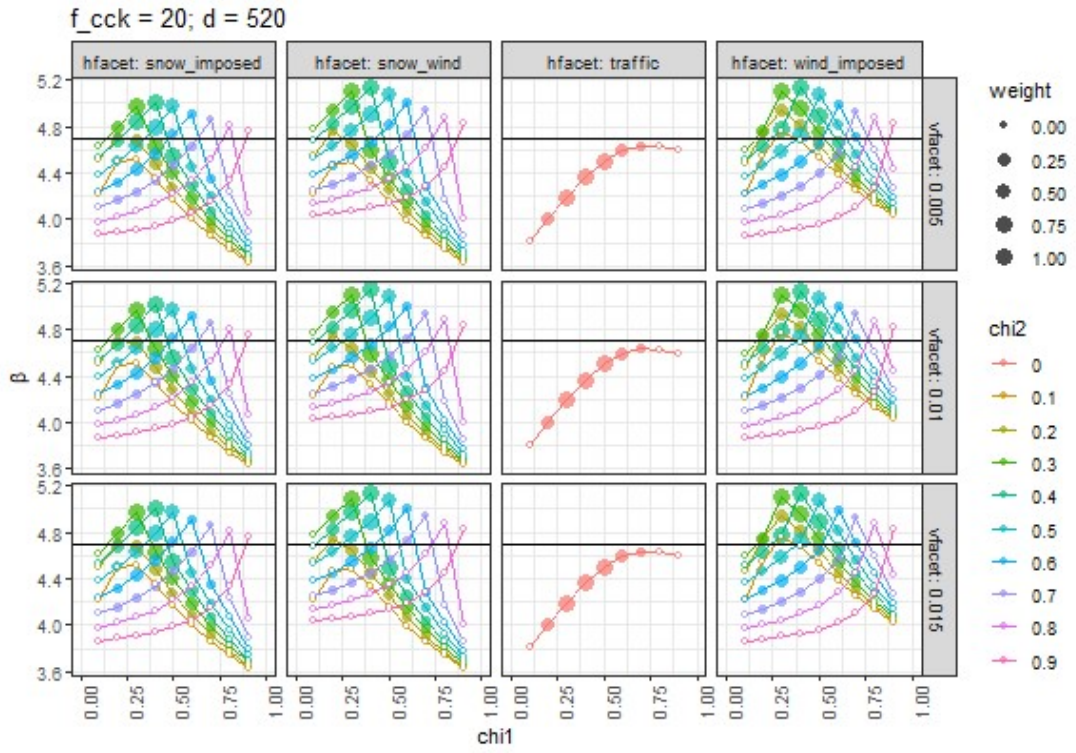

Figure B.5: Reliability indices β as a function of load ratio χ_1 with $d = 520$ mm for the subset $a_{cs} \geq 4\,d$ corresponding to the one-way shear resistance formula. Columns present different load combinations, while rows different value of longitudinal reinforcement ratios. Colors represent different values of χ_2 load ratios, while the marker size shows the magnitude of the weight of prevalence. The black horizontal line indicates the target reliability (4.7).

Slika B.5: Indeksi zanesljivosti β kot funkcija obtežnega faktorja χ_1 pri $d = 520$ mm za pogoj $a_{cs} \geq 4\,d$ enačbe strižne odpornosti; stolpci prikazujejo obtežne kombinacije, vrstice prikazujejo različne vrednosti koeficienta natezne armature; barve prikazujejo vrednosti obtežnega faktorja χ_2, velikost oznake na grafu prikazuje vrednost uteži; horizontalna polna črta prikazuje ciljni indeks zanesljivosti (4.7).

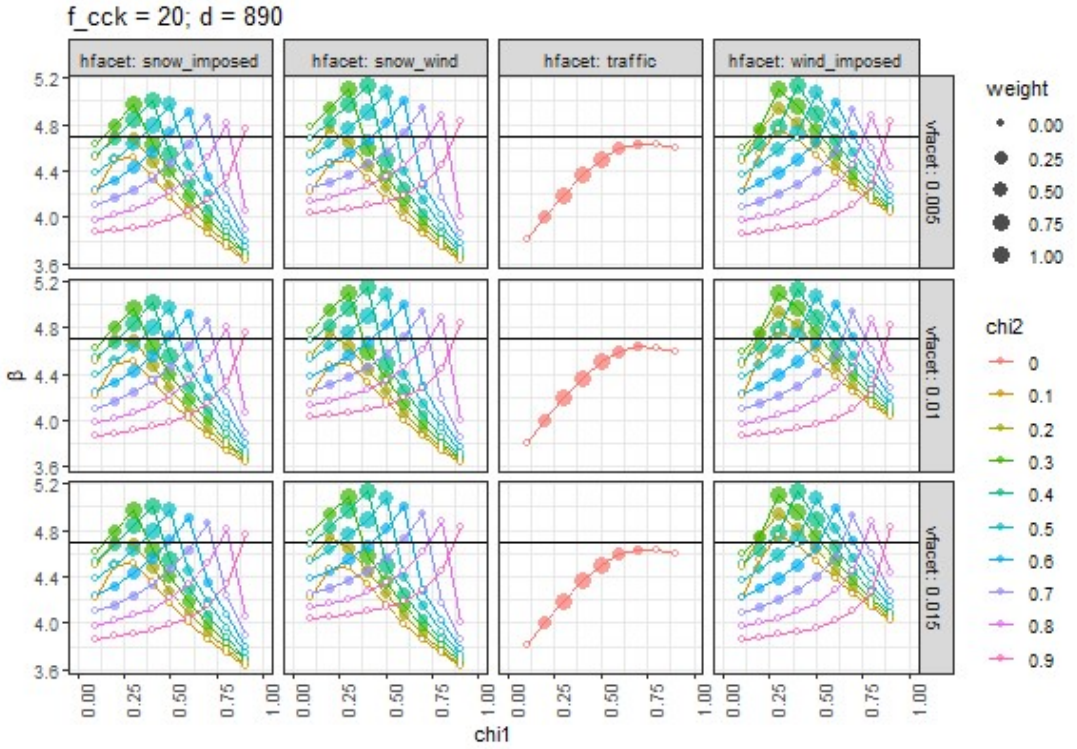

Figure B.6: Reliability indices β as a function of load ratio χ_1 with $d = 890$ mm for the subset $a_{cs} \geq 4d$ corresponding to the one-way shear resistance formula. Columns present different load combinations, while rows different value of longitudinal reinforcement ratios. Colors represent different values of χ_2 load ratios, while the marker size shows the magnitude of the weight of prevalence. The black horizontal line indicates the target reliability (4.7).

Slika B.6: Indeksi zanesljivosti β kot funkcija obtežnega faktorja χ_1 pri $d = 890$ mm za pogoj $a_{cs} \geq 4d$ enačbe strižne odpornosti; stolpci prikazujejo obtežne kombinacije, vrstice prikazujejo različne vrednosti koeficienta natezne armature; barve prikazujejo vrednosti obtežnega faktorja χ_2, velikost oznake na grafu prikazuje vrednost uteži; horizontalna polna črta prikazuje ciljni indeks zanesljivosti (4.7).

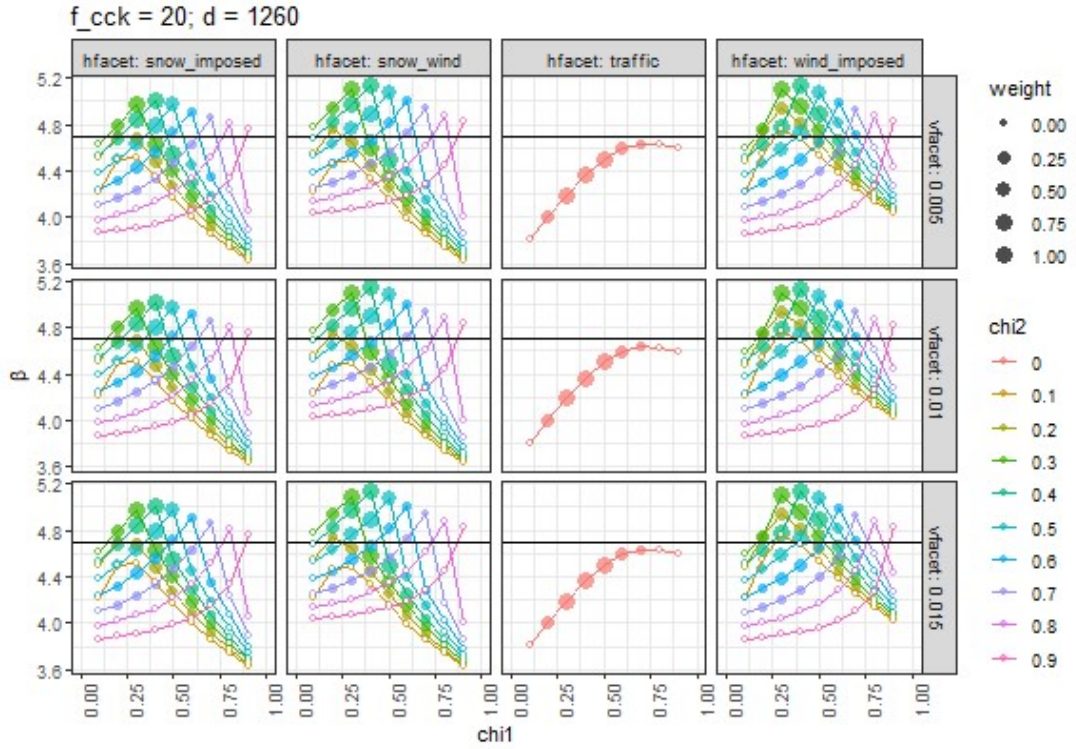

Figure B.7: Reliability indices β as a function of load ratio χ_1 with $d = 1260$ mm for the subset $a_{cs} \geq 4\,d$ corresponding to the one-way shear resistance formula. Columns present different load combinations, while rows different value of longitudinal reinforcement ratios. Colors represent different values of χ_2 load ratios, while the marker size shows the magnitude of the weight of prevalence. The black horizontal line indicates the target reliability (4.7).

Slika B.7: Indeksi zanesljivosti β kot funkcija obtežnega faktorja χ_1 pri $d = 1260$ mm za pogoj $a_{cs} \geq 4\,d$ enačbe strižne odpornosti; stolpci prikazujejo obtežne kombinacije, vrstice prikazujejo različne vrednosti koeficienta natezne armature; barve prikazujejo vrednosti obtežnega faktorja χ_2, velikost oznake na grafu prikazuje vrednost uteži; horizontalna polna črta prikazuje ciljni indeks zanesljivosti (4.7).

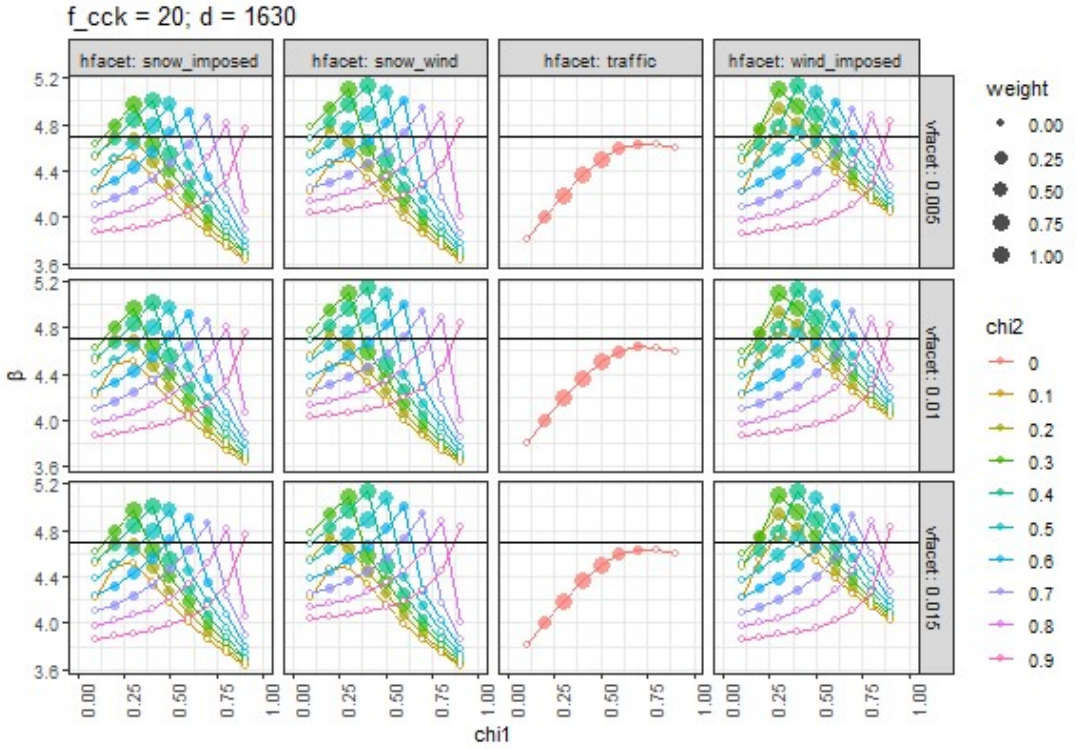

Figure B.8: Reliability indices β as a function of load ratio χ_1 with $d = 1630$ mm for the subset $a_{cs} \geq 4d$ corresponding to the one-way shear resistance formula. Columns present different load combinations, while rows different value of longitudinal reinforcement ratios. Colors represent different values of χ_2 load ratios, while the marker size shows the magnitude of the weight of prevalence. The black horizontal line indicates the target reliability (4.7).

Slika B.8: Indeksi zanesljivosti β kot funkcija obtežnega faktorja χ_1 pri $d = 1630$ mm za pogoj $a_{cs} \geq 4d$ enačbe strižne odpornosti; stolpci prikazujejo obtežne kombinacije, vrstice prikazujejo različne vrednosti koeficienta natezne armature; barve prikazujejo vrednosti obtežnega faktorja χ_2, velikost oznake na grafu prikazuje vrednost uteži; horizontalna polna črta prikazuje ciljni indeks zanesljivosti (4.7).

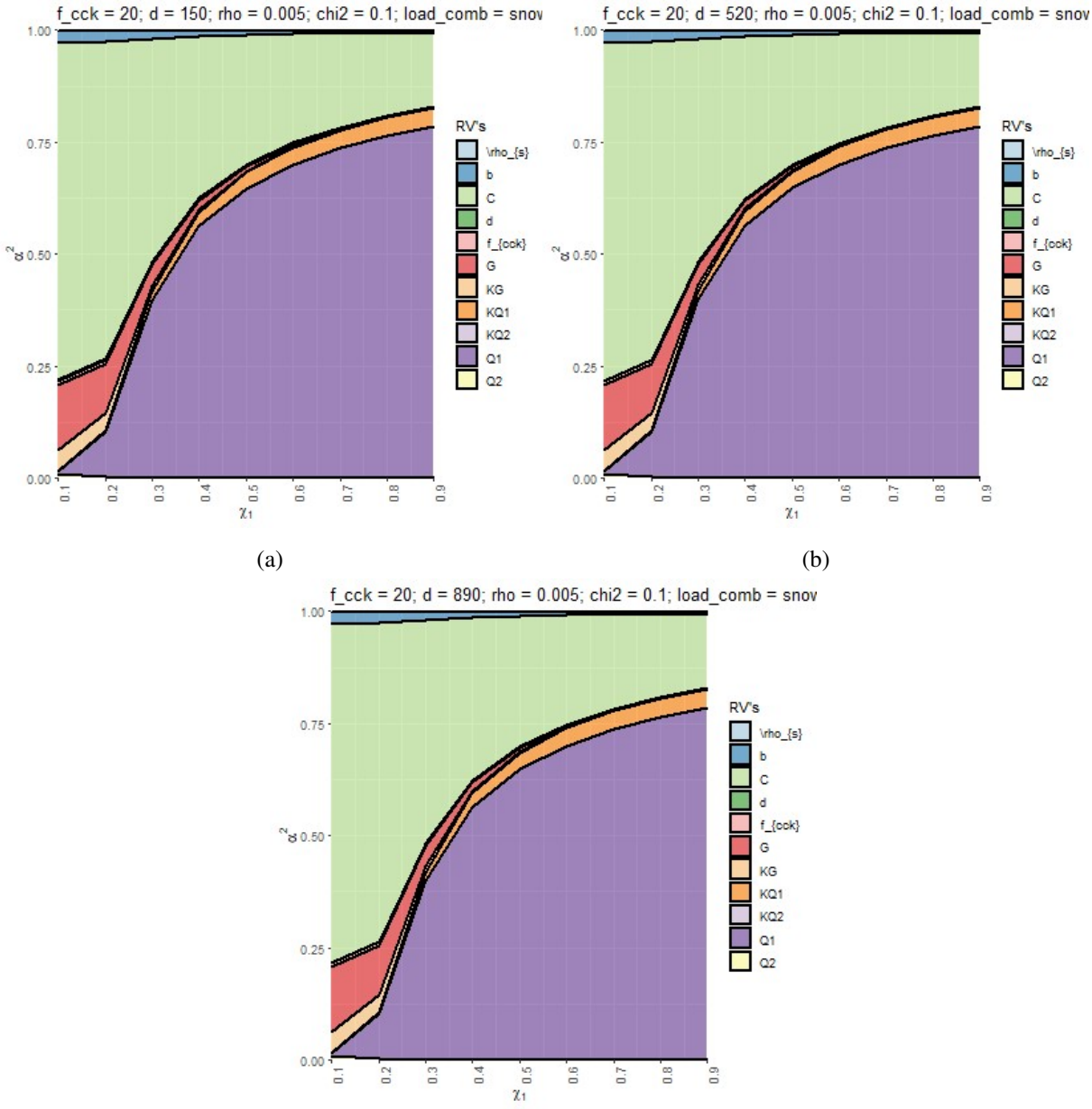

(a) (b)

(c)

Figure B.9: Sensitivity factors α^2 corresponding to subset $a_{cs} < 4d$ of the one-way shear resistance equation with the snow-imposed load combination and with different effective depth d: (a) 150 mm, (b) 520 mm, (c) 890 mm.

Slika B.9: Faktorji občutljivosti α^2, ki ustrezajo pogoju $a_{cs} < 4d$ enačbe strižne odpornosti za obtežno kombinacijo sneg-koristna obtežba in projektne vrednosti višine prereza d: (a) 150 mm, (b) 520 mm, (c) 890 mm.

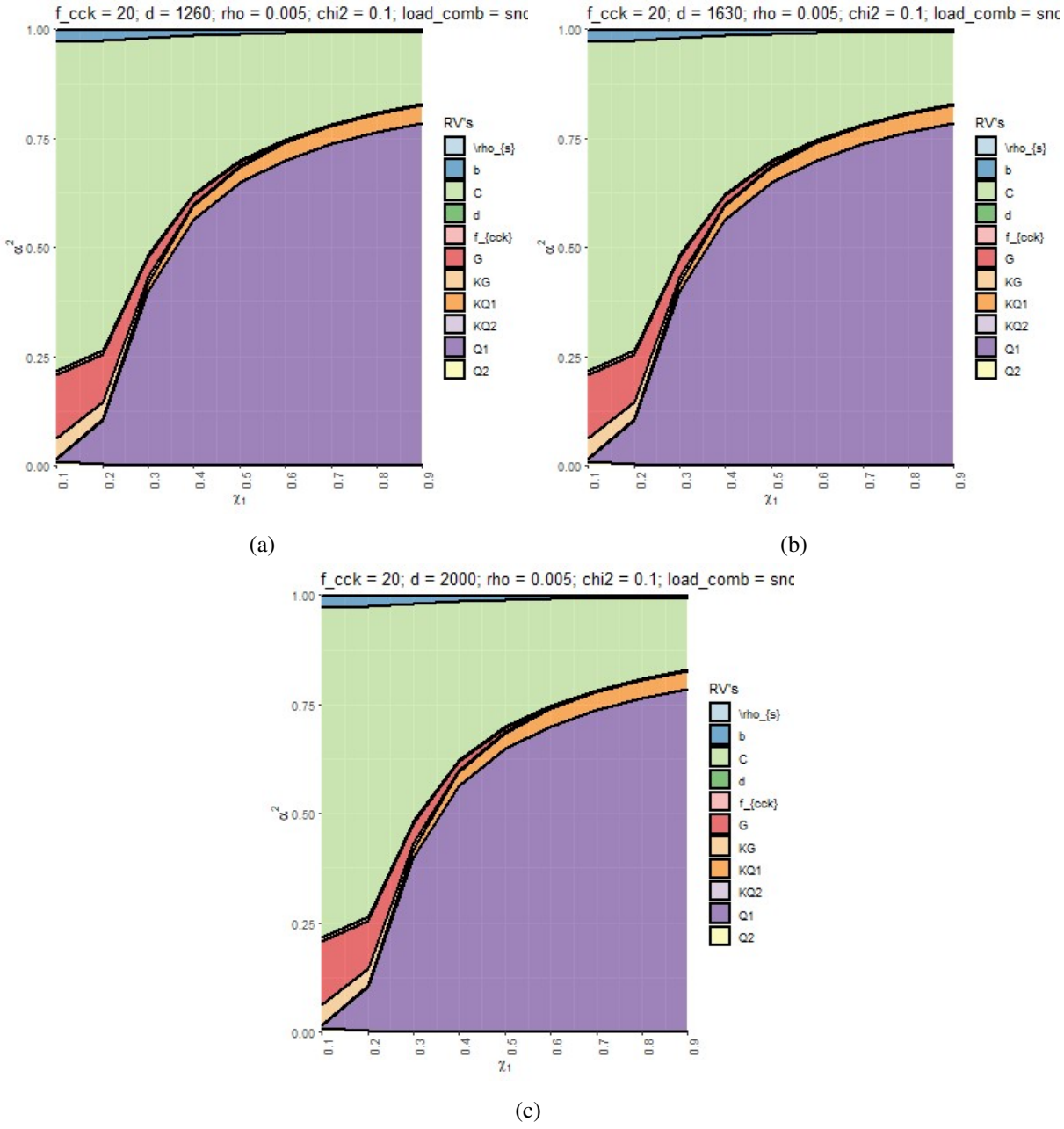

Figure B.10: Sensitivity factors α^2 corresponding to subset $a_{cs} < 4d$ of the one-way shear resistance equation with the snow-imposed load combination and with different effective depth d: (a) 1260 mm, (b) 1630 mm, (c) 2000 mm.

Slika B.10: Faktorji občutljivosti α^2, ki ustrezajo pogoju $a_{cs} < 4d$ enačbe strižne odpornosti za obtežno kombinacijo sneg-koristna obtežba in projektne vrednosti višine prereza d: (a) 1260 mm, (b) 1630 mm, (c) 2000 mm.

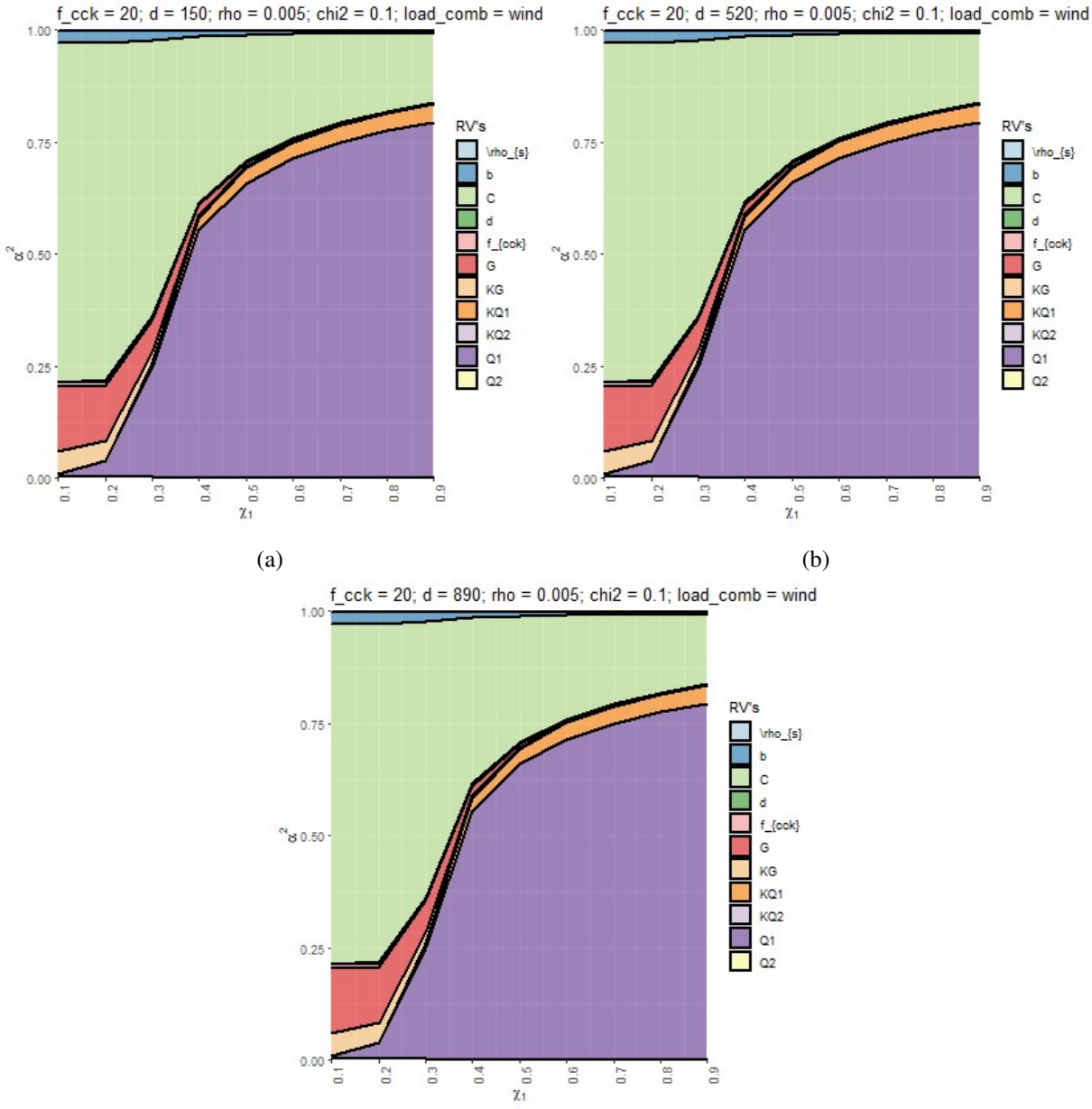

(a) (b)

(c)

Figure B.11: Sensitivity factors α^2 corresponding to subset $a_{cs} < 4d$ of the one-way shear resistance equation with the wind-imposed load combination and with different effective depth d: (a) 150 mm, (b) 520 mm, (c) 890 mm.

Slika B.11: Faktorji občutljivosti α^2, ki ustrezajo pogoju $a_{cs} < 4d$ enačbe strižne odpornosti za obtežno kombinacijo veter-koristna obtežba in projektne vrednosti višine prereza d: (a) 150 mm, (b) 520 mm, (c) 890 mm.

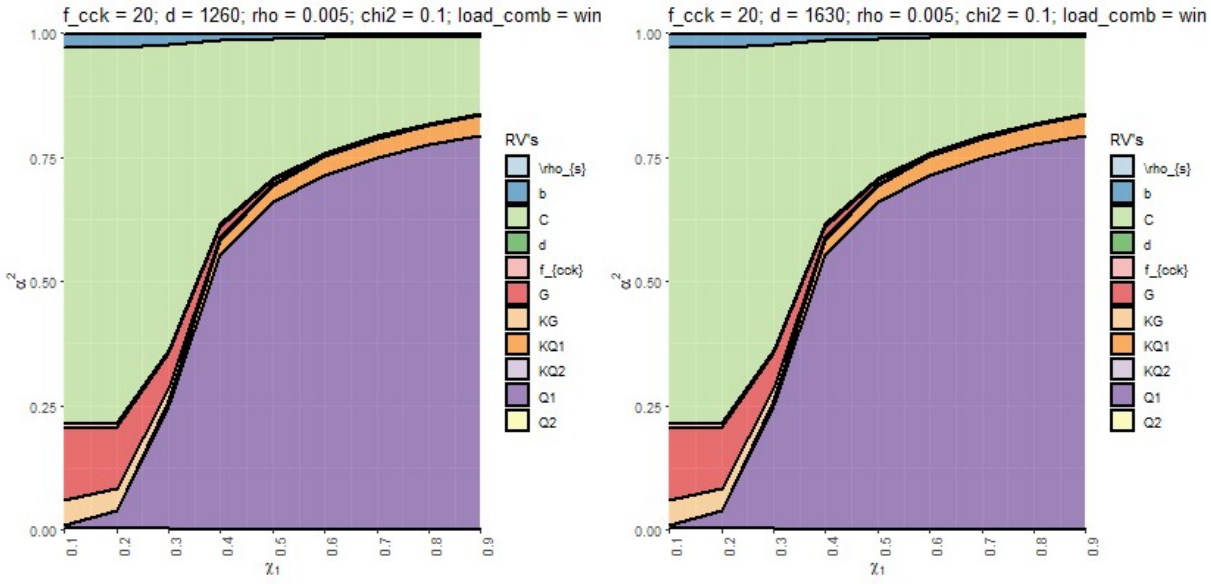

(a) (b)

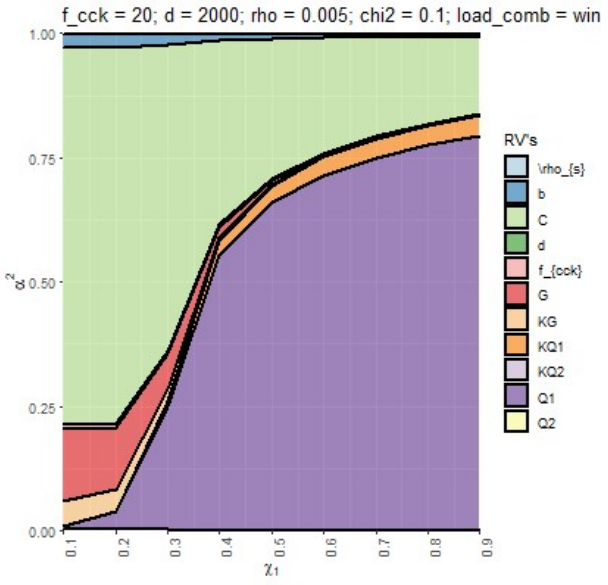

(c)

Figure B.12: Sensitivity factors α^2 corresponding to subset $a_{cs} < 4d$ of the one-way shear resistance equation with the wind-imposed load combination and with different effective depth d: (a) 1260 mm, (b) 1630 mm, (c) 2000 mm.

Slika B.12: Faktorji občutljivosti α^2, ki ustrezajo pogoju $a_{cs} < 4d$ enačbe strižne odpornosti za obtežno kombinacijo veter-koristna obtežba in projektne vrednosti višine prereza d: (a) 1260 mm, (b) 1630 mm, (c) 2000 mm.

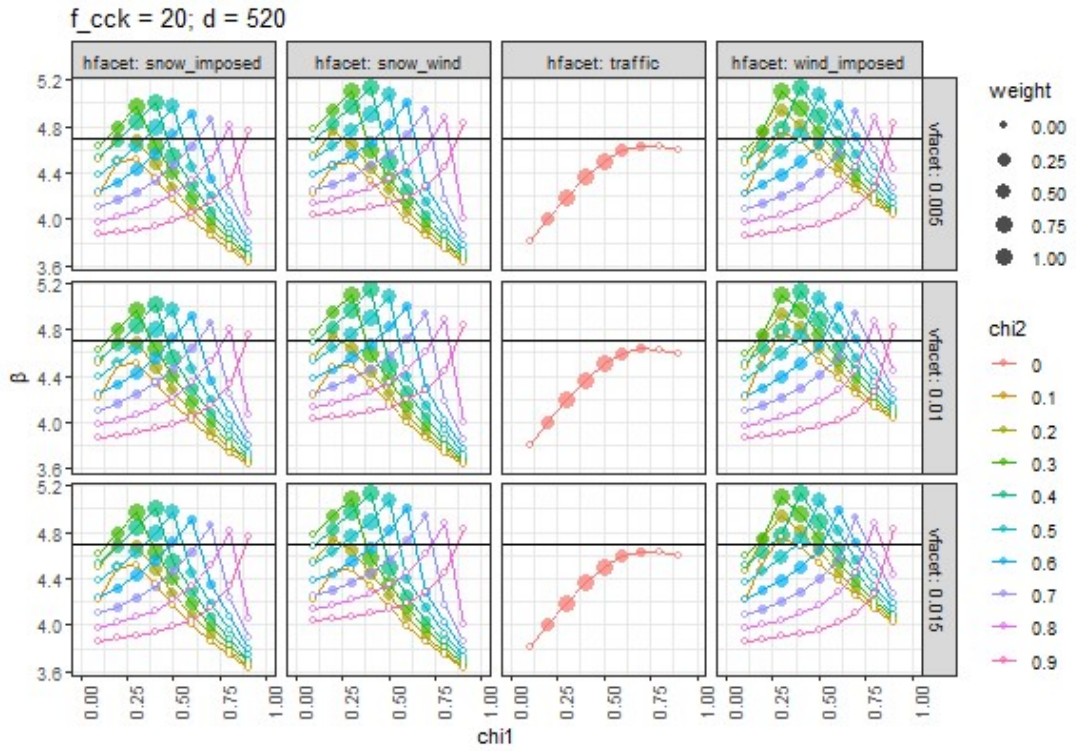

Figure B.13: Reliability indices β as a function of load ratio χ_1 with $d = 520$ mm for the subset $a_{cs} < 4\,d$ corresponding to the one-way shear resistance formula. Columns present different load combinations, while rows different value of longitudinal reinforcement ratios. Colors represent different values of χ_2 load ratios, while the marker size shows the magnitude of the weight of prevalence. The black horizontal line indicates the target reliability (4.7).

Slika B.13: Indeksi zanesljivosti β kot funkcija obtežnega faktorja χ_1 pri $d = 520$ mm za pogoj $a_{cs} < 4\,d$ enačbe strižne odpornosti; stolpci prikazujejo obtežne kombinacije, vrstice prikazujejo različne vrednosti koeficienta natezne armature; barve prikazujejo vrednosti obtežnega faktorja χ_2, velikost oznake na grafu prikazuje vrednost uteži; horizontalna polna črta prikazuje ciljni indeks zanesljivosti (4.7).

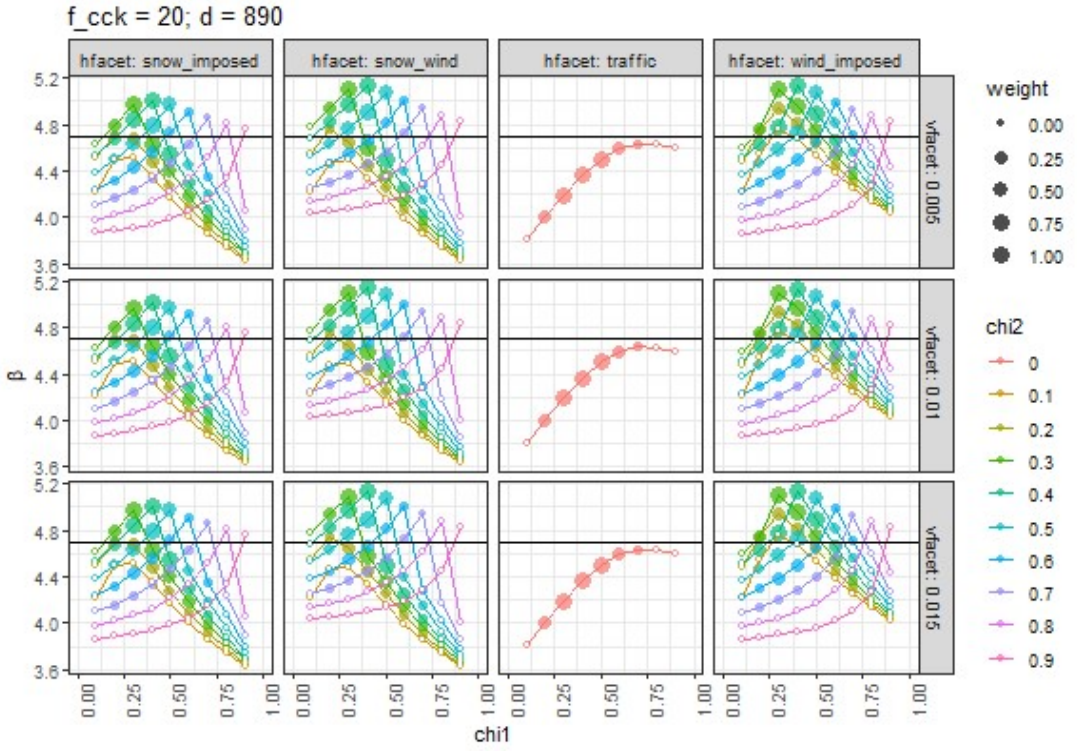

Figure B.14: Reliability indices β as a function of load ratio χ_1 with $d = 890$ mm for the subset $a_{cs} < 4\,d$ corresponding to the one-way shear resistance formula. Columns present different load combinations, while rows different value of longitudinal reinforcement ratios. Colors represent different values of χ_2 load ratios, while the marker size shows the magnitude of the weight of prevalence. The black horizontal line indicates the target reliability (4.7).

Slika B.14: Indeksi zanesljivosti β kot funkcija obtežnega faktorja χ_1 pri $d = 890$ mm za pogoj $a_{cs} < 4\,d$ enačbe strižne odpornosti; stolpci prikazujejo obtežne kombinacije, vrstice prikazujejo različne vrednosti koeficienta natezne armature; barve prikazujejo vrednosti obtežnega faktorja χ_2, velikost oznake na grafu prikazuje vrednost uteži; horizontalna polna črta prikazuje ciljni indeks zanesljivosti (4.7).

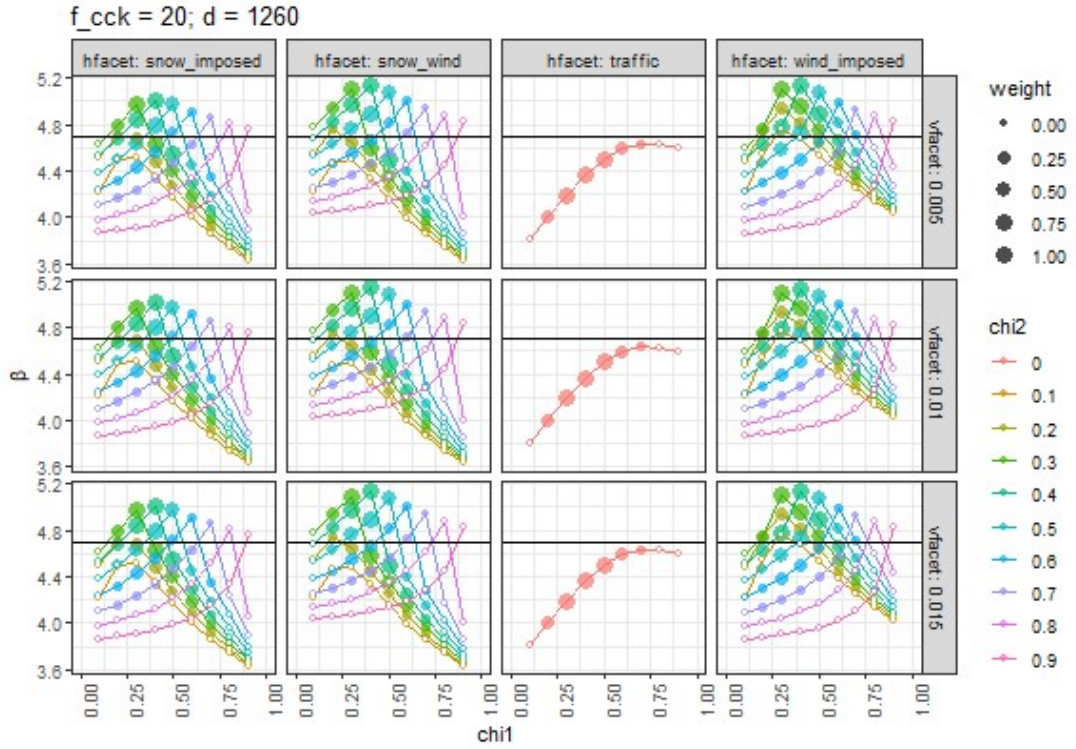

Figure B.15: Reliability indices β as a function of load ratio χ_1 with $d = 1260$ mm for the subset $a_{cs} < 4\,d$ corresponding to the one-way shear resistance formula. Columns present different load combinations, while rows different value of longitudinal reinforcement ratios. Colors represent different values of χ_2 load ratios, while the marker size shows the magnitude of the weight of prevalence. The black horizontal line indicates the target reliability (4.7).

Slika B.15: Indeksi zanesljivosti β kot funkcija obtežnega faktorja χ_1 pri $d = 1260$ mm za pogoj $a_{cs} < 4\,d$ enačbe strižne odpornosti; stolpci prikazujejo obtežne kombinacije, vrstice prikazujejo različne vrednosti koeficienta natezne armature; barve prikazujejo vrednosti obtežnega faktorja χ_2, velikost oznake na grafu prikazuje vrednost uteži; horizontalna polna črta prikazuje ciljni indeks zanesljivosti (4.7).

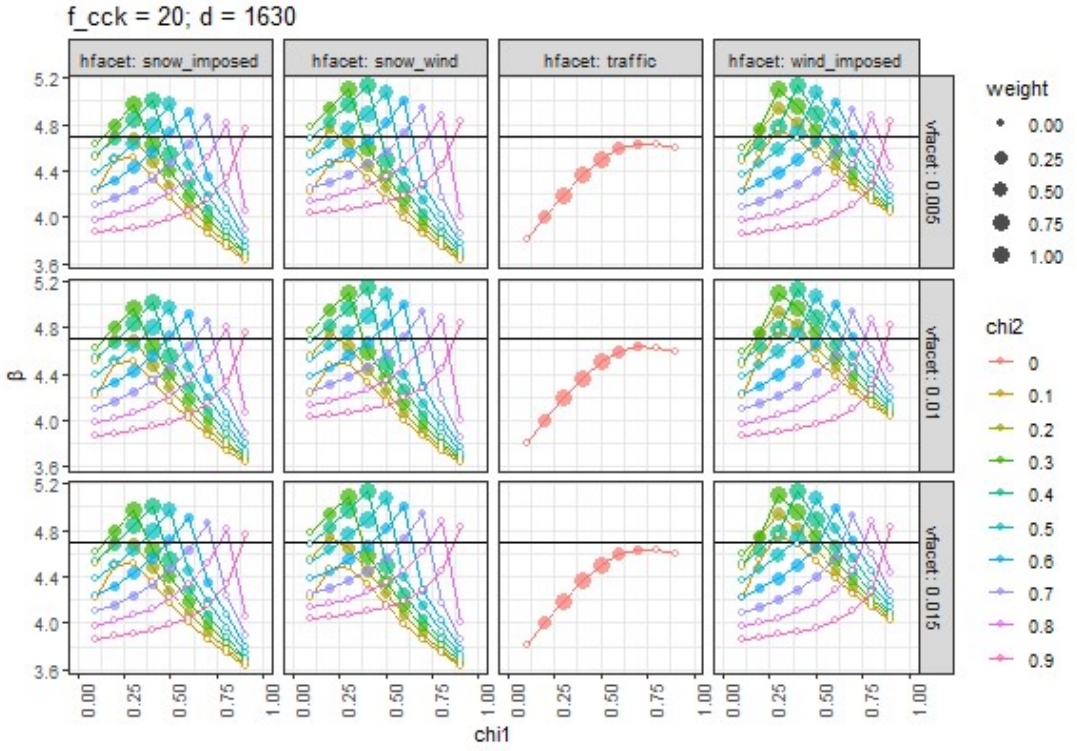

Figure B.16: Reliability indices β as a function of load ratio χ_1 with $d = 1630$ mm for the subset $a_{cs} < 4\,d$ corresponding to the one-way shear resistance formula. Columns present different load combinations, while rows different value of longitudinal reinforcement ratios. Colors represent different values of χ_2 load ratios, while the marker size shows the magnitude of the weight of prevalence. The black horizontal line indicates the target reliability (4.7).

Slika B.16: Indeksi zanesljivosti β kot funkcija obtežnega faktorja χ_1 pri $d = 1630$ mm za pogoj $a_{cs} < 4\,d$ enačbe strižne odpornosti; stolpci prikazujejo obtežne kombinacije, vrstice prikazujejo različne vrednosti koeficienta natezne armature; barve prikazujejo vrednosti obtežnega faktorja χ_2, velikost oznake na grafu prikazuje vrednost uteži; horizontalna polna črta prikazuje ciljni indeks zanesljivosti (4.7).

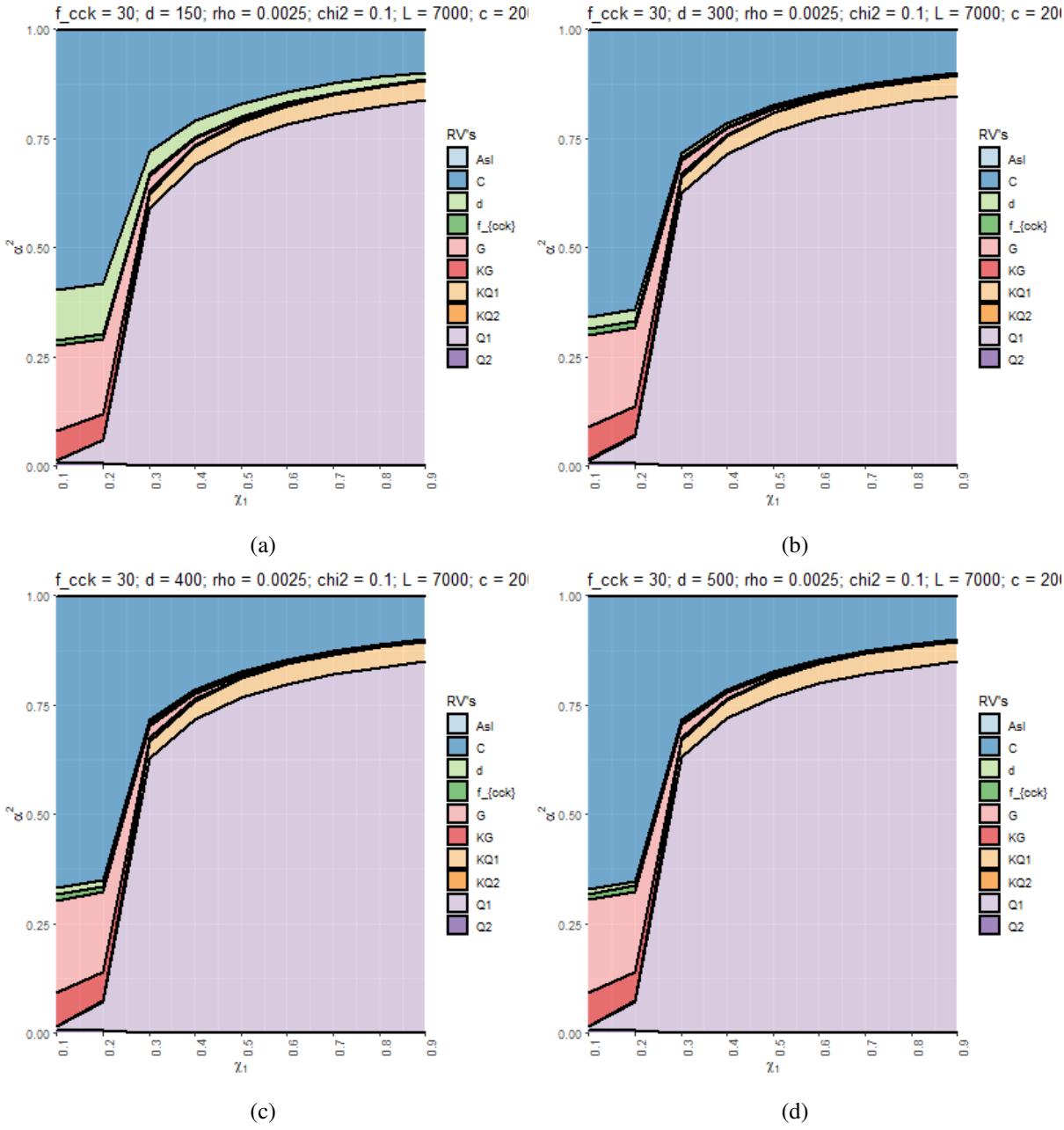

Figure B.17: Sensitivity factors α^2 corresponding to subset $a_p \leq 8\,d_v$ of the punching shear resistance equation with the snow-imposed load combination and with different effective depth d: (a) 150 mm, (b) 300 mm, (c) 400 mm, (d) 500 mm.

Slika B.17: Faktorji občutljivosti α^2, ki ustrezajo pogoju $a_p \leq 8\,d_v$ enačbe odpornosti proti preboju za obtežno kombinacijo sneg-koristna obtežba in projektne vrednosti višine prereza d: (a) 150 mm, (b) 300 mm, (c) 400 mm, (d) 500 mm.

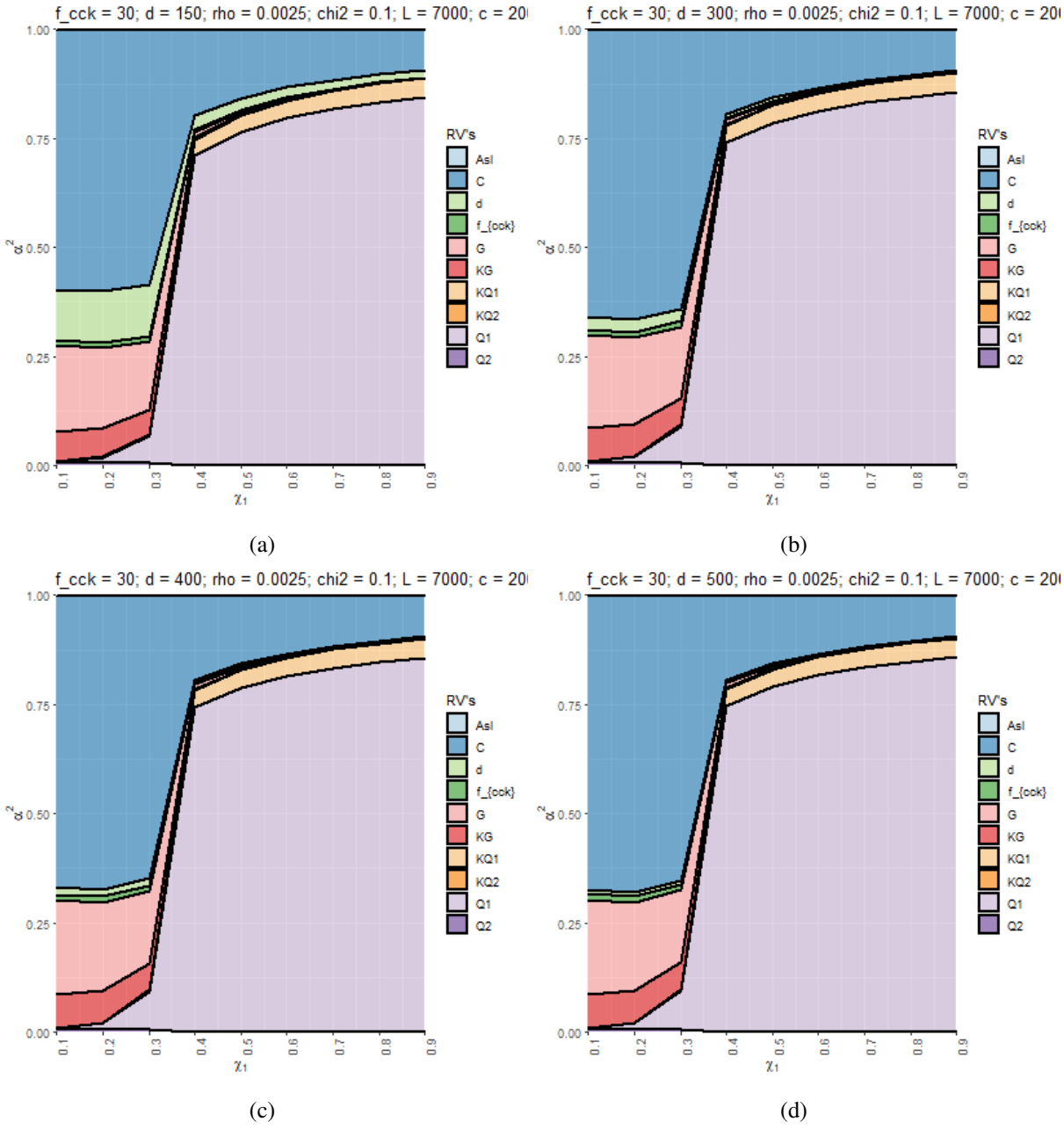

Figure B.18: Sensitivity factors α^2 corresponding to subset $a_p \leq 8\,d_v$ of the punching shear resistance equation with the wind-imposed load combination and with different effective depth d: (a) 150 mm, (b) 300 mm, (c) 400 mm, (d) 500 mm.

Slika B.18: Faktorji občutljivosti α^2, ki ustrezajo pogoju $a_p \leq 8\,d_v$ enačbe odpornosti proti preboju za obtežno kombinacijo veter-koristna obtežba in projektne vrednosti višine prereza d: (a) 150 mm, (b) 300 mm, (c) 400 mm, (d) 500 mm.

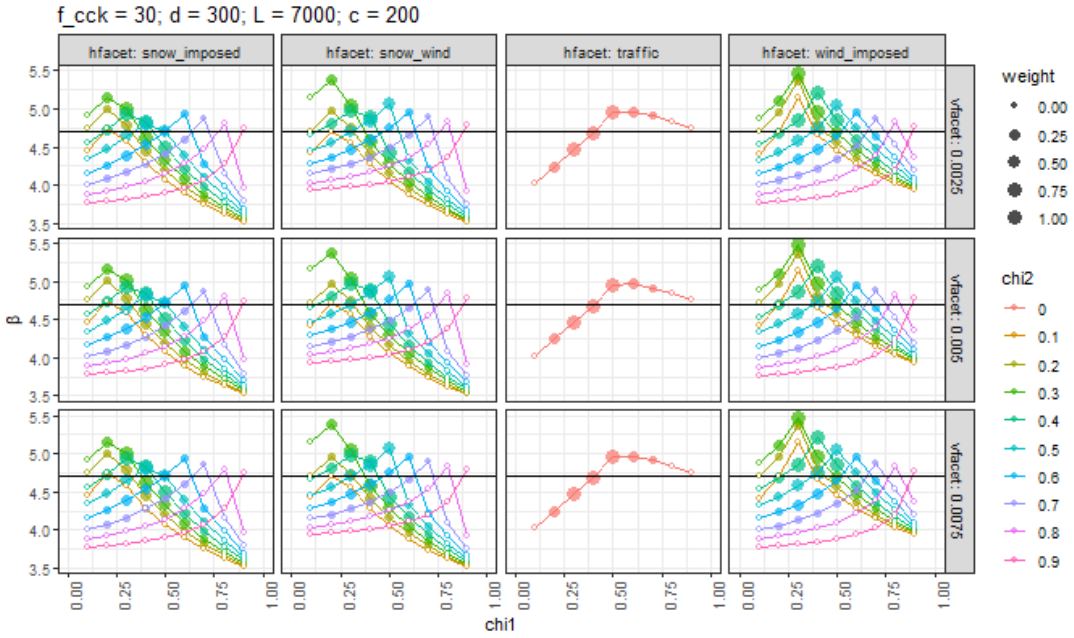

Figure B.19: Reliability indices β as a function of load ratio χ_1 with $d = 300$ mm for the subset $a_p \leq 8\,d_v$ corresponding to the punching shear resistance formula. Columns present different load combinations, while rows different value of longitudinal reinforcement ratios. Colors represent different values of χ_2 load ratios, while the marker size shows the magnitude of the weight of prevalence. The black horizontal line indicates the target reliability (4.7).

Slika B.19: Indeksi zanesljivosti β kot funkcija obtežnega faktorja χ_1 pri $d = 300$ mm za pogoj $a_p \leq 8\,d_v$ enačbe odpornosti proti preboju; stolpci prikazujejo obtežne kombinacije, vrstice prikazujejo različne vrednosti koeficienta natezne armature; barve prikazujejo vrednosti obtežnega faktorja χ_2, velikost oznake na grafu prikazuje vrednost uteži; horizontalna polna črta prikazuje ciljni indeks zanesljivosti (4.7).

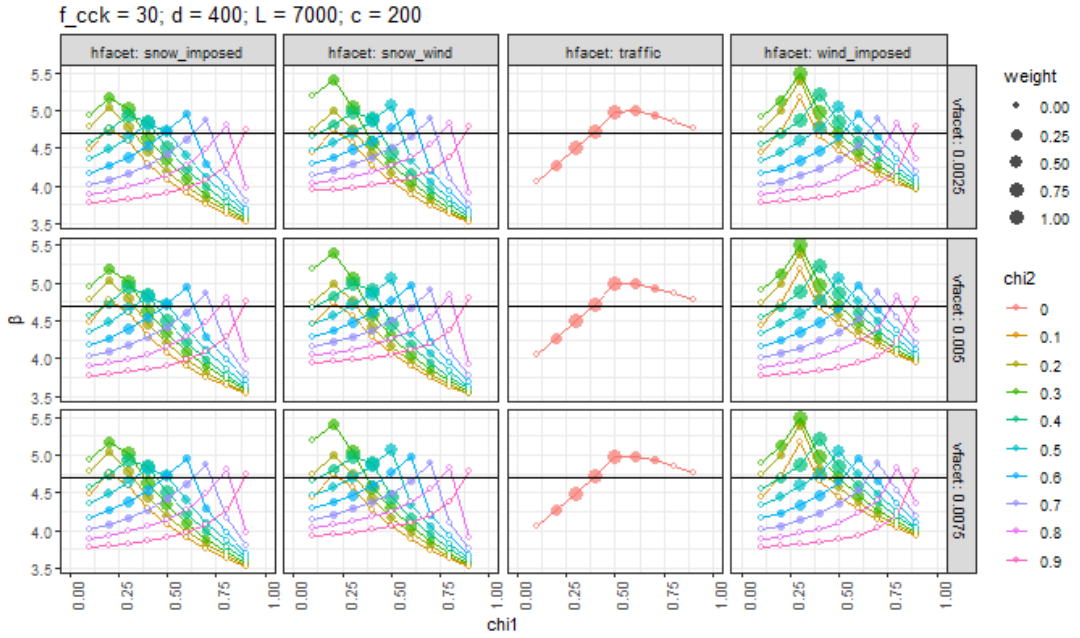

Figure B.20: Reliability indices β as a function of load ratio χ_1 with $d = 400$ mm for the subset $a_p \leq 8\,d_v$ corresponding to the punching shear resistance formula. Columns present different load combinations, while rows different value of longitudinal reinforcement ratios. Colors represent different values of χ_2 load ratios, while the marker size shows the magnitude of the weight of prevalence. The black horizontal line indicates the target reliability (4.7).

Slika B.20: Indeksi zanesljivosti β kot funkcija obtežnega faktorja χ_1 pri $d = 400$ mm za pogoj $a_p \leq 8\,d_v$ enačbe odpornosti proti preboju; stolpci prikazujejo obtežne kombinacije, vrstice prikazujejo različne vrednosti koeficienta natezne armature; barve prikazujejo vrednosti obtežnega faktorja χ_2, velikost oznake na grafu prikazuje vrednost uteži; horizontalna polna črta prikazuje ciljni indeks zanesljivosti (4.7).

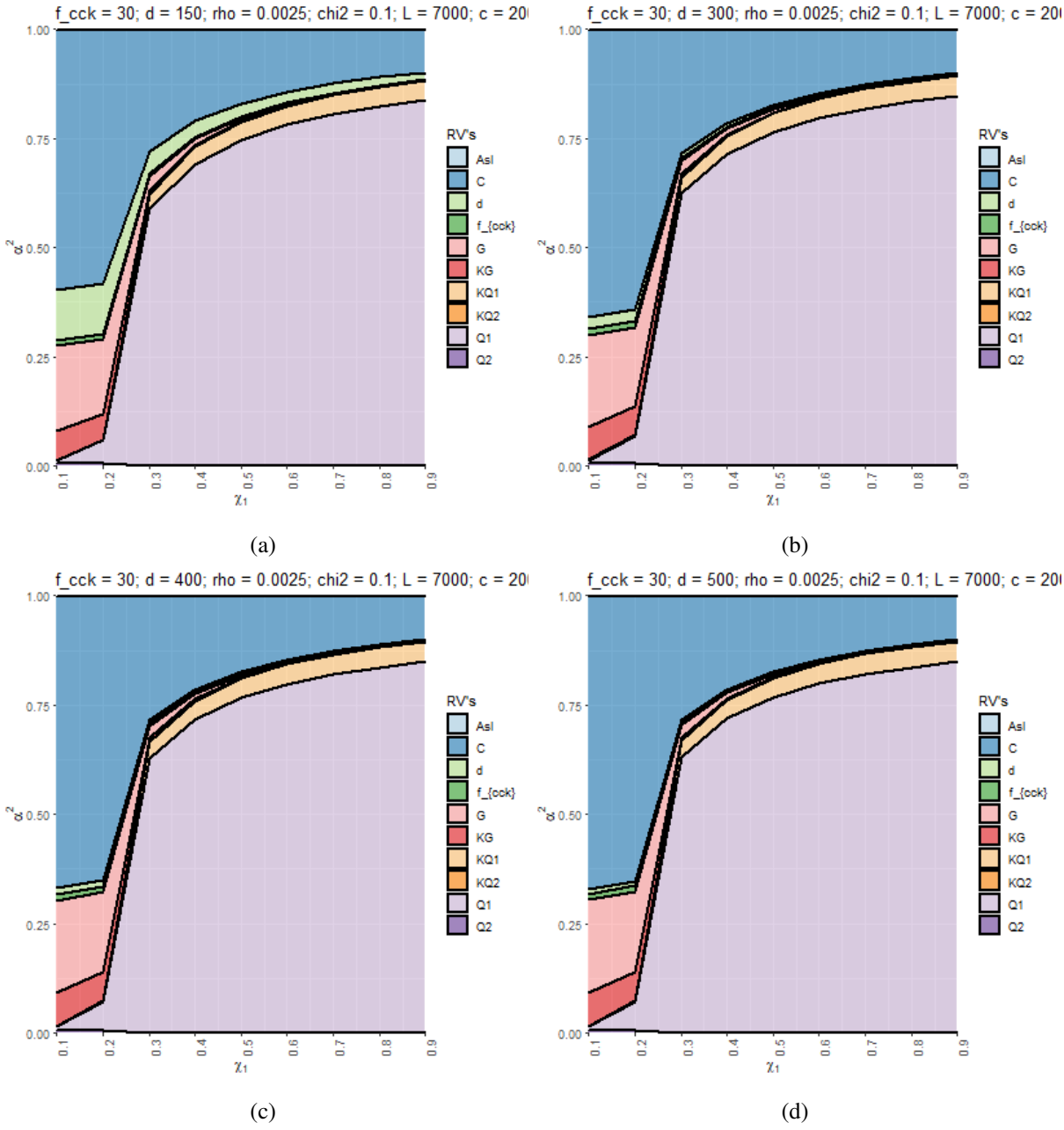

Figure B.21: Sensitivity factors α^2 corresponding to subset $a_p > 8\,d_v$ of the punching shear resistance equation with the snow-imposed load combination and with different effective depth d: (a) 150 mm, (b) 300 mm, (c) 400 mm, (d) 500 mm.

Slika B.21: Faktorji občutljivosti α^2, ki ustrezajo pogoju $a_p > 8\,d_v$ enačbe odpornosti proti preboju za obtežno kombinacijo sneg-koristna obtežba in projektne vrednosti višine prereza d: (a) 150 mm, (b) 300 mm, (c) 400 mm, (d) 500 mm.

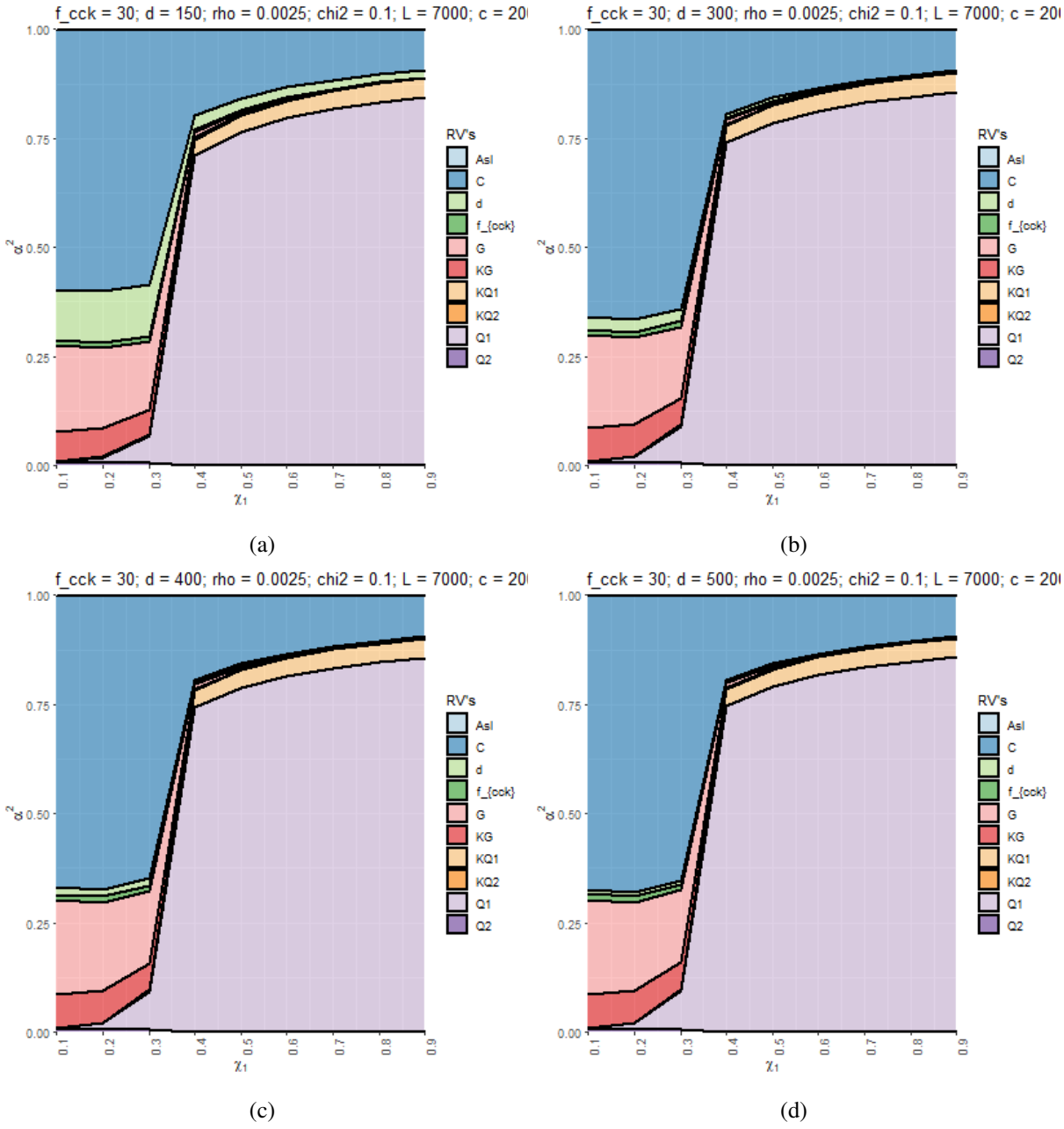

Figure B.22: Sensitivity factors α^2 corresponding to subset $a_p > 8\,d_v$ of the punching shear resistance equation with the wind-imposed load combination and with different effective depth d: (a) 150 mm, (b) 300 mm, (c) 400 mm, (d) 500 mm.

Slika B.22: Faktorji občutljivosti α^2, ki ustrezajo pogoju $a_p > 8\,d_v$ enačbe odpornosti proti preboju za obtežno kombinacijo veter-koristna obtežba in projektne vrednosti višine prereza d: (a) 150 mm, (b) 300 mm, (c) 400 mm, (d) 500 mm.

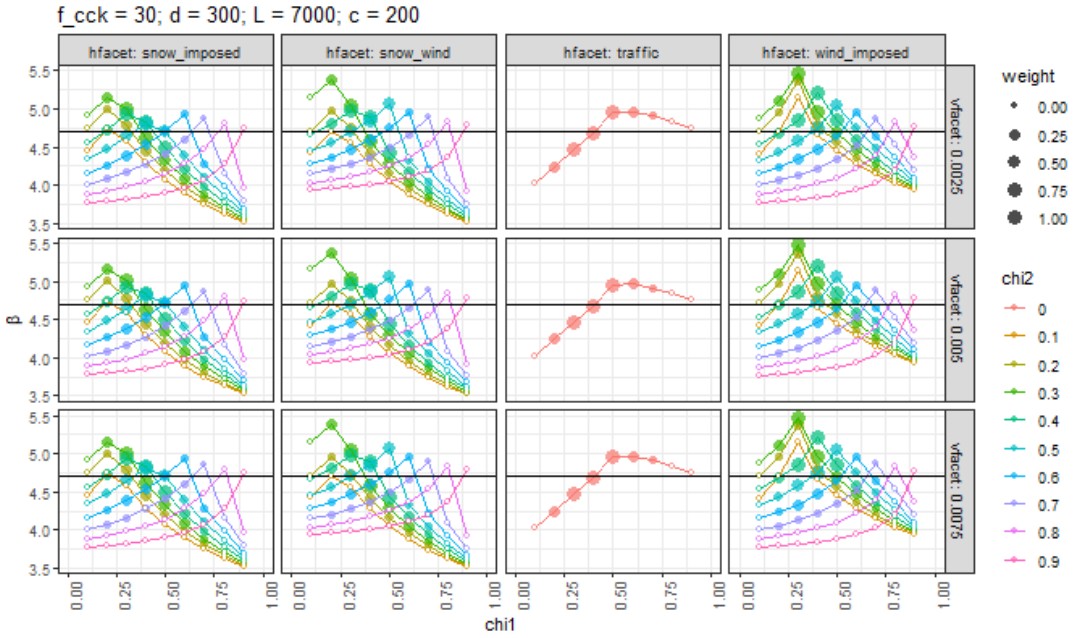

Figure B.23: Reliability indices β as a function of load ratio χ_1 with $d = 300$ mm for the subset $a_p > 8\,d_v$ corresponding to the punching shear resistance formula. Columns present different load combinations, while rows different value of longitudinal reinforcement ratios. Colors represent different values of χ_2 load ratios, while the marker size shows the magnitude of the weight of prevalence. The black horizontal line indicates the target reliability (4.7).

Slika B.23: Indeksi zanesljivosti β kot funkcija obtežnega faktorja χ_1 pri $d = 300$ mm za pogoj $a_p > 8\,d_v$ enačbe odpornosti proti preboju; stolpci prikazujejo obtežne kombinacije, vrstice prikazujejo različne vrednosti koeficienta natezne armature; barve prikazujejo vrednosti obtežnega faktorja χ_2, velikost oznake na grafu prikazuje vrednost uteži; horizontalna polna črta prikazuje ciljni indeks zanesljivosti (4.7).

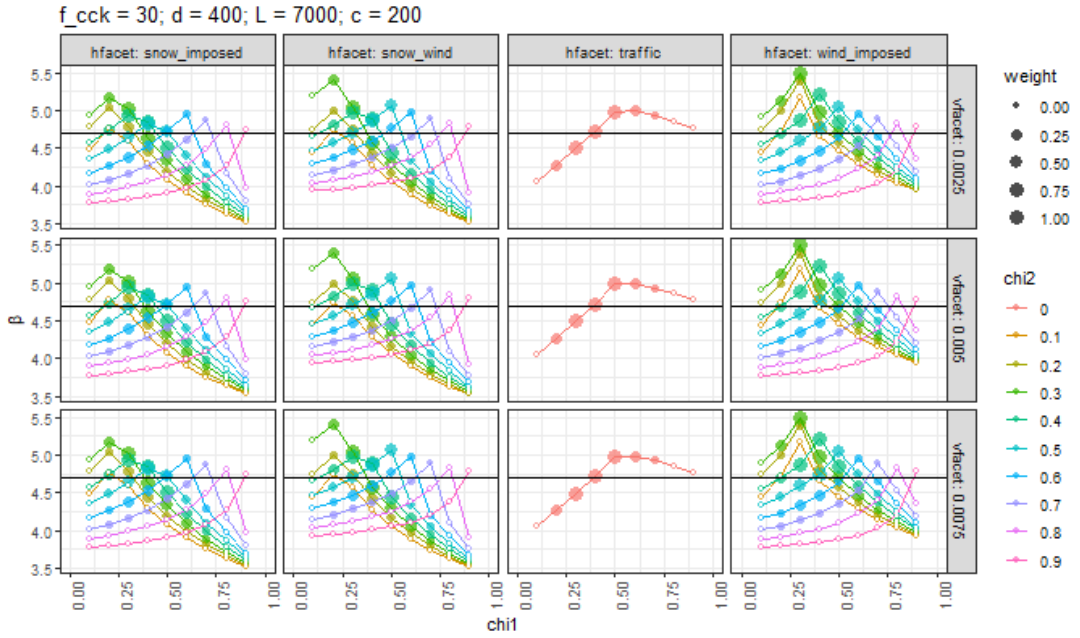

Figure B.24: Reliability indices β as a function of load ratio χ_1 with $d = 400$ mm for the subset $a_p > 8\,d_v$ corresponding to the punching shear resistance formula. Columns present different load combinations, while rows different value of longitudinal reinforcement ratios. Colors represent different values of χ_2 load ratios, while the marker size shows the magnitude of the weight of prevalence. The black horizontal line indicates the target reliability (4.7).

Slika B.24: Indeksi zanesljivosti β kot funkcija obtežnega faktorja χ_1 pri $d = 400$ mm za pogoj $a_p > 8\,d_v$ enačbe odpornosti proti preboju; stolpci prikazujejo obtežne kombinacije, vrstice prikazujejo različne vrednosti koeficienta natezne armature; barve prikazujejo vrednosti obtežnega faktorja χ_2, velikost oznake na grafu prikazuje vrednost uteži; horizontalna polna črta prikazuje ciljni indeks zanesljivosti (4.7).